

# Water and Salt Balance of Great Salt Lake, Utah, and Simulation of Water and Salt Movement through the Causeway, 1987–98

Rec'd  
2/20/01  
Kim/  
Greg  
(+CD  
Rom)

Water-Resources Investigations Report 00–4221

Prepared in cooperation with the  
UTAH DEPARTMENT OF NATURAL RESOURCES,  
DIVISION OF FORESTRY, FIRE, AND STATE LANDS, and  
TOOELE COUNTY, UTAH



**Cover photograph:** Union Pacific Railroad causeway across Great Salt Lake viewed from Lakeside, Utah. Gunnison Bay on left, Gilbert Bay on right, January 1998.

# **WATER AND SALT BALANCE OF GREAT SALT LAKE, UTAH, AND SIMULATION OF WATER AND SALT MOVEMENT THROUGH THE CAUSEWAY, 1987–98**

**By Brian L. Loving, Kidd M. Waddell, U.S. Geological Survey;  
and Craig W. Miller, Utah Department of Natural Resources, Division of  
Water Resources**

---

**U.S. GEOLOGICAL SURVEY**

**Water-Resources Investigations Report 00–4221**



**Prepared in cooperation with the  
UTAH DEPARTMENT OF NATURAL RESOURCES,  
DIVISION OF FORESTRY, FIRE, AND STATE LANDS, and  
TOOELE COUNTY, UTAH**

**Salt Lake City, Utah  
2000**

**U.S. DEPARTMENT OF THE INTERIOR**

**BRUCE BABBITT, Secretary**

**U.S. GEOLOGICAL SURVEY**

Charles G. Groat, Director

The use of trade, product, industry, or firm names is for descriptive purposes only and does not imply endorsement by the U.S. Government.

---

For additional information write to:

District Chief  
U.S. Geological Survey  
2329 West Orton Circle  
West Valley City, Utah 84119

Copies of this report can be purchased from:

U.S. Geological Survey  
Branch of Information Services  
Box 25286  
Denver Federal Center  
Denver, Colorado 80225

*Additional information about water resources in Utah is available on the World Wide Web at <http://ut.water.usgs.gov>*

# CONTENTS

Abstract .....	1
Introduction .....	2
Description of the study area .....	2
Purpose and scope .....	2
Acknowledgments .....	6
Water and salt balance of Great Salt Lake .....	6
Effects of causeway construction .....	6
Dissolved salt loads .....	8
Theoretical equations of water and salt balance for the divided lake .....	8
Trend of dissolved and precipitated salt loads in north and south parts, 1963–98 .....	9
Effect of causeway conveyance properties, 1987–98 .....	10
Stratification .....	14
Effects of the West Desert Pumping Project on loads of ions .....	14
Sources of error in computing loads of ions .....	15
Simulation of water and salt movement through the causeway .....	17
Calibration of the water and salt balance model, 1987–98 .....	18
Water-balance program .....	18
Water and salt balance model and causeway-fill flow .....	19
Simulation of major-ion loads as an independent check of model calibration .....	20
Limitations of the model .....	20
Simulated effects of breach dimension on the salinity balance between the north and south parts .....	25
Simulated effects of the West Desert Pumping Project on the salinity of the north and south parts .....	27
Sensitivity and error analyses .....	27
Summary .....	29
Information needed for more accurate water and salt balance calculations .....	30
References cited .....	30

## Appendixes

**A-1**

A. Water balance and boundary conditions .....	A-2
Correction of water-surface altitudes for the Boat Harbor gage, 1987–98 .....	A-5
Surface-water inflow .....	A-6
Bear River and Weber River basins .....	A-6
Jordan River basin .....	A-8
Other surface-water inflow .....	A-12
Ground-water inflow .....	A-12
Precipitation .....	A-13
Evaporation .....	A-14
West Desert Pumping Project .....	A-15
Calibration .....	A-16
Sensitivity and error analysis .....	A-17
B. Salt balance .....	B-1
Computation of salt load .....	B-1
Salt precipitation and re-solution .....	B-3
Stratification in Great Salt Lake .....	B-4
Effects of Bear River and Farmington Bays on salt load computations .....	B-7

## Appendixes—Continued

C. Flow through the causeway fill .....	C-1
Causeway properties .....	C-1
Modeling of the fill flow .....	C-1
Hydraulic properties .....	C-1
Selected causeway-fill flows .....	C-2
Methods used to compute causeway-fill flow .....	C-2
South-to-north flow .....	C-3
North-to-south flow .....	C-4
Fill-flow calibration .....	C-5
Computation of fill flow with the water and salt balance model .....	C-8
Sensitivity and error analysis .....	C-8
D. Flow through the causeway culverts .....	D-1
E. Flow through the causeway breach .....	E-1
F. Initial conditions and input used for calibration of water and salt balance model .....	F-1
Initial lake conditions .....	F-1
Causeway conditions .....	F-1
G. Model code (compact disc, in pocket at back of report)	
Water-balance program	
Water and salt balance model	
Glossary .....	Glossary 1
Abbreviations .....	Glossary 1

## FIGURES

1. Map showing location of study area and data-collection sites used to estimate inflow, water-surface altitude, and evaporation for Great Salt Lake, Utah, 1987–98. ....	3
2. Map showing location of breach and culverts in the causeway across Great Salt Lake, Utah .....	4
3. Diagrammatic cross section of the causeway across Great Salt Lake, Utah .....	4
4. Graphs showing dissolved-solids concentration of the south part, north part, and theoretically undivided lake, and water-surface altitude of the south and north parts of Great Salt Lake, Utah, 1959–98 .....	5
5. Schematic diagram of water balance for Great Salt Lake, Utah. ....	7
6. Schematic diagram of salt balance for Great Salt Lake, Utah. ....	7
7-11. Graphs showing:	
7. Dissolved and precipitated salt load in Great Salt Lake, Utah, 1963–98. ....	9
8. Flow through breach, culverts, and fill of causeway across Great Salt Lake, Utah, 1987–98 .	11
9. Altitude of water surface in the south part and theoretical interface between north and south part brines in the causeway across Great Salt Lake, Utah .....	13
10. Total magnesium and potassium loads in Great Salt Lake, Utah, 1966–99. ....	15
11. Difference between dissolved-solids concentration of the north and south part as computed from the sum of individual ion concentrations and as computed from specific-gravity measurements, 1966–99, Great Salt Lake, Utah. ....	17
12. Flow chart of Great Salt Lake water and salt balance model .....	19
13-16. Graphs showing:	
13. Simulated and measured head difference, water-surface altitude, density difference, density, and dissolved and cumulative precipitated salt load in the south and north parts of Great Salt Lake, Utah, before model calibration, 1987–98 .....	21

## FIGURES—Continued

13-16.	Graphs showing:—Continued	
14.	Simulated and measured breach flow, measured and estimated culvert flow, computed causeway-fill flow, total measured and estimated inflow, and estimated and computed evaporation in the south and north parts of Great Salt Lake, Utah, after model calibration, 1987–98. ....	22
15.	Simulated and measured head difference, water-surface altitude, density difference, density, and dissolved and cumulative precipitated salt load in the south and north parts of Great Salt Lake, Utah, after model calibration, 1987–98.....	23
16.	Simulated and measured loads of sodium, magnesium, potassium, and chloride in the south and north parts of Great Salt Lake, Utah, after model calibration, 1987–98 .....	24
17.	Schematic diagram showing approximate shape and dimensions of the breach (a) during August 1984 to July 1996 and (b) used in simulations of selected breach widths and bottom altitudes, Great Salt Lake, Utah, .....	25
18-A11.	Graphs showing:	
18.	Effects of selected breach widths and bottom altitudes on the dissolved-solids concentration of the south part as a percentage of that of the north part, 1987–98 hydrologic conditions, Great Salt Lake, Utah .....	27
A1.	Difference between datums used at the Boat Harbor gage and at the gages near the causeway Great Salt Lake, Utah, 1984–98.....	A-5
A2.	Inflow and evaporation for Great Salt Lake, Utah, 1987–98.....	A-17
A3.	Simulated and measured water-surface altitude of the south part of Great Salt Lake, Utah, before and after calibration of water balance, 1987–98. ....	A-18
A4.	Simulations showing sensitivity of the south part water-surface altitude to a 13-percent error in surface-water inflow, Great Salt Lake, Utah. ....	A-19
A5.	Simulations showing the sensitivity of the south part water-surface altitude to a 100-percent error in ground-water inflow, Great Salt Lake, Utah.. ....	A-19
A6.	Simulations showing sensitivity of the south part water-surface altitude to a 10-percent error in precipitation, Great Salt Lake, Utah.. ....	A-20
A7.	Simulations showing sensitivity of the south part water-surface altitude to the maximum positive and negative errors from all sources of inflow, Great Salt Lake, Utah.....	A-20
A8.	Simulations showing sensitivity of the south part water-surface altitude to a 0.7-percent error in change in north part volume, Great Salt Lake, Utah.. ....	A-21
A9.	Simulations showing sensitivity of the south part water-surface altitude to a 10-percent error in estimated outflow to and return flow from West Pond, Great Salt Lake, Utah.....	A-21
A10.	Simulations showing sensitivity of the south part water-surface altitude to a 10-percent error in evaporation, Great Salt Lake, Utah.....	A-22
A11.	Simulations showing sensitivity of the south part water-surface altitude to the maximum positive and negative errors from all sources of inflow and outflow, Great Salt Lake, Utah....	A-22
B1.	Map showing sites where chemical samples have been collected from Great Salt Lake by the Utah Geological Survey. ....	B-2
B2.	Diagram of a load calculation for a hypothetical lake divided into 10-foot-thick layers with two sampling sites .....	B-3
B3-B5.	Graphs showing:	
B3.	Approximate dissolved-solids concentration gradients for south part of Great Salt Lake, Utah, on selected dates, 1967–98. ....	B-5
B4.	Approximate dissolved-solids concentration gradients for north part of Great Salt Lake, Utah, on selected dates, 1980–98. ....	B-6

## FIGURES—Continued

### B3-B5. Graphs showing:—Continued

B5. Percentage of total south part volume contained in the Bear River and Farmington Bays, Great Salt Lake, Utah .....	B-7
C1. Diagram of model grid of the cross section of causeway fill across Great Salt Lake, Utah, showing intrinsic permeability values of cells .....	C-2
C2. Schematic diagram of flow through a cross section of the causeway fill; interfaces between new, old, and non-permeable fill; and the relation of the new and old fill interface to the south and north flows through the fill, Great Salt Lake, Utah .....	C-7
C3-C6. Graphs showing:	
C3. North-to-south flow through the causeway fill as computed from the fill-flow model and from the water and salt balance equations for Great Salt Lake, Utah .....	C-9
C4. Measured and estimated flows through the culverts and breach and model-computed flows through the causeway fill for Great Salt Lake, Utah. ....	C-10
C5. Values for each parameter of the north-to-south fill-flow equation on December 15, 1992, Great Salt Lake, Utah. ....	C-11
C6. Values for each parameter of the north-to-south fill-flow equation on December 15, 1987, Great Salt Lake, Utah .....	C-12
D1. Schematic cross section of the east culvert in the causeway across Great Salt Lake, Utah, showing bidirectional, stratified flow and related hydraulic properties.....	D-1
D2. Schematic cross sections showing flow regimes modeled for unsubmerged culverts in Great Salt Lake, Utah.....	D-2
D3. Flow chart of subroutine used to compute flow through submerged and unsubmerged culverts and the breach in the causeway across Great Salt Lake, Utah. ....	D-3
D4. Schematic cross sections showing flow regimes modeled for submerged culverts in the causeway across Great Salt Lake, Utah. ....	D-4
E1. Graph showing comparison of model-computed and measured south-to-north flow through the breach in the causeway across Great Salt Lake, Utah, 1987–98.....	E-4
E2. Graph showing comparison of model-computed and measured north-to-south flow through the breach in the causeway across Great Salt Lake, Utah, 1987–98.....	E-4

## TABLES

1.	Major modifications to the original model of Waddell and Bolke (1973). .....	18
2.	Simulated dissolved-solids concentration of the south part as a percentage of that of the north part for selected breach dimensions, Great Salt Lake, Utah, December 31, 1998.....	26
3.	Results of model simulations showing comparison of salinities in Great Salt Lake, Utah, with a 290-ft-wide rectangular breach of selected bottom altitudes .....	26
4.	Results of a model simulation showing comparison of salinities in Great Salt Lake, Utah, with and without the West Desert Pumping Project.....	28
A1.	Area and volume of Great Salt Lake, Utah, and of the Magnesium Corporation of America evaporation ponds. ....	A-3
A2.	South part water-surface altitude corrected to the datum used for the north part water-surface altitudes, Great Salt Lake, Utah .....	A-7
A3.	Streamflow-gaging stations used to estimate monthly surface-water inflow to Great Salt Lake, Utah, 1987–98.....	A-7
A4.	Statistical summary of regression estimates of monthly surface-water inflow to Great Salt Lake, Utah, 1987–98.....	A-8
A5.	Estimated monthly and annual inflow for all streams and canals to Great Salt Lake, Utah, 1987–98	A-9
A6.	Estimated monthly and annual surface-water inflow to Great Salt Lake, Utah, 1987–98 .....	A-12
A7.	Estimated ground-water inflow to Great Salt Lake, Utah, 1987–98 .....	A-12
A8.	Average annual precipitation and evaporation of freshwater for selected water-surface altitudes of Great Salt Lake, Utah, 1987–98.....	A-14
A9.	Pan evaporation and percentage of mean pan evaporation (1931–73) for five sites near Great Salt Lake, Utah, June through September 1987–98 .....	A-15
C1.	South-to-north flow through the causeway fill as computed by the fill-flow model, Great Salt Lake, Utah. ....	C-3
C2.	North-to-south flow through the causeway fill as computed by the fill-flow model, Great Salt Lake, Utah. ....	C-4
C3.	Post-breach flow through the causeway fill as computed by the fill-flow model, Great Salt Lake, Utah. ....	C-5
C4.	Interpolation matrix for south-to-north flow through the causeway fill, Great Salt Lake, Utah. ....	C-6
C5.	Summary of intermediate and final interpolated south-to-north flow for selected boundary conditions, Great Salt Lake, Utah .....	C-6
D1.	Water-surface altitude and brine density in Great Salt Lake, Utah, and flow through the east and west culverts in the causeway across Great Salt Lake, Utah, 1986–98.....	D-6
E1.	Water-surface altitude, head difference, and brine density in Great Salt Lake and flow through the breach in the causeway across Great Salt Lake, Utah, 1987–98.....	E-2

## CONVERSION FACTORS, VERTICAL DATUM, AND ABBREVIATED WATER-QUALITY UNITS

Multiply	By	To obtain
acre	4,047	square meter
acre-foot (acre-ft)	1,233	cubic meter
acre-foot (acre-ft)	0.001233	cubic hectometer
acre-foot per day (acre-ft/d)	0.014276	cubic meter per second
cubic foot per second (ft <sup>3</sup> /s)	0.02832	cubic meter per second
foot (ft)	0.3048	meter
foot per second (ft/s)	0.3048	meter per second
inch (in.)	25.4	millimeter
mile (mi)	1.609	kilometer
square foot (ft <sup>2</sup> )	0.092903	square meter
square mile (mi <sup>2</sup> )	2.590	square kilometer
ton	0.9072	metric ton or megagram
tons per acre-foot (tons/acre-ft)	0.735467	grams per liter
tons per day (tons/d)	0.9072	metric tons or megagram per day

Degree Celsius (°C) may be converted to degree Fahrenheit (°F) by using the following equation:

$$^{\circ}\text{F} = 9/5(^{\circ}\text{C}) + 32.$$

Degree Fahrenheit (°F) may be converted to degree Celsius (°C) by using the following equation:

$$^{\circ}\text{C} = 5/9(^{\circ}\text{F} - 32).$$

**Sea level:** In this report, “sea level” refers to the National Geodetic Vertical Datum of 1929—a geodetic datum derived from a general adjustment of the first-order level nets of the United States and Canada, formerly called Sea Level Datum of 1929.

Chemical concentration is reported only in metric units. Chemical concentration is reported in grams per milliliter (g/mL) or grams per liter (g/L). Grams per liter is a unit expressing the weight of solute per unit volume (liter) of water.

# Water and Salt Balance of Great Salt Lake, Utah, and Simulation of Water and Salt Movement Through the Causeway, 1987–98

By Brian L. Loving<sup>1</sup>, Kidd M. Waddell<sup>1</sup>, and Craig W. Miller<sup>2</sup>

## ABSTRACT

The Southern Pacific Transportation Company completed a rock-fill causeway across Great Salt Lake in 1959. The effect of the causeway was to change the water and salt balance of Great Salt Lake by creating two separate but interconnected parts of the lake, with more than 95 percent of freshwater surface inflow entering the lake south of the causeway.

The water and salt balance of Great Salt Lake primarily depends on the amount of inflow from tributary streams and the conveyance properties of the causeway that divides the lake into south and north parts. The conveyance properties of the causeway consist of two 15-foot-wide culverts, a 290-foot-wide breach, and permeable rock-fill material.

The dissolved-solids concentrations of the north and south parts were approximately equal at the time the causeway was completed in 1959, but by 1972, the concentration was about 200 grams per liter greater in the north part than in the south, and by December 1998, the concentration was 250 grams per liter greater in the north than in the south. The theoretical concentration that would have occurred in an undivided lake in December 1998 was 190 grams per liter. In 1998 the concentration in the south part was about 90 grams per liter, or 100 grams per liter less than the theoretical concentration for an undivided lake. In 1998 the concentration in the north part was about 340 grams per liter, or 150 grams per liter more than the theoretical concentration for an undivided lake.

A water and salt balance model of Great Salt Lake, Utah, developed by the U.S. Geological Survey in 1973, was modified to incorporate the effects of changes in the conveyance properties of the causeway and withdrawals from the lake as part of the West Desert Pumping Project during 1987–89. Additional capability was added to the model to simulate (1) stratified flow through submerged culverts, and (2) loads and concentrations of chloride, magnesium, potassium, and sodium in the lake.

The calibrated model was used to simulate the effects of several combinations of breach depths and widths on the dissolved-solids concentration in each part of the lake. The simulations indicated that deepening the breach is more effective in reducing the difference in concentration between the two parts of the lake than widening without deepening the breach. In December 1998, the dissolved-solids concentration of the south part of the lake was 28 percent of the concentration in the north part. If the breach had been deepened from 4,200 feet to 4,195 feet in January 1987, the dissolved-solids concentration of the south part would have been 38 percent of that of the north part by December 1998. Deepening the breach to 4,190 feet in January 1987 would have increased the dissolved-solids concentration of the south part to 55 percent of that of the north part by December 1998. By comparison, widening the breach from 290 feet to 600 feet, without deepening it, would have increased the dissolved-solids concentration of the south part to 33 percent of that of the north part.

During 1987–92, about 500 million tons of salt, including 17.5 million tons of magnesium and 16 million tons of potassium, were removed from the lake as part of the West Desert Pumping

---

<sup>1</sup>Hydrologist, U.S. Geological Survey, Salt Lake City, Utah.

<sup>2</sup>PE, Engineer Specialist, Utah Department of Natural Resources, Water Resources Division, Salt Lake City, Utah.

Project. The pumps only operated during April 1987 to June 1989, but there was some return flow from West Pond to the lake during 1990–92. Model simulation indicated that had there been no West Desert Pumping Project, the dissolved-solids concentration in the north part would have been 3 grams per liter higher, and the concentration in the south part 9 grams per liter higher by December 1998.

## INTRODUCTION

According to Wold, Thomas, and Waddell (1997, p. 1), “Prior to construction of a railroad causeway during 1957–59, the hydrologic characteristics of Great Salt Lake, Utah, were typical of a closed lake having no outlet to the sea. After completion of the causeway (figs. 1 and 2) in 1959, the water and salt balance of the lake changed. The causeway divides the lake into a south and a north part (fig. 3), with slightly more than one-third of the surface area of the lake being north of the causeway. Because more than 95 percent of freshwater surface inflow enters the lake south of the causeway, the causeway has interrupted the circulation and caused substantial changes to the hydrology and chemistry of the lake.”

Previous modeling of the water and salt balance incorporated the causeway conveyance properties and hydrologic conditions that existed during 1959–86. Waddell and Bolke (1973) described the effects of the causeway on the water and salt balance of Great Salt Lake and developed a model to simulate the effects of the causeway on the salt balance for variable culvert widths and tributary inflows to the lake. This original model of Waddell and Bolke was calibrated for causeway conveyance and hydrologic conditions existing during 1969–72. This model was valid until about 1981. During the 1980s, fill material was frequently added to the causeway (figs. 2 and 3) to maintain the top of the causeway above the water surface. During 1983, the two 15-ft-wide culverts became submerged beneath the rising water surface and eventually filled with debris; in August 1984, a 290-ft-wide breach was opened near the western end of the causeway. Because these new conditions warranted revision of the model, Wold, Thomas, and Waddell (1997) modified the original model and recalibrated it for 1980–86.

Since 1986, additional changes in the causeway conveyance properties and withdrawals for the West Desert Pumping Project have made it necessary to

revise the model of Wold, Thomas, and Waddell (1997). In this report, the 1997 model was modified and recalibrated to incorporate the changes that occurred during 1987–98.

Many of the explanatory statements pertaining to historical trends and technical aspects of the water and salt balance model have been taken from the two prior reports of Waddell and Bolke (1973) and Wold, Thomas, and Waddell (1997).

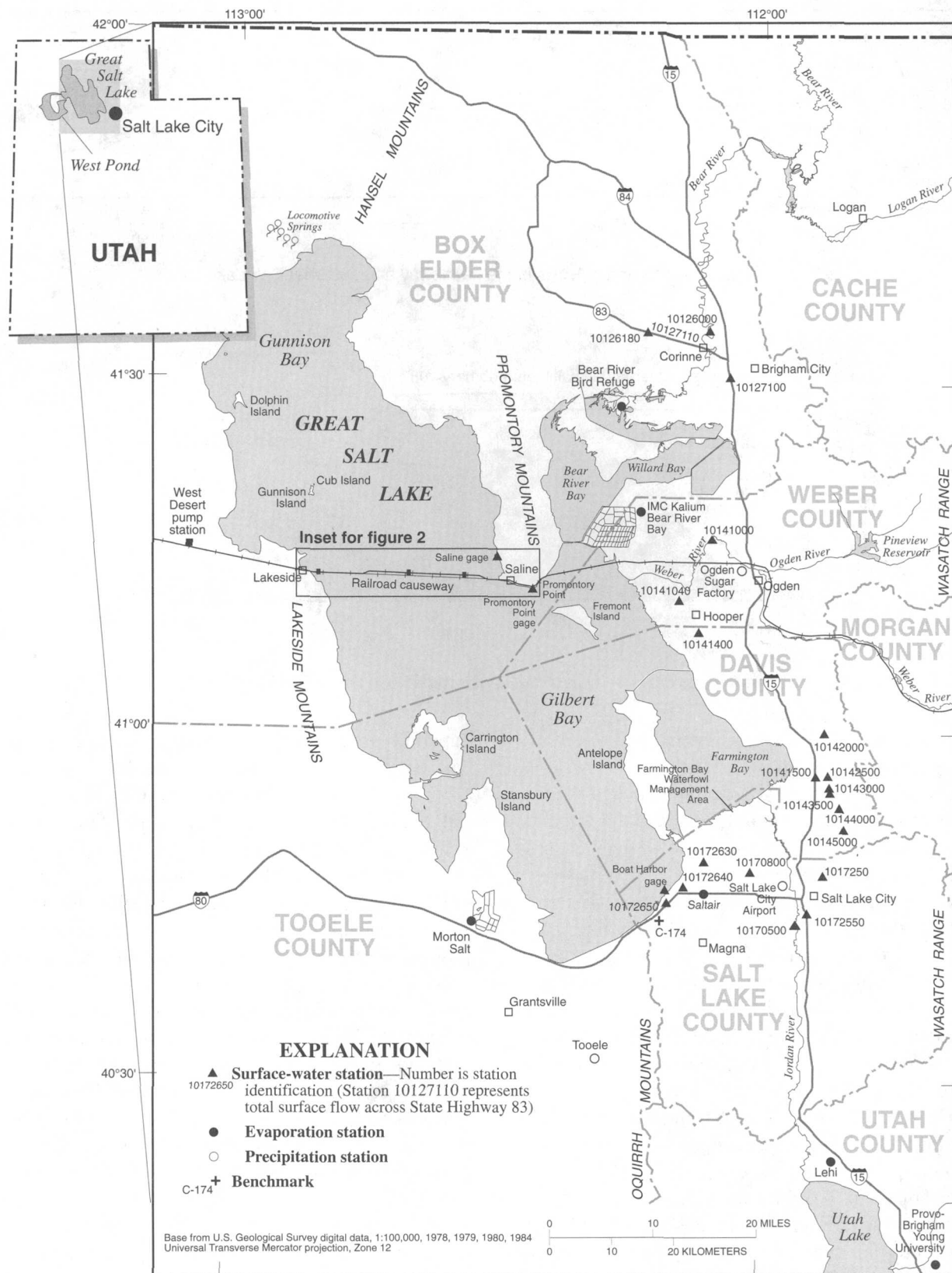
The study was done because continued freshening of the south part of the lake during the 1990s has caused concern about the ecology of the lake. The purpose of this study is to update earlier mathematical models of the lake that can be used to (1) understand the causes of historical changes in the water and salt balance and (2) to predict the effects of modifying the conveyance properties of the causeway on the water and salt balance of the lake.

## Description of the Study Area

Great Salt Lake is a closed lake located in semi-arid northwestern Utah in the Basin and Range Physiographic Province (Fenneman, 1931). The lake is bordered on the west by desert and on the east by the Wasatch Range. Great Salt Lake is a remnant of freshwater Lake Bonneville, which existed about 10 to 15 thousand years ago. Lake Bonneville covered much of western Utah and small parts of Idaho and Nevada, and was about 1,000 ft deep at the deepest part. In 1963, when Great Salt Lake was at its lowest water-surface altitude in recent history at about 4,191 ft, it covered about 950 mi<sup>2</sup> and had a maximum depth of about 25 ft. In 1986, when Great Salt Lake was at its highest water-surface altitude in recent history at about 4,212 ft, it covered about 2,400 mi<sup>2</sup> and had a maximum depth of about 45 ft.

## Purpose and Scope

This report presents the results of a study that was done to update the model developed by Waddell and Bolke (1973), which was later modified by Wold, Thomas, and Waddell (1997). The report contains the results of the study, and the appendixes describe the major components of the model in detail. Included are a description of the calibration of the model, results of simulations for different breach dimensions, and the effect of the West Desert Pumping Project on the water and salt balance of the lake. The code of the program



**Figure 1.** Location of study area and data-collection sites used to estimate inflow, water-surface altitude, and evaporation for Great Salt Lake, Utah, 1987–98. (Modified from Wold, Thomas, and Waddell (1997, fig. 1)).

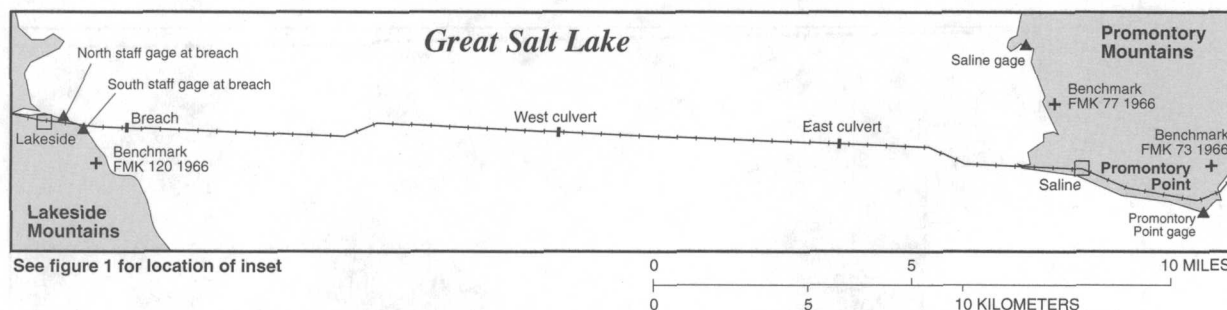


Figure 2. Location of breach and culverts in the causeway across Great Salt Lake, Utah.

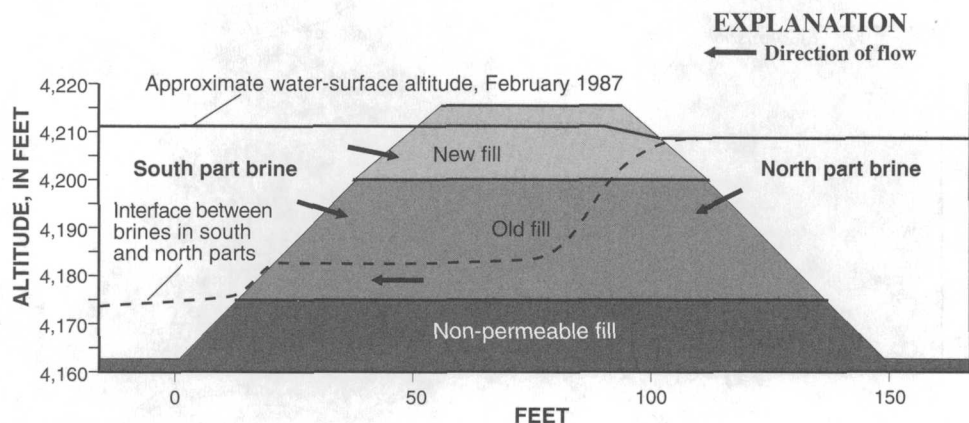


Figure 3. Diagrammatic cross section of the causeway across Great Salt Lake, Utah.

developed for the model is included in appendix G on the compact disc at the end of the report.

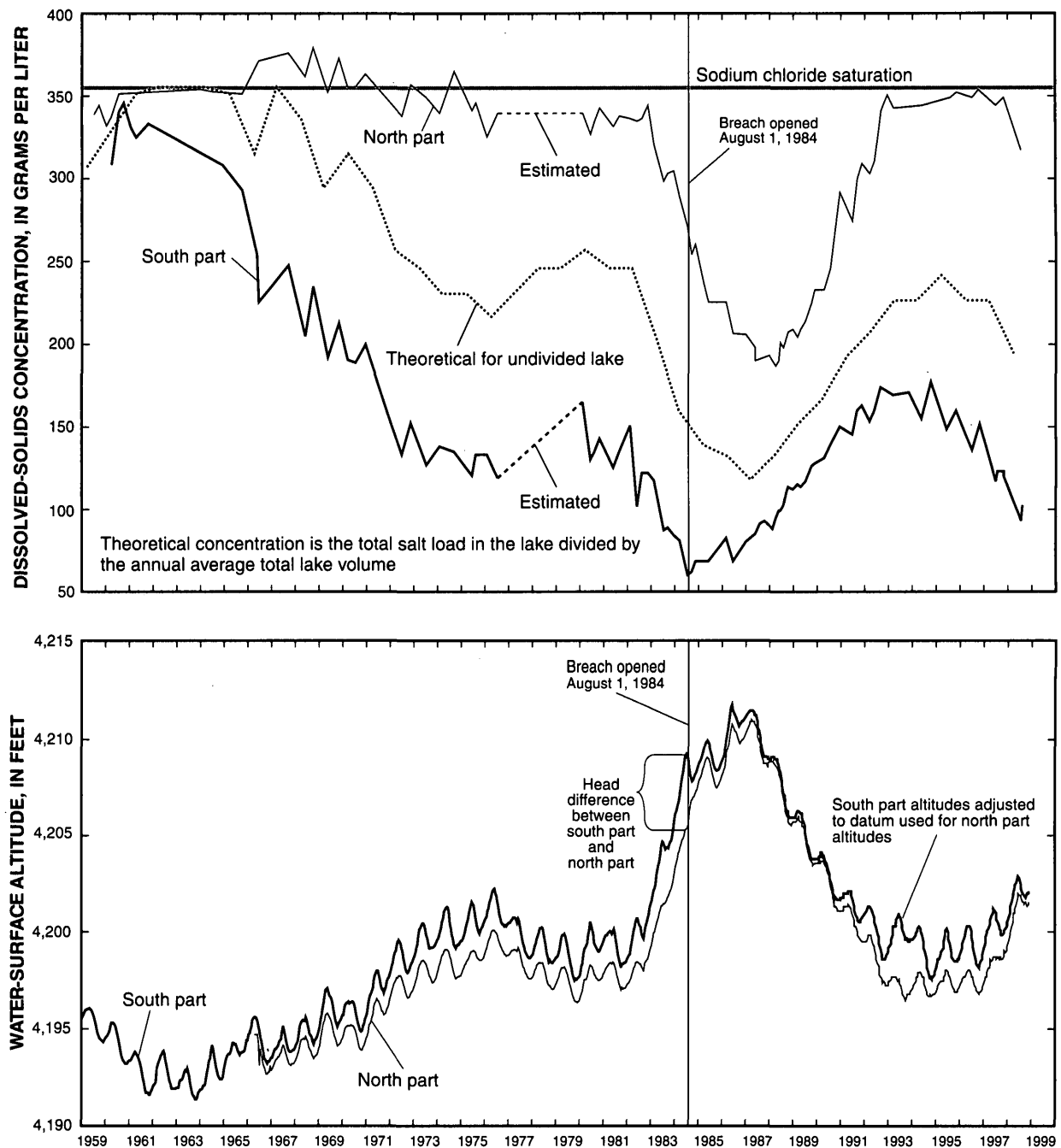
During the study of Waddell and Bolke (1973), the altitude of the culvert bottoms were about 4,180 ft for the east culvert and about 4,183 ft for the west culvert. The altitudes of the ceilings of the culverts were not documented, but are believed to have been near 4,203 ft for the east culvert, and 4,206 ft for the west culvert. As a result of settling, by 1998 the altitude of the culvert ceilings had subsided to about 4,195 ft for the east culvert and about 4,198 ft for the west culvert. Since about 1983, the settling in combination with higher lake levels (fig. 4) has caused the culverts to be submerged.

The model of Wold, Thomas, and Waddell (1997) was modified to incorporate changes to the hydraulic conveyance properties of the causeway that have occurred since 1986, and for the effects of the withdrawals from the lake as part of the West Desert Pumping Project during 1987–89. The major changes to the hydraulic conveyance properties include provision for flow through submerged culverts and reduced flow through the causeway fill. To check the calibration, the

capability to compute the concentration and load of four major ions was added to the model.

For this study, the equations of Holley and Waddell (1976) were modified to account for flow through submerged culverts (E.R. Holley, University of Texas, written commun., 1998; see appendix D). Submerged culvert flows were measured during 1996–98; but because the culvert openings were partially or fully plugged with debris, the cross-sectional areas of the culverts could not be defined, and measurements could not be used to verify the theoretical equations for flow through the submerged culverts. Flows computed with these equations for non-submerged culverts were evaluated by comparing them with measured flows through non-submerged culverts and the breach. Non-submerged, relatively open culvert flows were measured prior to about 1983 (Wold, Thomas, and Waddell, 1997). Also, during 1987–94 and 1996–98, measurements of non-submerged flow through the breach were made and used to verify the theoretical equations.

The causeway-fill flow was computed with the procedures presented by Wold, Thomas, and Waddell (1997, p. 38), but the flow through the deeper, older fill was reduced by a constant factor (see section “Water



**Figure 4.** Dissolved-solids concentration of the south part, north part, and theoretically undivided lake, and water-surface altitude of the south and north parts of Great Salt Lake, Utah, 1959–98.

and Salt Balance Model and causeway-fill flow”). Wold, Thomas, and Waddell (1997, p. 4) used the two-constituent solute-transport model of Sanford and Konikow (1985) to simulate flows through the fill (referred to in this report as the fill-flow model). No additional field data were collected during this study to directly evaluate the hydraulic properties of the fill. The seepage computed by the fill-flow model was indirectly evaluated and revised by comparing the water and salt balance computed by the model with independent computations of the water and salt balance from measured data.

Freshwater surface inflow, precipitation on the lake surface, and evaporation data were compiled for Great Salt Lake for monthly intervals during 1987–98 and used as input to the model. The water and salt balances were computed from monitoring data collected during 1987–98. Dissolved salt load was computed for the south and north parts of Great Salt Lake and used to evaluate the model for the calibration period, 1987–98.

## Acknowledgments

Special acknowledgment is extended to Lloyd H. Austin and Norman E. Stauffer, Jr., Utah Department of Natural Resources, Division of Water Resources; J. Wallace Gwynn, Utah Department of Natural Resources, Utah Geological Survey; and Karl Kappe, Utah Department of Natural Resources, Division of Forestry, Fire, and State Lands for their aid in the planning of this study and for providing interim technical reviews of the study as it progressed. Special appreciation is given to Edward R. Holley, University of Texas at Austin, for derivation of equations for bidirectional flow through submerged culverts.

## WATER AND SALT BALANCE OF GREAT SALT LAKE

Prior to completion of the causeway in 1959, the hydrologic characteristics of Great Salt Lake were typical of a closed lake having no outlet to the sea. The water-surface altitude rose and fell in response to the balance between evaporation from the surface and inflow to the lake from runoff, ground-water inflow, and precipitation on the surface. During periods when the water-surface altitude fell, surface area and volume decreased and dissolved-solids concentration increased. During periods when the water-surface altitude rose, surface area and volume increased and dissolved-solids concentration decreased. The lake was

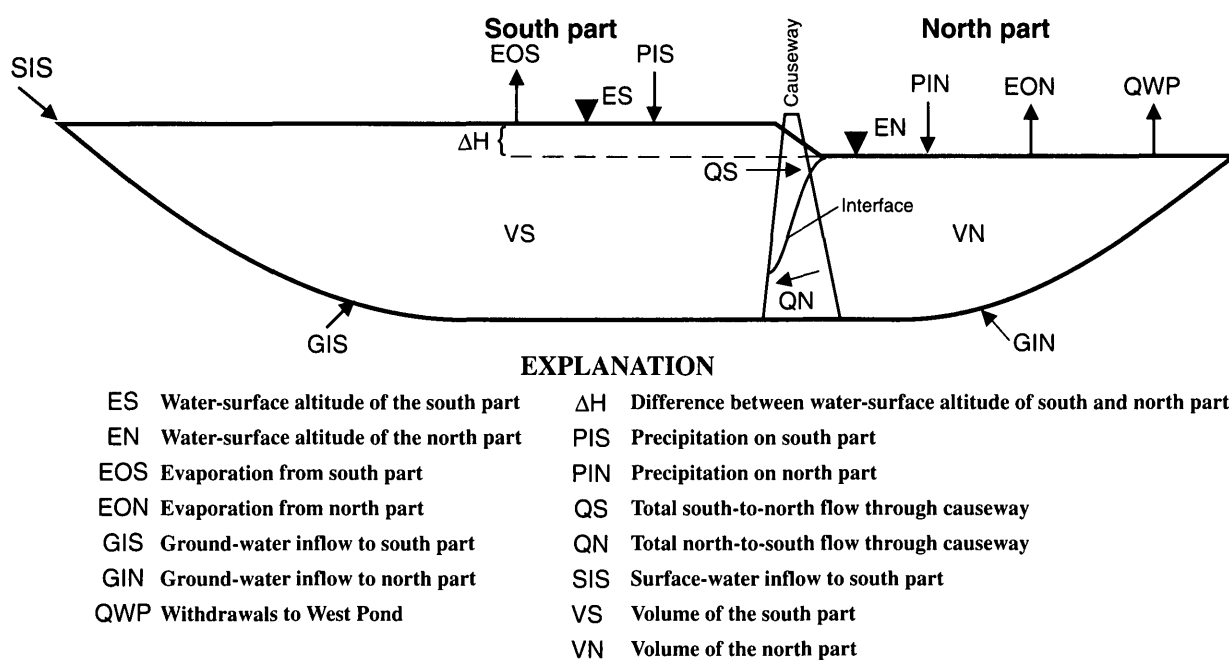
thought to be well mixed and to have no stratification, and salt precipitation was thought to occur throughout the entire lake when the lake volume was small enough for the salt concentration to exceed the saturation level for sodium chloride.

## Effects of Causeway Construction

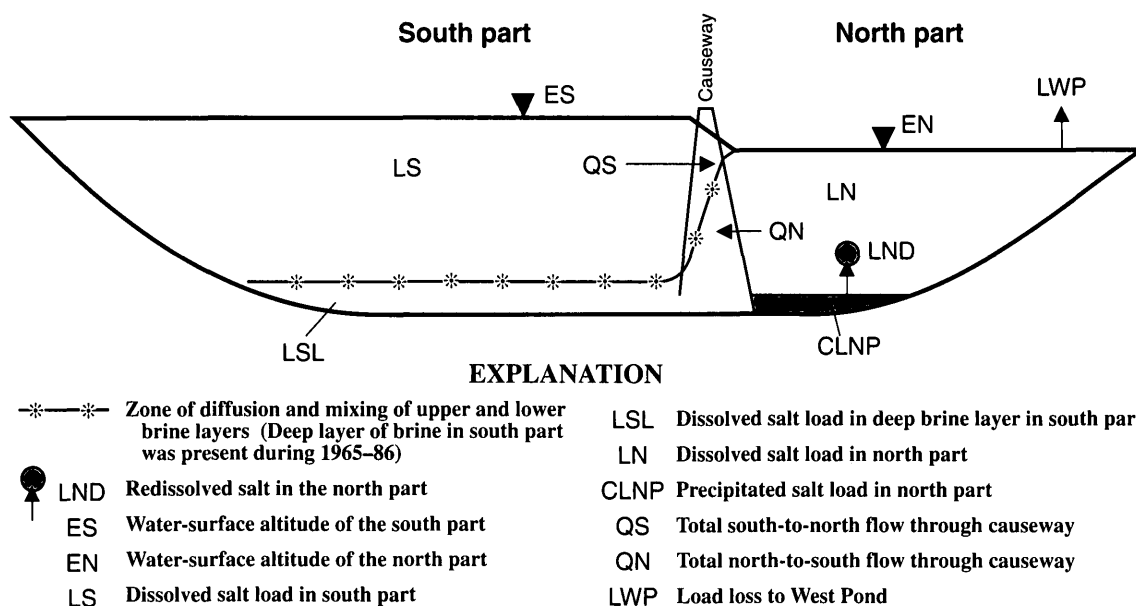
During 1959–84, the railroad causeway conveyance properties consisted of two 15-ft-wide by 23-ft-high culverts (see appendix D) and the hydraulic properties of the causeway rock-fill material. The effect of the causeway construction was to change the water and salt balance of Great Salt Lake by creating two separate but interconnected parts of the lake with different water-surface altitudes and dissolved-solids concentrations. A 290-ft-wide breach was added in 1984, to provide for additional circulation when the altitude of the south part was above 4,200 ft.

Because almost all surface-water inflow is to the south part (fig. 1), the water in the south part is less saline than the water in the north part (fig. 4), and the water-surface altitude of the south part (*ES*, fig. 5) is higher than that of the north part (*EN*). The differences between the water-surface altitudes and densities of the south and north parts provides the potential for brine to flow in both directions through the causeway conveyances (*QS* and *QN*, figs. 5 and 6). In general, the less dense brine from the south part flows northward through the upper part of the causeway conveyances (culverts, breach, and causeway fill) and the more dense brine from the north part flows southward through the lower part of the causeway conveyances.

Restricted circulation in the lake is indicated by a theoretical water and salt balance for an undivided lake, as well as historical trends in the dissolved salt loads for the north and south parts. The theoretical dissolved-solids concentration for an undivided Great Salt Lake was computed to compare with concentrations that actually occurred in the north and south parts of the lake during 1959–98 (fig. 4). The dissolved-solids concentrations of the north and south parts were approximately equal at the time the causeway was completed in 1959, but began diverging by 1961 (fig. 4). In 1972, the concentration was about 200 g/L greater in the north than in the south part, and by 1998 the concentration was 250 g/L greater in the north than in the south. The theoretical concentration that would have occurred in an undivided lake in December 1998 was 190 g/L. In 1998, the concentration in the south part was about 90 g/L, or 100 g/L less than the theoretical concentration for an undivided



**Figure 5.** Schematic diagram of water balance for Great Salt Lake, Utah.



**Figure 6.** Schematic diagram of salt balance for Great Salt Lake, Utah.

lake. In 1998, the concentration in the north was about 340 g/L, or 150 g/L greater than the theoretical for an undivided lake.

## Dissolved Salt Loads

The dissolved solids in the freshwater inflow to Great Salt Lake contributes a relatively insignificant part of the total salt load contained in the lake; thus, the total salt load can be assumed to be constant for a large number of years. Hahl (1968, p. 20) determined the salt load contributed from freshwater inflow to be less than 0.0035 billion ton per year. During a 100-year period, surface-water inflow would add about 0.35 billion ton of salt to the lake, which is 8 percent of the current total load of 4.5 billion tons. The addition of dissolved salt from inflow to Great Salt Lake is roughly equal to the amount of salt mined from the lake (J. W. Gwynn, Utah Geological Survey, oral commun., 2000). The chemical composition of the inflowing dissolved salt, however, is probably different than that extracted for mining.

Total salt loads were determined during periods when salinity was well below saturation with respect to sodium chloride. During those periods, it can be assumed that essentially all of the salt is dissolved and that the load of salt can be computed as the product of the volume and concentration. During 1985–86, when the water-surface altitude was near historic highs and the salinity was below saturation with respect to sodium chloride in both parts, the total salt load was estimated to be 5.0 billion tons. A prior study by Wold, Thomas, and Waddell (1997, p. 7) estimated the total salt load to be 4.9 billion tons on the basis of salinities measured in 1976. For purposes of water and salt balance computation in this study, 5.0 billion tons of total salt load was used. About 0.5 billion ton of dissolved salt was pumped to the West Desert during 1987–89, thereby reducing the total load of salt in Great Salt Lake to about 4.5 billion tons (see section on “Effects of the West Desert Pumping Project on loads of ions”).

## Theoretical Equations of Water and Salt Balance for the Divided Lake

A general relation between the water and salt balance of the north and south parts was derived in terms of the total flows north-to-south ( $QN$ ) and south-to-north ( $QS$ ) through the causeway. The change in the dissolved-solids load for the north part (fig. 6) can be expressed as:

$$QS \cdot CS - QN \cdot CN = \Delta LN + \Delta CLNP + LWP \quad (1)$$

where

- $CS$  = dissolved-solids concentration of the south part;
- $CN$  = dissolved-solids concentration of the north part;
- $QS$  = fill flow + culvert flow + breach flow (all from the south to north part);
- $QN$  = fill flow + culvert flow + breach flow (all from the north to south part);
- $\Delta LN$  = change in the dissolved-solids load of the north part;
- $\Delta CLNP$  = change in the precipitated salt load of the north part due to precipitation (+) or re-solution (-); and
- $LWP$  = load of salt pumped from (+), or returned to (-) the north part of Great Salt Lake as part of the West Desert Pumping Project.

Solving equation 1 for  $QS$ :

$$QS = \frac{1}{CS} [\Delta LN + \Delta CLNP + LWP] + QN \cdot \frac{CN}{CS} \quad (2)$$

From figure 5, the water balance for the north part is:

$$\Delta VN = PIN + GIN - EON + QS - QN - QWP \quad (3)$$

where

- $PIN$  = precipitation on the north part;
- $GIN$  = ground-water inflow to the north part;
- $\Delta VN$  = change in volume in north part;
- $EON$  = evaporation from the north part;
- $QWP$  = volume of water pumped from (+) or returned to (-) north part of Great Salt Lake as part of the West Desert Pumping Project.

Solving equation 3 for  $QS$ :

$$QS = \Delta VN - PIN - GIN + EON + QN + QWP \quad (4)$$

Equating equations 2 and 4 and solving for  $QN$ :

$$QN = \frac{CS}{CN - CS} [\Delta VN - PIN - GIN + EON + QWP - \frac{\Delta LN}{CS} - \frac{\Delta CLNP}{CS} - \frac{LWP}{CS}] \quad (5)$$

Most of the variables in equation 5 are dynamically related; when the value of one variable changes, the values of the other variables change. The exceptions to this are ground-water inflow to the north part ( $GIN$ ), outflow of water ( $QWP$ ) and salt load ( $LWP$ ) to West

Pond as part of the West Desert Pumping Project (see section titled “Effects of the West Desert Pumping Project on loads of ions”), and the conveyance properties of the causeway (dimensions of culverts and breach, and hydraulic properties of the fill). South-to-north flow,  $Q_S$ , and north-to-south flow,  $Q_N$ , are largely dependent on the specific hydraulic characteristics of the fill, culverts, and breach and are discussed in appendices C, D, and E, respectively.

The balance of salt between the north and south parts can be changed either by redistribution of some of the freshwater surface inflow to the south part ( $SIS$ , fig. 5) into the north part or by changing the conveyance properties of the causeway. For example, diversion of some of the flow of the Bear River into the north part would change the balance of salt between the north and south parts. However, modification of causeway conveyance properties was considered as the only practical means of changing the salt balance for a specified net freshwater inflow. A water and salt balance computer model was used to facilitate the calculations needed to evaluate the effects of changing the conveyance properties on the water and salt balance of the lake.

## Trend of Dissolved and Precipitated Salt Loads in North and South Parts, 1963–98

The trend of total dissolved salt load (fig. 7) can be used as an indication of salt precipitation (CLNP, fig. 6) or re-solution ( $LND$ ). Because the total amount of salt available in the lake can be assumed to be constant for a large number of years, an increase in total dissolved salt load represents re-solution of salt, and a decrease in total dissolved salt load represents precipitation of salt. The only exception to this occurred as a result of the West Desert Pumping Project during 1987–92, when there was a 0.5 billion ton net loss of dissolved salt from the lake as a result of pumpage and return flow.

In 1963, shortly after completion of the causeway, the water surface declined to its lowest recorded altitude (4,191.35 ft) and volume. At this low volume, the south and north parts of the lake were saturated with respect to sodium chloride, and a salt crust formed on the lake bed south and north of the causeway (Madison, 1970, p. 12). The total dissolved salt load during 1963 was about 4.1 billion tons, and the precipitated salt load was about 0.9 billion tons.

During 1964–71, the water-surface altitude of the lake generally rose (fig. 4) and the dissolved-solids

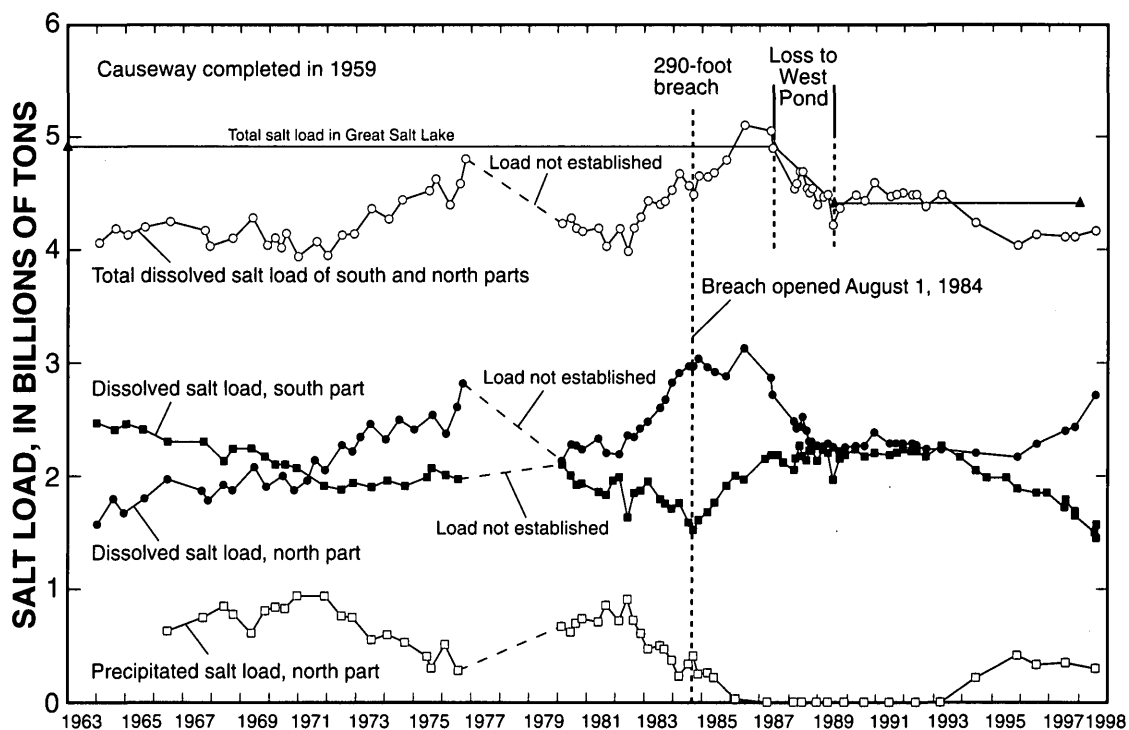


Figure 7. Dissolved and precipitated salt load in Great Salt Lake, Utah, 1963–98.

concentration in the south part decreased because of increased surface-water inflow (and associated increase of lake volume) and the net movement of the dissolved salt load to the north part (fig. 7). The load loss from the south part ceased during 1972 and was nil during 1972–80, which indicates that the balance of dissolved salt loads between the south and north parts was near equilibrium for the inflow conditions and causeway conveyance properties existing during that period. The dissolved salt load in the north part increased during 1972–76 because of re-solution of the salt crust in the north part as the water-surface altitude rose and the volume of the lake increased. Most of the salt that precipitated throughout the entire lake during 1959–63 probably dissolved from the south part by 1972, but the precipitated salt in the north part could not re-dissolve because the brine in the north part was at or near saturation.

During 1980–86, average annual inflow was about 240 percent greater than the long-term average for 1931–76 (Wold, Thomas, and Waddell, 1997, p. 8). This record inflow caused the water-surface altitude of the south part to rise about 14 ft, reaching an historic high of about 4,212 ft on June 3, 1986 (fig. 4). To keep up with the rising water surface, the causeway fill was raised and widened during this period, changing the hydraulic characteristics of the fill and affecting the salt balance of the lake (see appendix C). The record inflows from January 1980 to July 1984 caused about 0.5 billion tons of dissolved salt to move from the south to the north part (fig. 7). The dissolved salt load of the north part was also increased as a result of the re-solution of precipitated salt. The precipitated salt was dissolved because the increase in the lake volume caused the dissolved-solids concentration in the north part to decrease below saturation.

In August 1984, to combat the rising level of Great Salt Lake, the State of Utah completed construction of a 290-ft opening (breach) on the western edge of the causeway (fig. 2). The breach, which increased causeway conveyance for water-surface altitudes above 4,200 ft, was designed to reduce the head differential that had developed between the north and south parts (fig. 4). The effect of the breach was to increase south-to-north flow by about 50 percent and more than double north-to-south flow when compared with average flow through the causeway from January 1980 to July 1984 (Wold, Thomas, and Waddell, 1997, p. 8).

Because of the increased flow through the causeway, the head difference between the south and north parts decreased from an average of about 3.5 ft prior to

the breach opening, to a range of about 0.5 to 1.0 ft within 3 months after the breach was opened (fig. 4). Associated with this rapid decrease in head difference was an increase in the altitude at which the pressure gradient was conducive to north-to-south flow through both the fill ( $QNF$ ) and the breach ( $QNB$ ). The increased flow in both directions through the causeway generally caused the dissolved salt load to increase in the south and decrease in the north (fig. 7). From August 1, 1984, when the breach was opened, to May 1989, a net dissolved salt load of about 0.5 billion ton moved from the north to south part.

During 1987–94, the water-surface altitude of the lake generally decreased because annual evaporation was greater than inflow (fig. 4, and appendix A, fig. A2). As water-surface altitude decreased, flow through the causeway generally decreased because of less depth of flow above the breach bottom and within the permeable part of the causeway fill (above 4,175 ft) (fig. 8). By 1992, the water-surface altitude of both parts was near the altitude of the bottom of the breach (4,200 ft); consequently, there was almost no breach or culvert flow, and north-to-south fill flow was less than 25 percent of what it was in early 1987 (fig. 8).

#### Effect of Causeway Conveyance Properties, 1987–98

For a specified inflow to the lake, increases in the dimensions of the culverts and breach and increases in the permeability of the fill material will result in increased flow through the causeway ( $QS$  and  $QN$ ) and a decrease in the difference between the dissolved-solids concentration of north and south parts ( $CS$  and  $CN$ ). To illustrate the effects of the conveyance properties on net load gain or loss, equation 5 was simplified for the conditions of no West Pond pumping ( $QWP$  and  $LWP = 0$ ) and a constant inflow of freshwater:

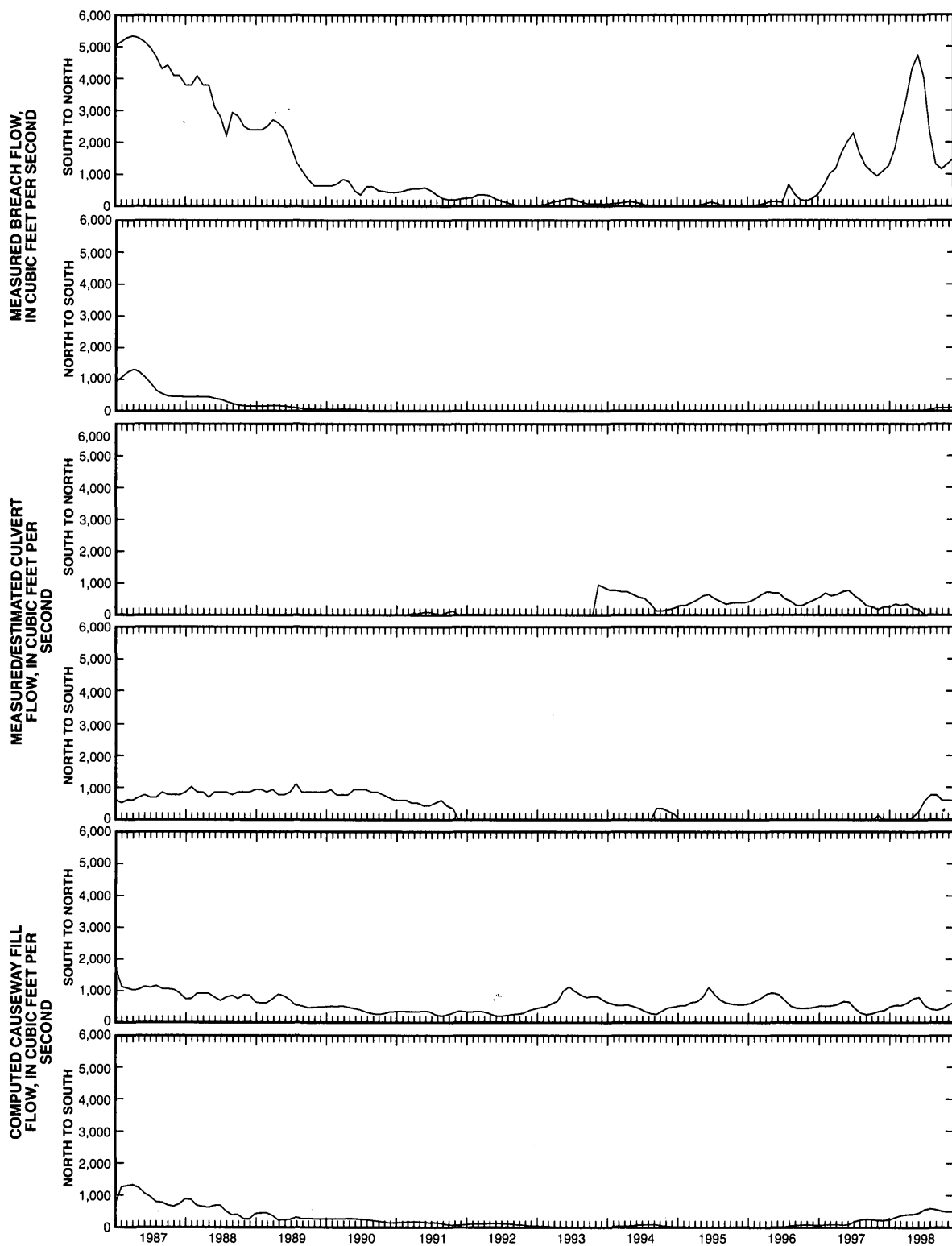
$$QS \cdot CS = QN \cdot CN$$

or

$$QS/QN = CN/CS. \quad (6)$$

If  $CS = CN$  then  $QS = QN$ . This is the condition that would exist with no causeway, assuming complete mixing between the north and south parts.

If  $QS > QN$ , which generally has occurred since the causeway was constructed, then  $CS < CN$ . For example, if the ratio of  $QS$  to  $QN$  were 2.0 for a constant freshwater inflow, then the ratio of  $CN$  to  $CS$  would eventually approach 2.0. Therefore if the concentration of the north part ( $CN$ ) were constant at 350 g/L, the



**Figure 8.** Flow through breach, culverts, and fill of causeway across Great Salt Lake, Utah, 1987–98.

[Flow in cubic feet per second. Fill: Flow computed using model; Culvert: Flow compiled from flow measurements made by U.S. Geological Survey (ReMillard and others, 1986, and Herbert and others, 1997, 1998, 1999), No culvert flow is inferred from January 1, 1992, through November 30, 1993, as a result of debris plugging the culverts; Breach: Flow compiled from measurements made by U.S. Geological Survey (ReMillard and others, 1987, 1988, 1989, 1990, 1991, 1992, 1993 and Herbert and others, 1997, 1998, 1999)]

concentration of the south part ( $CS$ ) would approach about 175 g/L.

The general trends of salt loads and how they are related to the conveyance properties of the causeway and the water-surface altitude of the lake (inflow) can be explained with equation 6. The water-surface altitude of the south part ranged from about 4,212 ft in 1987 to about 4,202 ft in 1990. During much of this period, the causeway conveyance properties were increased as a result of the water-surface altitude being several feet above the bottom (4,200 ft) of the 290-ft-wide breach. The causeway fill was also raised and widened, which changed the hydraulic properties for flow through the fill (see appendix C). The flow through the breach allowed the south-to-north head difference to decrease from an average of about 3.5 ft in 1984 to less than 1.0 ft within 3 months after the opening of the breach.

When bidirectional flow exists there is an interface between the flows. The interface between these flows is not a sharp boundary but a diffused zone that can vary in thickness depending on the densities, velocities, and medium, or opening through which it is flowing (figs. 3, and D1 in appendix D). The zone of diffusion, or interface between the north and south brines near the middle of the causeway fill ranges from about 2 to 5 ft in thickness, and in the breach ranges from about 1 to 3 ft in thickness.

For the purpose of explaining the interfacial depth and its relation to bidirectional flow, assume that the causeway is replaced by an impermeable wall separating the south and north parts. Under this condition there would be no flow and pressures on either side of the wall would be hydrostatic. Because of the higher elevation of the south part, the hydrostatic pressure gradient on the upper part of the wall is from south to north. Because the brine in the north part has a higher density than that of the south part, it is possible for conditions to occur where there is a depth below which the pressure gradient from north to south would be equal to the pressure from south to north. Above this depth of equal pressure, conditions would be conducive to south-to-north flow, and below this depth would be conditions conducive to north-to-south flow.

In the causeway, however, flow is occurring and static conditions do not exist. The interfacial depth slopes from near the water surface on the north edge of the causeway, to a greater depth where the north-to-south flow exits the causeway into the south part (figs. 3, and D1 in appendix D). With equation 7, the altitude of the interface can be approximated by the Ghyben-

Hertzberg principle (Badon-Ghyben, 1888; and Herzberg, 1901) (see appendix C). The altitude computed with equation 7 approximates the upper surface of the north-to-south flow near where it exits on the south edge of the fill or breach.

$$\text{Altitude of Interface} = ES - \Delta H \cdot \rho_n / (\rho_n - \rho_s) \quad (7)$$

where:

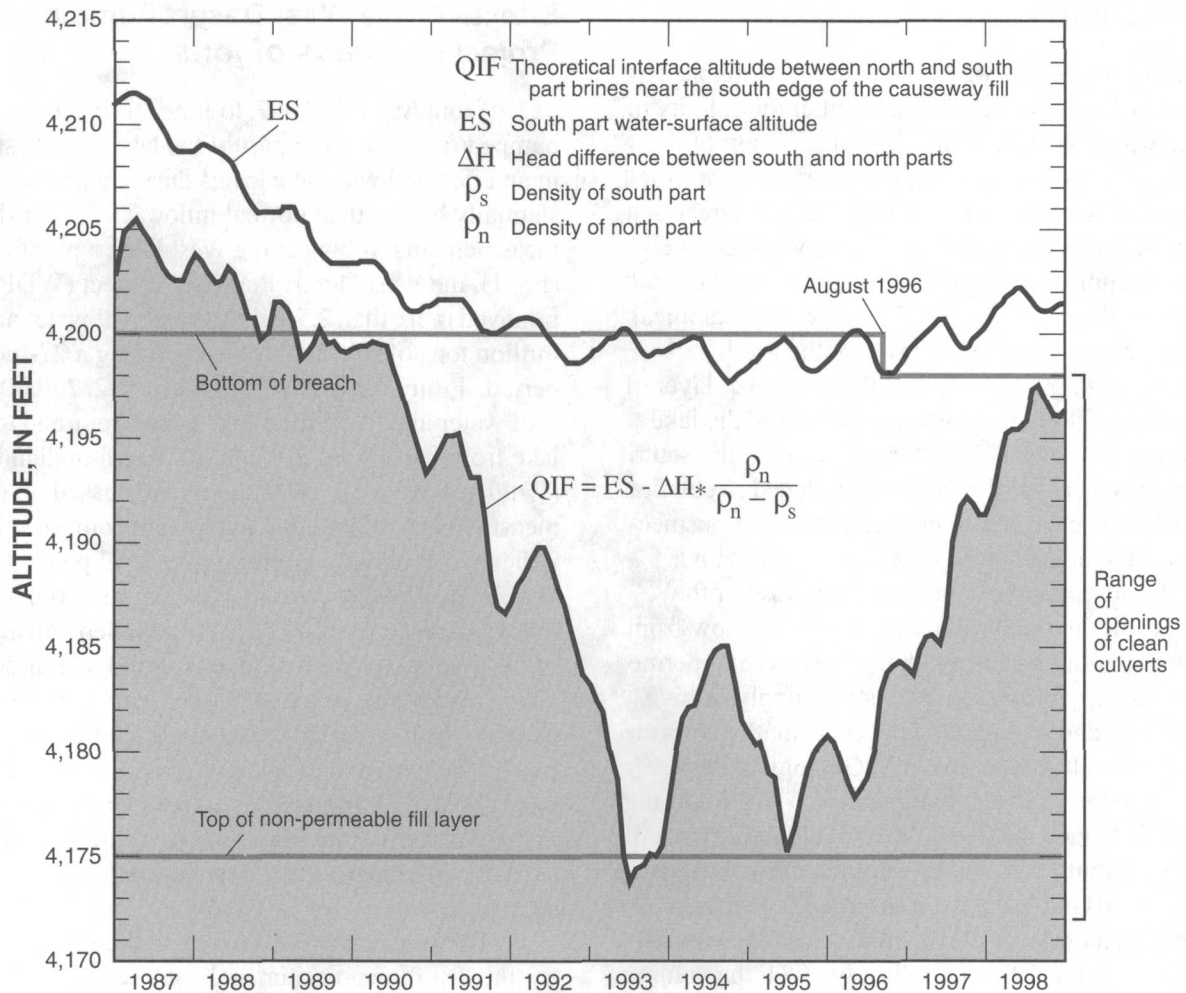
- $ES$  = water-surface altitude of the south part, in ft;
- $\Delta H$  = difference between the water-surface altitudes of the south and north parts, in ft;
- $\rho_s$  = density of the south part in g/mL; and
- $\rho_n$  = density of the north part in g/mL.

The head difference remained at about 1.0 ft or less until 1991, and as a result, the altitude below which the pressure gradient was conducive to north-to-south flow ( $QN$ ) through the culverts, breach, and fill was above 4,200 ft during most of 1987–90 (fig. 9).

The interface altitude ranged from about 4,205 ft in 1987 to about 4,176 ft in 1993. The altitude of the top of the no-flow zone for the causeway fill was determined to be about 4,175 ft (see appendix C). Thus, for an interface altitude near 4,205 ft there is about 30 ft of cross-sectional depth through which north-to-south flow can occur through the fill, and for an interface altitude of 4,176 ft there is only 1 ft of cross-sectional depth through which north-to-south flow can occur. Also, the higher the interface, the more the potential exists for north-to-south flow to occur through the culverts, if open.

Although  $\Delta H$ ,  $\rho_s$ , and  $\rho_n$  are interdependent,  $\Delta H$  responds much faster to change in the conveyance properties than does  $\rho_s$ , and  $\rho_n$ . The south-to-north flow through the breach occurs in an open channel with a free surface and therefore maintains a low head difference ( $\Delta H$ ) when the altitude of the water surface in the south part is above the bottom of the breach. Eventually, with mixing in the north and south parts, the salinities and densities,  $\rho_s$  and  $\rho_n$ , reach a new equilibrium with  $\Delta H$ , depending on the conveyance properties and amount of inflow. Generally, the ratio of  $QS$  to  $QN$  will decrease with decreasing  $\Delta H$  and increase with increasing  $\Delta H$ . A decrease in the ratio of  $QS$  to  $QN$  is favorable to more net movement of salts to the south part, and an increase in the ratio is favorable to more net movement to the north part.

During 1987–90, the ratios of  $QS$  to  $QN$  ranged from about 1.97 to 1.45, compared to the ratio of  $CN$  to



**Figure 9.** Altitude of water surface in the south part and theoretical interface between north and south part brines in the causeway across Great Salt Lake, Utah.

*CS* of about 2.1 to 1.8, which caused considerable net transfer of dissolved salts back to the south part. In 1992, the water-surface altitude of the south part dropped below 4,200 ft and remained so during most of 1992–96. During this time, there was little breach flow (fig. 8) and the head difference began increasing, peaking at about 3.5 ft in 1993. Associated with the increase of head difference was a rapid decline in the altitude at which the pressure gradient was conducive to north-to-south flows (fig. 9), and by 1993 the depth had plunged to about 4,176 feet, at which time the ratio of *QS* to *QN* peaked at 65.

The water-surface altitude of the south part began increasing in about 1997 and the ratio of *QS* to *QN* had decreased to about 4 by 1998. The ratios of *QS* to *QN*

were much greater than the ratio of *CS* to *CN* during much of 1991–98 and resulted in considerable net movement of dissolved solids to the north part through 1998. The net loss of dissolved load from the south part during 1991–98 occurred primarily because of the decreased conveyance created by the water-surface altitude being near or below the bottom of the breach and the interface being so deep into the fill for much of the period.

By 1998, the water-surface altitude of the south part increased to about 4.5 ft above the bottom of the breach. South-to-north breach flows increased, the head difference dropped below 1.0 ft, and altitude of the pressure gradient conducive to north-to-south flow rose to about 4,197 ft.

## Stratification

Before the causeway was built, the available data were not adequate to determine whether the salinity of the lake was stratified. Since the construction of the causeway, the lake has at times been vertically stratified (appendix B, section titled "Stratification in Great Salt Lake"). A lower layer of denser brine with relatively constant volume was first observed in 1965 in the south part of the lake (*LSL*, fig. 6). This layer had chemical characteristics similar to the brine in the north part. Madison (1970, p. 12) observed that the lower layer of brine in the south part occurred everywhere the lake bottom was below 4,175 ft. Stratification in the south part occurred because the causeway reduced circulation in the lake. The causeway created the conditions necessary for the north part to achieve and maintain a higher density than the south part. Because of the higher density in the north part, brine could flow from the north to south part through the culverts and permeable fill, thereby providing a constant supply of high-density brine and maintaining the deep south part brine layer. Data collected by the U.S. Geological Survey (USGS) and the Utah Geological Survey (UGS) during 1973–74 indicated that the volume of the lower layer of brine in the south part and the altitude of the interface with the overlying brine were essentially unchanged, even though the water-surface altitude had increased by several feet. From 1972 through July 1984, the volume of the deep layer of brine in the south part and the altitude of the interface with the overlying brine increased, and the interface in the south part became more diffused.

During 1984, when the breach was opened, increased causeway conveyance combined with record surface-water inflow produced a large amount of flow through the causeway in both the north and south directions. There was little or no stratification in the north part prior to 1984, but during 1984 both parts became stratified. Stratification decreased during 1988–91 but persisted in both parts through 1991. As surface-water inflow and causeway conveyance decreased during 1988–91, flow through the causeway (*QS* and *QN*) also decreased and the salinity stratification gradually diminished and did not recur during 1992–98. In October 1998, samples were collected only to a depth of 4,172.5 ft and stratification below this depth would not have been detected. The stratification in both the north and south parts occurred because the increase in rates of south-to-north (*QS*) and north-to-south (*QN*) flows were greater than the rate of mixing in either part.

## Effects of the West Desert Pumping Project on Loads of Ions

From April 10, 1987, to June 30, 1989, water was pumped from the north part of the lake into West Pond in an effort to lower lake levels during a period of substantially higher than normal inflow. On the basis of measurements of flow at the West Desert pump station (fig. 1), the West Desert Pumping Project (WDPP) removed more than 2.5 million acre-ft of water and 695 million tons of salt from the lake during a 27-month period. From January 1990 to June 1992, 200,000 acre-ft of water and 94 million tons of salt returned to the lake from West Pond through the Newfoundland Weir (Wold and Waddell, 1994). Estimates based on direct measurements of salt flowing to and from West Pond indicate that about 0.6 billion ton, or 12 percent of the dissolved-solids load for the lake, were left in West Pond as a result of the WDPP. As an independent check of the amount of salt lost to West Pond, the dissolved-solids load of the lake just before April 1987 was compared to the load just after the return flow had ceased in 1992. The loss of total salt to West Pond was estimated to be about 0.5 billion ton or 10 percent of the total salt in the lake before the WDPP (fig. 7), and this sum was used for this study for the calculations in the salt balance equations.

Because of the importance to the mineral industry, the loss of magnesium and potassium to West Pond also was estimated from historical chemical data for Great Salt Lake. The most complete, continuous record of spatially distributed ion-concentration data available for Great Salt Lake is the data collected by the UGS. The loads of magnesium and potassium in Great Salt Lake were computed for 1966–99 with the UGS data. The methods used for computing dissolved-solids load are described in appendix B.

Prior to the WDPP (1966–86) as well as after (1991–98), both magnesium and potassium loads had a declining trend (fig. 10). The trend lines during 1966–86 indicate a loss of 11 million tons of magnesium and 12.5 million tons of potassium. The trend lines during 1991–99 indicate a loss of 7 million tons of magnesium and 3.5 million tons of potassium. The only known factor that could contribute to this decline is withdrawal by the mining industry.

Comparison of magnesium and potassium loads just before and after the WDPP indicates that about 17.5 million tons of magnesium (12 percent of the pre-WDPP total magnesium) and 16 million tons of potassium (18 percent of the pre-WDPP total potassium)

	Prior to West Desert Pumping Project (1966–86)	During West Desert Pumping Project (1987–89)	After West Desert Pumping Project (1991–98)
Magnesium load, loss in millions of tons	11	17.5	7
Potassium load, loss in millions of tons	12.5	16	3.5

from the lake were lost to West Pond as a result of the WDPP. Because all of the salt in the lake was dissolved during the WDPP, the percentage of the lake's total loads of magnesium, potassium, and total dissolved solids (sum of all ions) lost to West Pond were assumed to be the same. The 12-percent loss of magnesium agrees with the 10- to 12-percent loss computed for dissolved solids, but the computed potassium loss was 6

percent greater than the computed dissolved-solids loss.

The computed loads of magnesium and potassium are highly variable from measurement to measurement (fig. 10). Computed loads of magnesium and potassium each had standard errors from the trend lines of 8 percent of the mean loads during 1966–86. Because of the magnitude of the variability relative to the losses to West Pond, it cannot be inferred that the computed losses of total magnesium and potassium during the WDPP are substantially different from that computed for total dissolved solids.

### Sources of Error in Computing Loads of Ions

Spatial error associated with representing large parts of the lake with a small number of samples, and analytical error associated with analysis of brines, are sources of error in computing loads or masses of salts in Great Salt Lake. If the brine samples used for a load calculation do not represent an average vertical profile of the entire lake, then the load calculation can be in error because of the large volume of the lake (load = concentration \* volume). In general, the more spatially

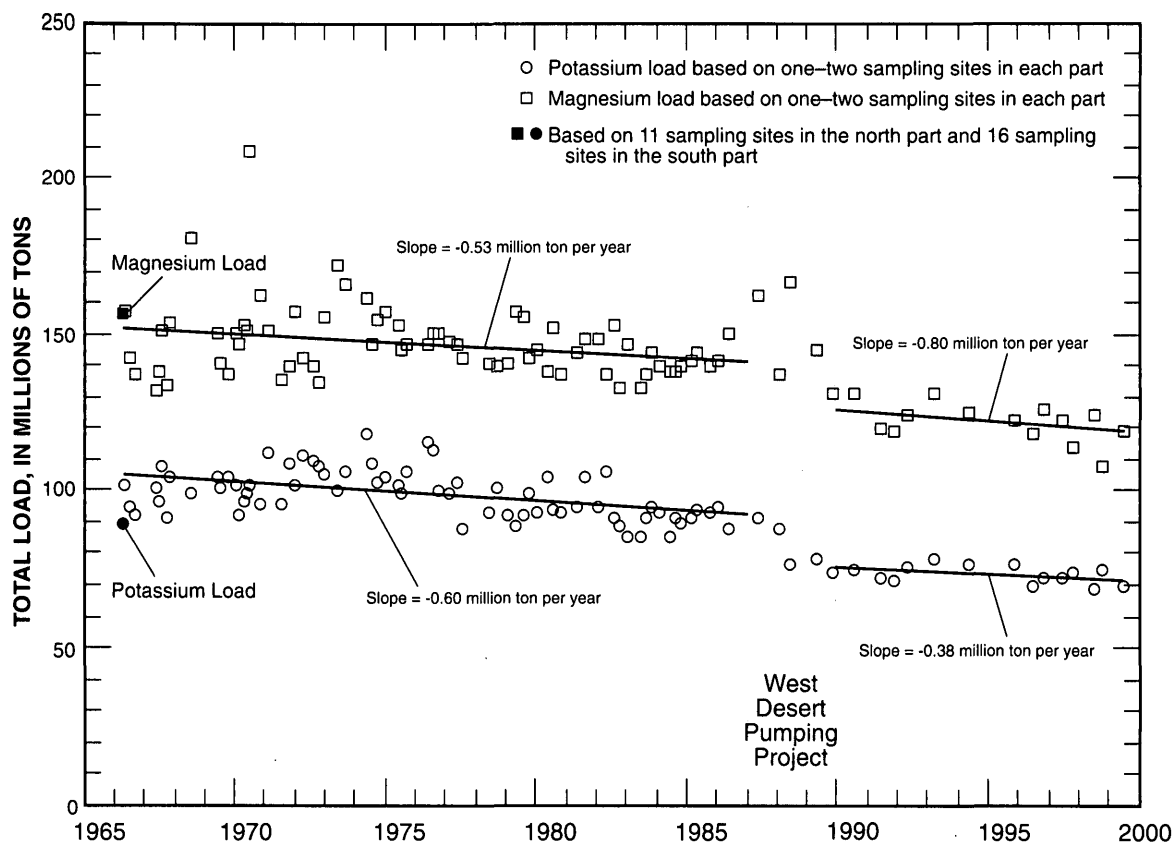


Figure 10. Total magnesium and potassium loads in Great Salt Lake, Utah, 1966–99.

distributed the sample sites, the smaller the spatial error.

Spatial error can result from both areal differences and stratification. The bay areas, where most of the freshwater inflow occurs, are typically of lower dissolved-solids concentration than the main body of the lake and are the primary cause of areal differences in the south part of the lake. Historically, stratification has been small in the north part of the lake, but at times substantial in the south part. The major exception was during the historic rise in lake levels during 1983–87, and particularly after opening of the causeway breach during 1984, when both parts were stratified.

Loads of dissolved solids used in this report were determined from measurements at three to nine sites in each part of the lake, whereas individual ion loads were determined from measurements at only one to two sites in each part of the lake. Specific-gravity measurements, corrected to 20° C, are a simple and reliable way to estimate dissolved-solids concentration; therefore, a large number of specific-gravity measurements were made from which to estimate dissolved-solids loads, rather than using summation of individual ion loads.

To provide an estimate of how much spatial error is involved in the computation of loads in the lake, a comparison was made of loads based on vertical profiles at one sampling site in each part of the lake and at three to nine sites in each part, for two different sampling periods. One period was when the lake stratified following the historic high lake levels in 1987, and the other was in 1992 when the lake was well mixed and had very little areal or vertical stratification.

During 1987, the load of dissolved solids computed from a vertical profile of samples at one site in each part was 4.94 billion tons, and from four to nine sampling sites in each part was 4.83 billion tons. The load computed from vertical profiles at 2 sites was about 2 percent higher than the load computed from 13 sites. In comparison, during 1992 when the lake was well mixed both vertically and areally, the load based on measurements from two sites was only 1 percent higher than the load based on measurements from eight sites.

Only in the south part of the lake has a significant areal difference in salinity occurred. This difference is a result of the bay areas, where freshwater from the Bear, Weber, and Jordan Rivers enters the lake. Although the bay areas generally are fresher than the main south part of the lake, consideration of the volume of the bay areas compared to that of the main south part indicates only small error in computing loads of dis-

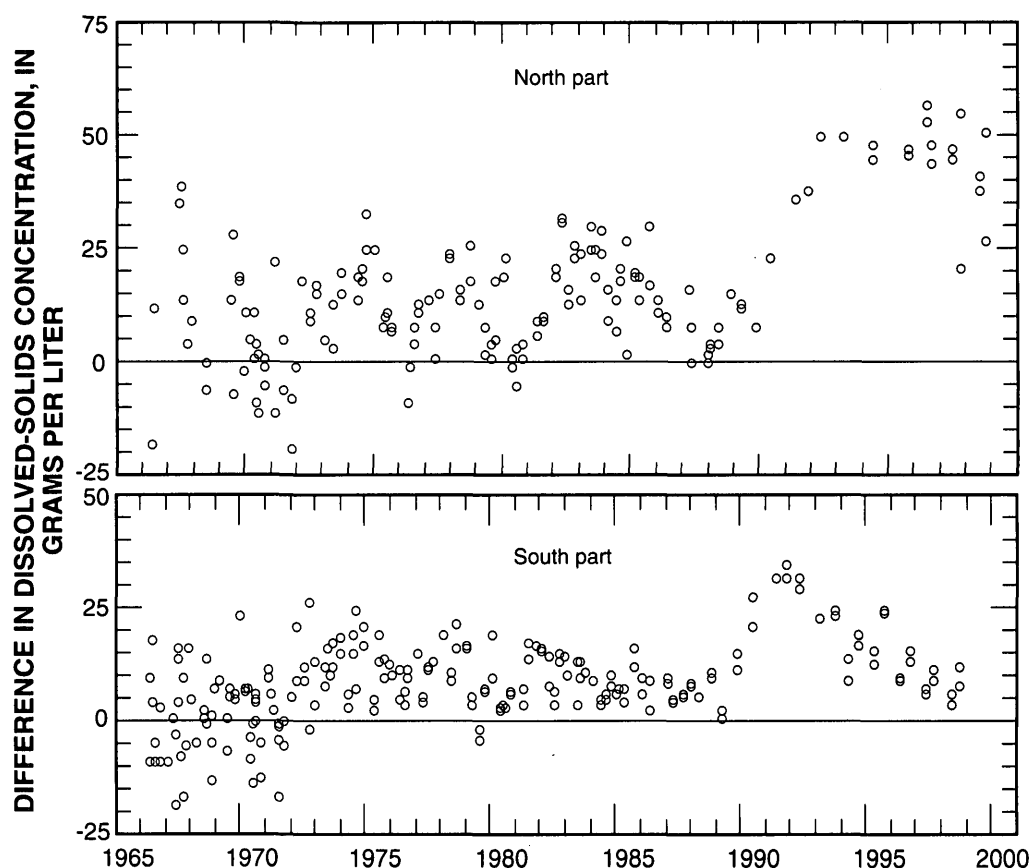
solved solids. In this report, computation of loads of dissolved solids is based on the assumption that the bay areas have the same concentration as the main south part of the lake (see appendix B).

Inherent in the computation of dissolved solids from the sum of the ions is the cumulative error associated with the determination of each ion. Laboratories and methods for analyzing brines changed during 1965–98 and may have contributed to the differences between the dissolved solids as computed from specific gravity and the sum of the ions (fig. 11). Methods used for measuring specific gravity during 1965–98 were basically the same and are considered to have small analytical error due to the simplicity of the measurement and the excellent relation between specific gravity and dissolved solids (Waddell and Bolke, 1973, p. 35).

The differences between dissolved solids as computed from the sum of the ions and specific gravity were evaluated in an effort to determine the possible causes and effects these differences might have on the calculation of losses of specific ions, such as potassium and magnesium resulting from the WDPP, or the exchange of dissolved salts between the north and south parts of Great Salt Lake. Possible causes of these differences in dissolved solids are ion-balance errors and (or) analytical bias. Ion-balance errors were evaluated as the difference between the sum of the cations (sodium, potassium, and magnesium) and anions (chloride and sulfate) in terms of equivalents per liter. During 1976–98, the error was about plus or minus 6 percent and was not large enough to cause the differences seen in the dissolved solids; thus, these differences may be a result of analytical bias.

Irrespective of the analytical techniques used by the laboratories, the brines generally are diluted substantially prior to analysis. Small errors in dilution can lead to large errors in the final computation of ion concentrations even if the analysis of the diluted brine is quite accurate. Because of the viscous nature of the concentrated brines, small aliquots pipetted to volumetric flasks for large dilution can result in underestimating the actual dilution. Standard pipettes are calibrated for use with fluids of viscosity less than that of Great Salt Lake brine, and as a result, may deliver less than the amount indicated for the pipette.

Potassium and magnesium concentrations are too low relative to the differences in dissolved-solids concentrations as computed from the sum of the ions and from specific gravity (fig. 11) to account for these differences. Sodium and chloride comprise about 85 to 90 percent of the dissolved-solids concentration. For the



**Figure 11.** Difference between dissolved-solids concentration computed from the sum of individual ion concentrations and as computed from specific-gravity measurements, 1966–99, for the north and south parts of Great Salt Lake, Utah.

cations and anions to balance and still have a discrepancy in the dissolved-solids concentration, sodium and chloride would have to be biased low in approximately the same ratio.

The higher differences between dissolved-solids concentrations as computed from the sum of the ions and from specific gravity (fig. 11) in the north part as compared to that of the south part may indicate dilution errors. During 1988–98, the concentrations of all ions in the north part were about 2 to 3.5 times greater than those in the south part and would require more dilution and possibly result in greater sources of error than for brines in the south part.

Prior to about 1991 the dissolved-solids concentration computed from the sum of the ions in the north part ranged from about 0 to 25 g/L less than that computed from specific gravity (fig. 11). After about 1991, the difference increased to about 50 g/L. Prior to 1991, in the south part the difference ranged from about 0 to 20 g/L, increased to about 30 g/L after 1991, and then slowly decreased to almost 0 by 1998.

In consideration of the possible analytical bias, perhaps from dilution errors, the losses of potassium and magnesium from the lake after 1988 may be overestimated. Because there is indication that the analytical bias increases as the dissolved-ion(s) concentration increases (figs. 4 and 11), the samples collected from the north part of the lake would have a greater analytical error or bias than those from the south. The error biasing concentrations low would also appear as load losses, especially in the north part, and may account for the difference between the expected and computed losses of potassium during the WDPP.

## **SIMULATION OF WATER AND SALT MOVEMENT THROUGH THE CAUSEWAY**

The original model developed by Waddell and Bolke (1973) was used during the 1970s by the Utah Department of Natural Resources to simulate water and salt movement through the causeway and to determine

the effects of causeway modifications on the salt balance between the two parts of the lake. The original model also was used to simulate the effects of different widths of culvert or breach openings on the head difference between the south and north parts of the lake. The simulations made by the original model were used to help design the breach that was constructed in the causeway in 1984 to help alleviate flooding along the shores of the south part of the lake.

The original model simulates the effects of the causeway on the water and salt balance of the lake for variable rates of inflow. The main components of and modifications to the original model are shown in table 1. The current model has all the simulation capabilities of the original model but also can simulate effects of the breach, flow through submerged culverts, and loads of four major ions.

## Calibration of the Water and Salt Balance Model, 1987–98

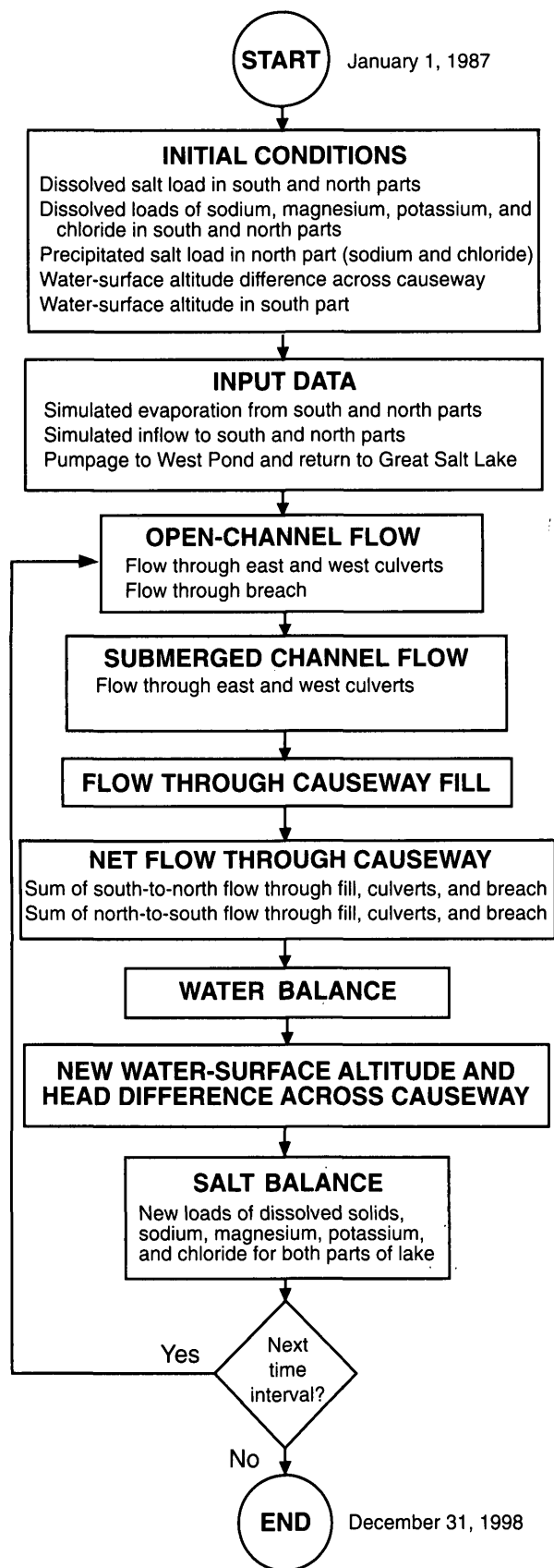
Model calibration involved a water-balance program that was used to calibrate the hydrologic and climatic variables that are input to the water and salt balance model. The water and salt balance model was then used to calibrate the causeway-fill flows (fig. 12).

### Water-Balance Program

Monthly values of measured and estimated surface inflow, ground-water inflow, precipitation on the lake surface, and evaporation were compiled for 1987–98. The input data were evaluated with a water-balance program (Wold, Thomas, and Waddell, 1997, appendix A). The purpose of the water-balance program was to test, and if necessary, modify the independent estimates

**Table 1.** Major modifications to the original model of Waddell and Bolke (1973)

Component	First modification (Wold, Thomas, and Waddell, 1997)	Second modification (for current model)
<b><i>Initial Conditions</i></b>	<ul style="list-style-type: none"> <li>Revised water-surface altitude, area, and volume relations (George Pyper, U.S. Geological Survey, written commun., 1986)</li> </ul>	<ul style="list-style-type: none"> <li>Revised water-surface altitude, area, and volume relations to account for MagCorp dike that was breached in June 1986 and repaired in January 1994</li> <li>Added dissolved loads of individual major ions</li> </ul>
<b><i>Input Data</i></b>	<ul style="list-style-type: none"> <li>Compiled inflow and evaporation for 1980–86</li> </ul>	<ul style="list-style-type: none"> <li>Compiled inflow and evaporation for 1987–98</li> <li>Compiled withdrawals and return flows of water and dissolved solids to and from West Pond</li> </ul>
<b><i>Open-channel Flow</i></b>	<ul style="list-style-type: none"> <li>Replaced energy equations for open-channel flow with equations of Holley and Waddell (1976)</li> <li>Added the breach as a channel for which flow could be computed</li> </ul>	<ul style="list-style-type: none"> <li>Added equations to account for flow through submerged culverts</li> <li>Revised the equations that convert flow computed for a rectangular-shaped breach to flow through a trapezoidal-shaped breach</li> </ul>
<b><i>Flow Through Causeway Fill</i></b>	<ul style="list-style-type: none"> <li>Computed fill flow with solute-transport model of Sanford and Konikow (1985)</li> <li>Modified the fill-flow computations to account for changes in the hydraulic conductivity of the fill</li> </ul>	<ul style="list-style-type: none"> <li>Modified the fill-flow computations to account for changes in the hydraulic conductivity of the original fill</li> </ul>



**Figure 12.** Flow chart of Great Salt Lake water and salt balance model.

of monthly inflow, precipitation, and evaporation. The water-balance program computes water-surface altitudes from the monthly input and compares them to measured altitudes during 1987–98.

Computations of the water-surface altitude made with the independent estimates of inflow and evaporation indicate that there was either too much evaporation or too little inflow. Most of the surface-water inflow (*SIS*) and pumpage to West Pond (*QWP*) were measured, and ground-water inflow (*GIS* and *GIN*) is very small when compared to other inflow sources. Thus, most of the error in the water balance was probably from a combination of error in precipitation and evaporation. Although there is probably some error in the amount of precipitation, only evaporation was adjusted as part of the water-balance data evaluation. The maximum adjustment to evaporation during 1 year was 8 percent, and adjustment averaged 4 percent during 1987–98 (see fig. A2 in appendix A).

#### Water and Salt Balance Model and Causeway-Fill Flow

The water and salt balance model was used to evaluate the causeway-fill flows for 1987–98. Evaporation, as adjusted in the water balance program, and the same inflow, were used as input to the water and salt balance model.

Causeway-fill flow (*QSF* and *QNF*) was considered to be the least accurate component of the causeway flows (*QS* and *QN*). Therefore, by using the measured breach flows (*QSB* and *QNB*, see appendix E) and estimated and measured culvert flows (*QSC* and *QNC*, see appendix D) in the model, all error between the measured and simulated values of the water and salt balance variables was assumed to be the result of errors in the causeway-fill flow (see appendix E).

During the calibration of the water and salt balance model, it was assumed that the hydraulic-conductivity values used in the fill-flow model (see appendix C) were responsible for the errors between the simulated and measured water-surface altitudes (*ES* and *EN*), salt loads (*LS*, *LN*, and *CLNP*), and densities ( $\rho_s$ , and  $\rho_n$ ). The model was calibrated by assuming that a change in the hydraulic conductivity was directly proportional to a change in the fill flow. With this assumption, constant factors were used to reduce the fill flows and were evaluated by comparison of simulated water-surface altitudes, salt loads, and densities with measured values during 1987–98.

To calibrate the model for 1980–86, Wold, Thomas, and Waddell (1997, p. 12) reduced the hydraulic conductivity of the fill to 40 percent of what Waddell and Bolke (1973) determined it to be. Comparison of simulated and measured water-surface altitudes (*ES* and *EN*), salt loads (*LS*, *LN*, and *CLNP*), and densities ( $\rho_s$ , and  $\rho_n$ ) indicated that the hydraulic conductivity of the fill had continued to decrease during the 1980s and 1990s (fig. 13). By reducing the causeway-fill flows by a constant factor, the simulated and measured water-surface altitude, salt loads, and densities were in closer agreement.

After several trials of assigning a single hydraulic-conductivity value to the entire vertical profile of causeway fill, it was decided to assign the new fill added during the high lake levels of the 1980s a different hydraulic conductivity than the original fill below it (fig. 3). The best match of simulated and measured water-surface altitudes, salt loads, and densities for the 1987–98 calibration occurred when the new fill was assigned the same hydraulic conductivity used by Waddell and Bolke (1973) and the original fill below it was reduced to 10 percent of the 1973 conductivity. The methods used to compute fill flow are described in more detail in appendix C. No other components of the water and salt balance were changed as part of the calibration. The final calibration values of breach, culvert, and fill flow, and the water balance parameters for 1987–98, are shown in figure 14.

After the calibration of fill flows, the sensitivity and accuracy of the simulated water and salt balance components were evaluated by comparison with measured data (fig. 15). The components most sensitive to adjustment of the hydraulic conductivity of the fill are head difference ( $\Delta H$ , fig. 5), density difference ( $\Delta \rho$ ), and precipitated salt load in the north part (*CLNP*, fig. 6). The maximum differences between simulated and measured head differences were + 0.5 ft and - 0.9 ft, with the largest differences occurring during 1992–96 (see appendix A, “Correction of water-surface altitudes for the Boat Harbor Gage, 1987–98”). Simulated density difference closely matched measured values, with the largest difference being about 0.008 g/mL. Simulated precipitated salt loads in the north part (*CLNP*, fig. 6) matched estimated loads in 1994 and 1998, but during 1995–97 they were 0.014 to 0.277 billion ton higher than estimated loads. During 1993–98, dissolved salt loads of the south part were simulated from 0.080 to 0.220 billion ton lower than measured.

Although all error in the water and salt balance was attributed to the causeway-fill flow, the differences

between simulated and measured values result from the combined error from the causeway fill, culvert, and breach flow. Most of these differences can be attributed to errors in the estimated culvert flow during 1987–96, when culvert flow was not monitored.

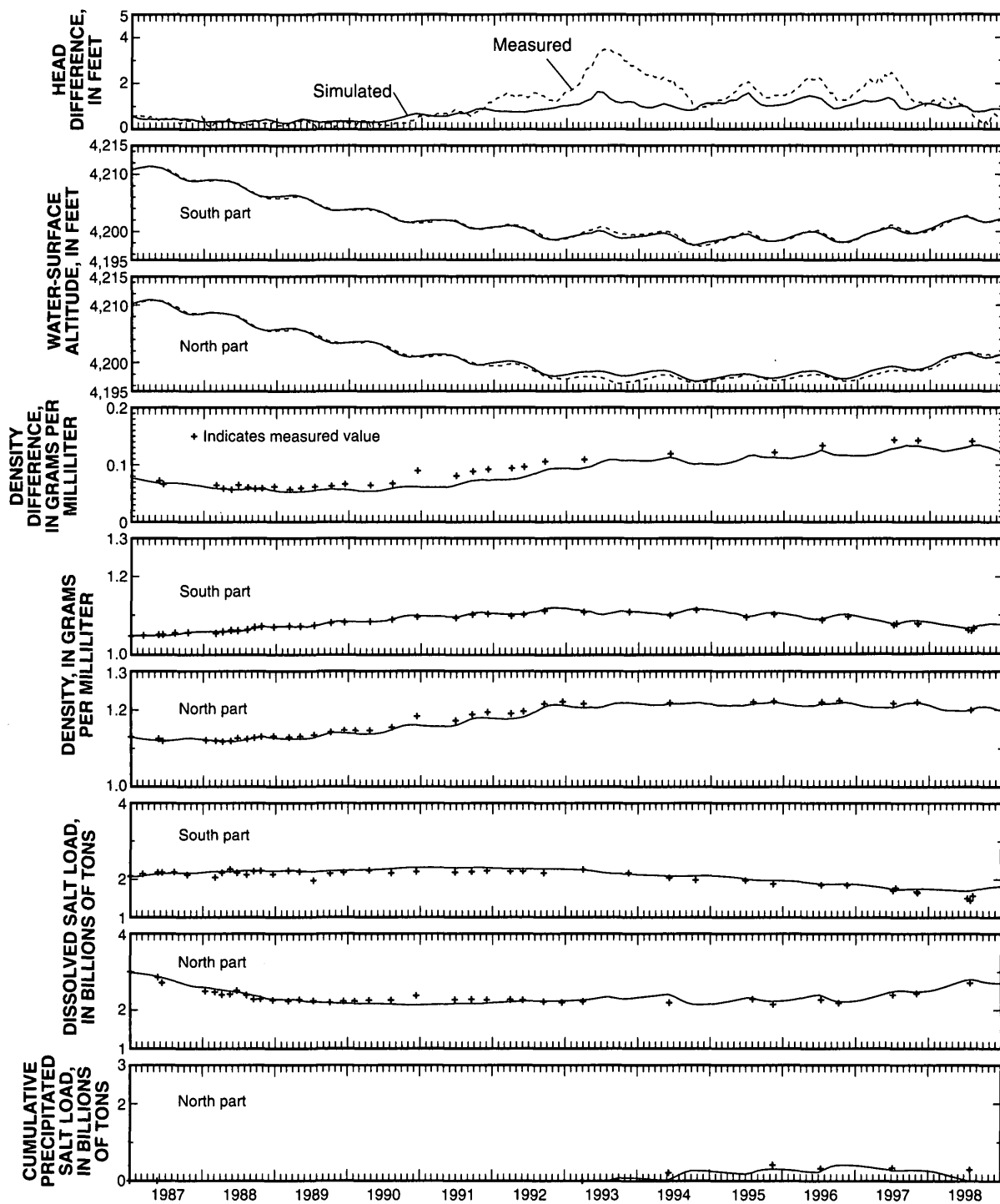
The subroutine used to calculate breach flow was evaluated independently of the model by comparing computed and measured flow for observed boundary conditions (figs. E1 and E2, appendix E). The accuracy of model-computed breach flows is discussed in appendix E.

## Simulation of Major-Ion Loads as an Independent Check of Model Calibration

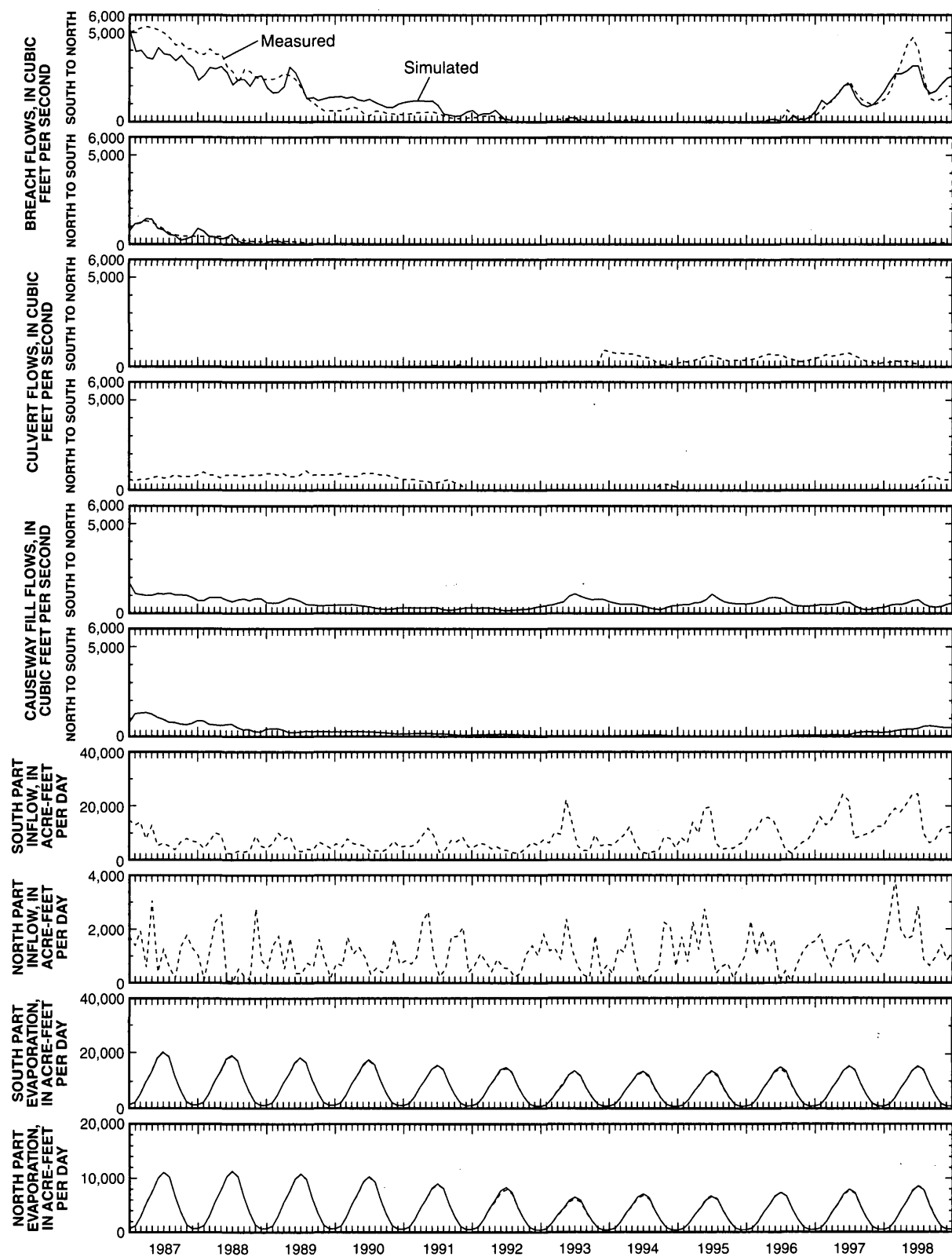
The dissolved loads of four major ions (sodium, magnesium, potassium, and chloride) were simulated to independently check the model accuracy after the model had been calibrated. As discussed earlier in the section “Sources of error in computing loads of ions,” ion loads vary widely. Because of this variation, the model did not match the measured loads of individual ions as well as the total dissolved-solids loads computed from specific-gravity measurements. Simulated south part loads matched measured loads reasonably well for all four ions (fig. 16). Simulated north part loads matched measured loads well for sodium and chloride, but not as well for magnesium or potassium.

## Limitations of the Model

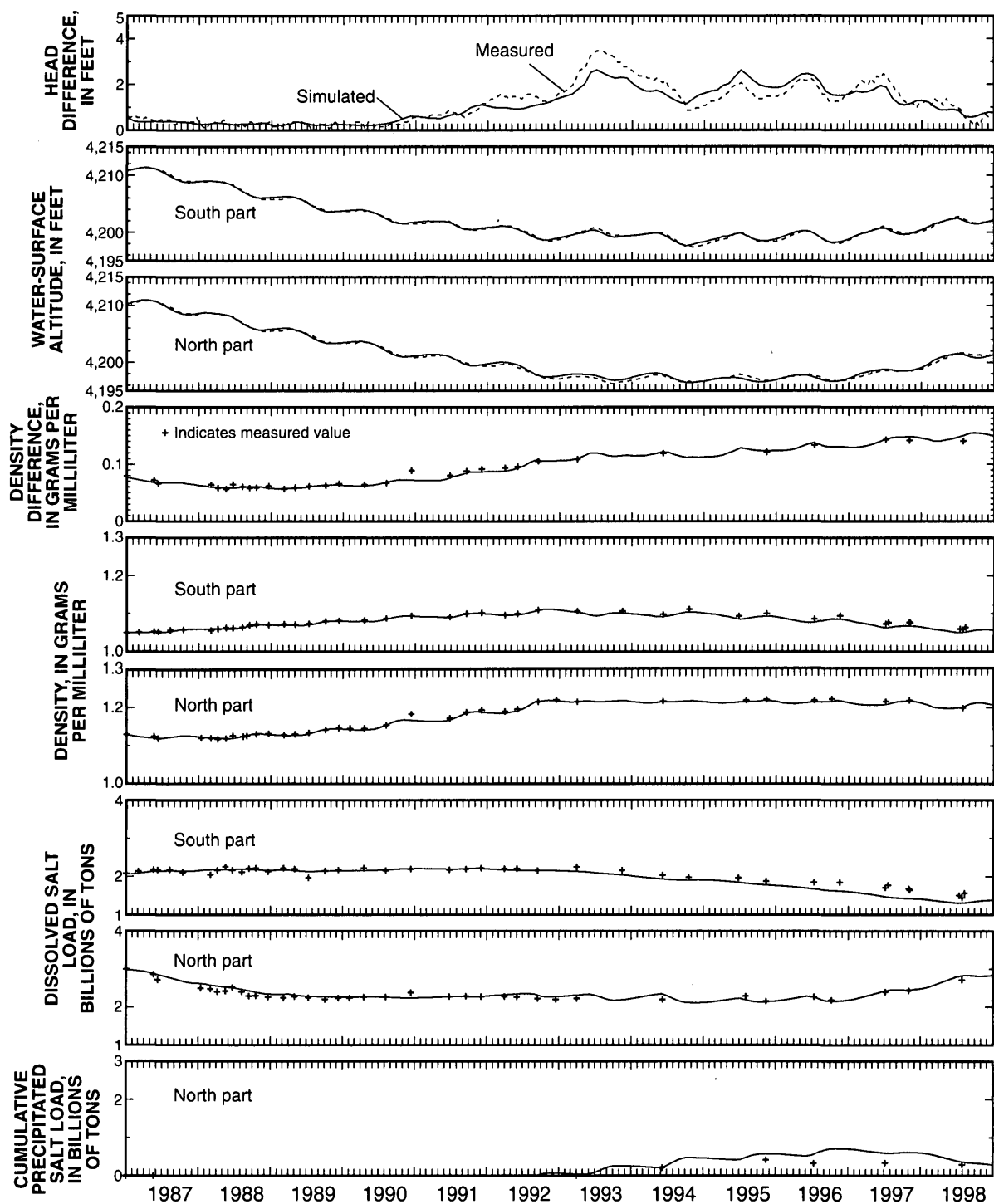
- The model’s optimum operating range for water-surface altitudes is from 4,191 to 4,212 ft.
- The model is limited to positive head differences between south and north parts (south is higher) and positive density differences between north and south parts (north is greater). The model is valid for head differences ranging from about 0.1 to 3.9 ft and density differences ranging from about 0.02 to 0.15 g/mL.
- The model simulates water and salt movement across the causeway by using any combination of up to two culverts or breaches but can be easily modified to simulate any number of culverts or breaches.
- Model simulations were made with the assumption that the altitude of the breach bottom remained constant at 4,200 ft from January 1987 to August 1996. The breach was deepened to 4,198 ft in August



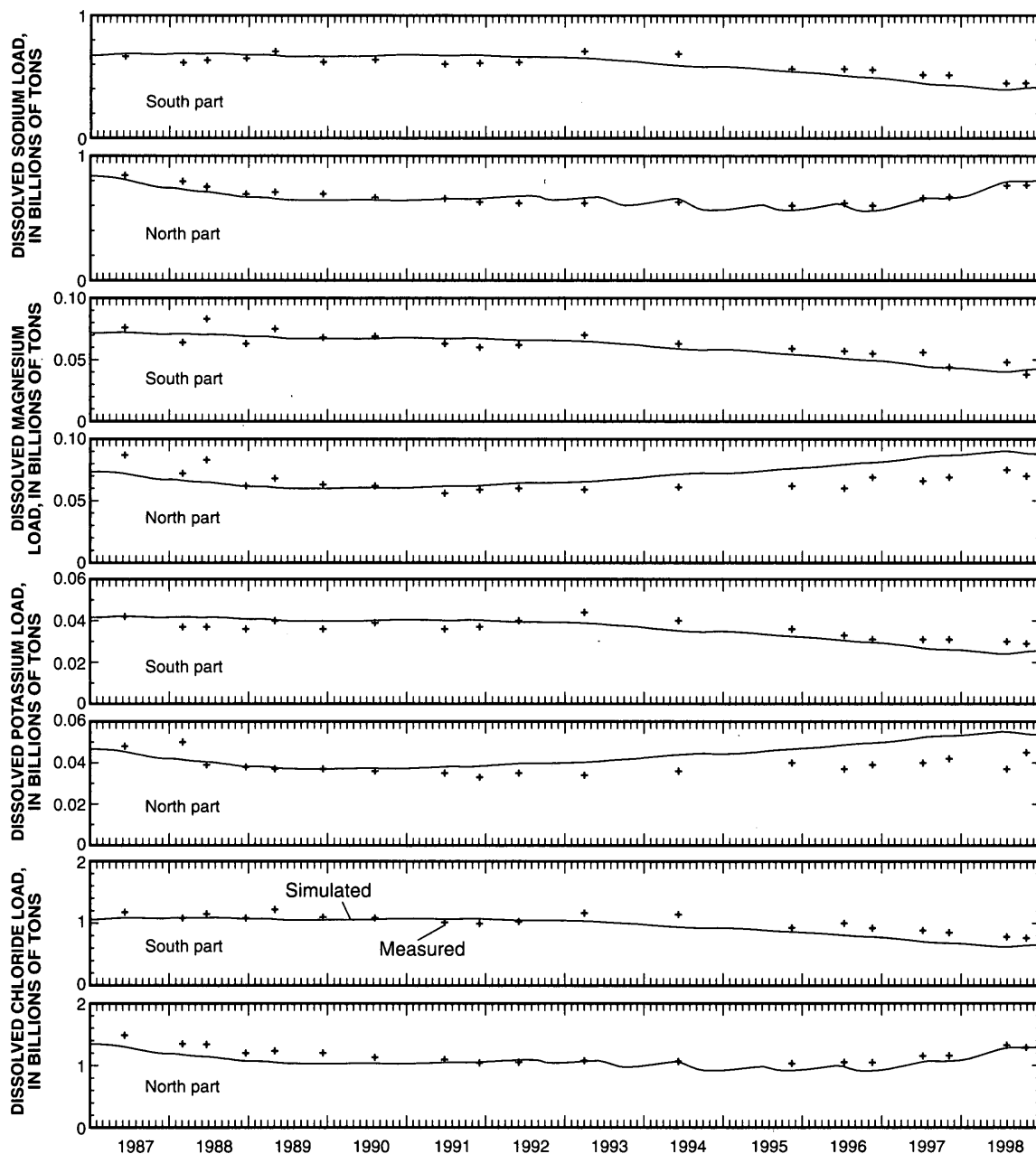
**Figure 13.** Simulated and measured head difference, water-surface altitude, density difference, density, and dissolved and cumulative precipitated salt load in the south and north parts of Great Salt Lake, Utah, before model calibration, 1987–98.



**Figure 14.** Simulated and measured breach flow, measured and estimated culvert flow, computed causeway-fill flow, total measured and estimated inflow, and estimated and computed evaporation in the south and north parts of Great Salt Lake, Utah, after model calibration, 1987–98.



**Figure 15.** Simulated and measured head difference, water-surface altitude, density difference, density, and dissolved and cumulative precipitated salt load in the south and north parts of Great Salt Lake, Utah, after model calibration, 1987–98.



**Figure 16.** Simulated and measured loads of sodium, magnesium, potassium, and chloride in the south and north parts of Great Salt Lake, Utah, after model calibration, 1987–98.

1996 and was assumed to be constant from August 1996 to December 1998.

- Water-surface altitude affects the amount of water and dissolved solids moving through the causeway. When the water-surface altitude is less than or equal to the altitude of the bottom of the breach (4,200 ft before August 1996; 4,198 ft after), flow occurs only through the culverts and fill. Because computation of fill flow has more uncertainty than computation of breach flow, simulated water-surface

altitudes less than the breach-bottom altitude may have more error than those above the breach-bottom altitude, when the breach is the dominant means of conveyance.

- During this study, the density of the water was assumed to be uniform along the length of the causeway. Data collected by Waddell and Bolke (1973, table 8) show that there was little variation in the density of the water along the length of the causeway. No data were available, however, to

determine if density boundary conditions along the length of the causeway were uniform after construction of the breach or after more fill material was added to raise the causeway.

- Model simulations were made with the assumption that inaccuracies of the hydraulic-conductivity values used in the fill-flow model were responsible for the errors between the simulated and measured values of head difference and between dissolved and precipitated salt loads, so that the flow computed by the fill-flow model was reduced by a series of constant factors until the minimum error between simulated and measured values was attained (see appendix C).

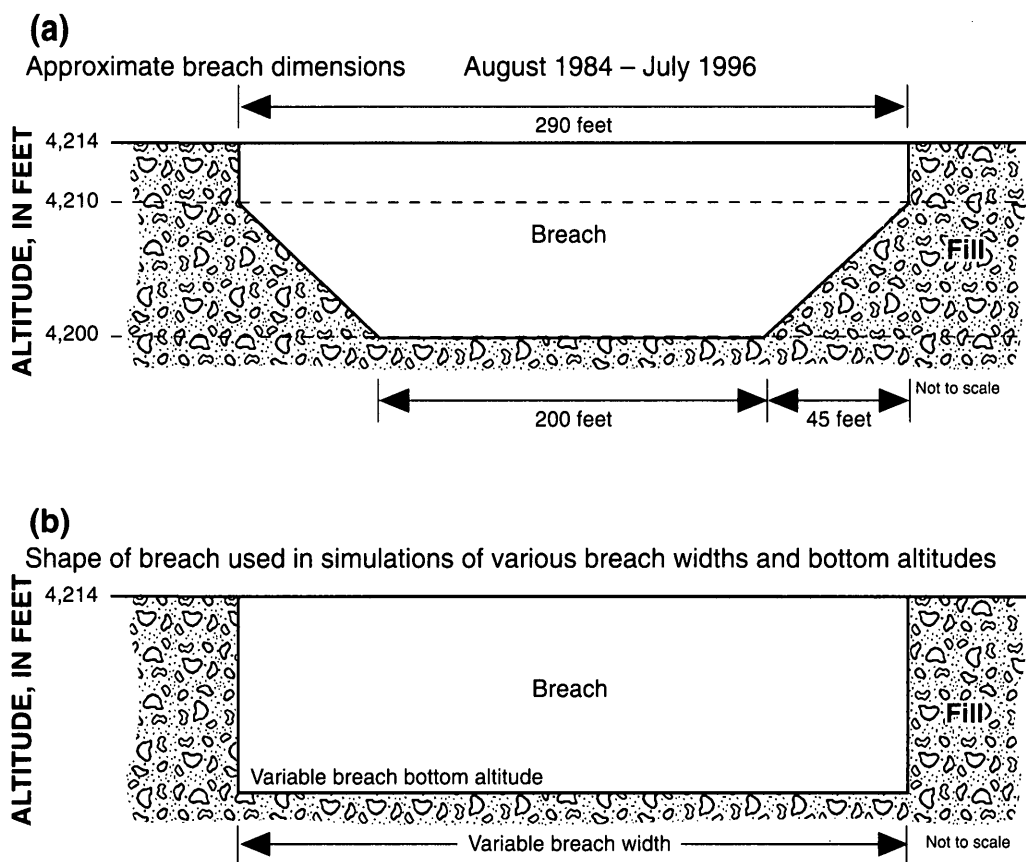
### Simulated Effects of Breach Dimension on the Salinity Balance Between the North and South Parts

The calibrated model was used to simulate the effect of several combinations of breach depth and width on the salinity in each part of the lake. The 1987–98 inflows and evaporation were used as a baseline sim-

ulation (along with estimated culvert flows and West Pond withdrawals for the period). During 1987–98, the lake experienced a wide range of surface-water inflows and water-surface altitudes, providing hydrologic conditions suitable for evaluating the effect of variable breach dimensions.

During 1987–98, the general shape of the breach was trapezoidal, with the widest opening (about 290 ft) at the top of the breach and the narrowest opening (about 200 ft) at the bottom (fig. 17a). The altitude of the bottom of the breach was about 4,200 ft until August of 1996, when it was deepened to an effective altitude of 4,198 ft. For the simulations of different breach dimensions, the breach shape was assumed to be rectangular with the same width at the bottom as at the top (fig. 17b).

Model simulations (tables 2 and 3, and fig. 18) indicate that deepening the breach is more effective in reducing the difference in dissolved-solids concentration between the two parts of the lake than widening the breach without deepening the breach. In December 1998, the dissolved-solids concentration of the south part of the lake was 94 g/L, or 28 percent of the concentration in the north part. If the breach had been modified from its



**Figure 17.** Approximate shape and dimensions of the breach (a) during August 1984 to July 1996, and (b) used in simulations of selected breach widths and bottom altitudes, Great Salt Lake, Utah.

**Table 2.** Simulated dissolved-solids concentration of the south part as a percentage of that of the north part for selected breach dimensions, Great Salt Lake, Utah, December 31, 1998

[Assumes breach dimensions were modified from existing dimensions on January 1, 1987; —, breach dimensions produced head differences too small for the model to simulate breach or fill flows]

Breach width, in feet	Altitude of the bottom of breach, in feet						
	4,198	4,195	4,193	4,190	4,185	4,180	4,175
100	27	30	31	38	48	55	60
150	28	32	35	44	54	—	—
200	29	33	40	49	59	—	—
250	30	35	44	53	—	—	—
<sup>2</sup> 290	30	38	46	55	—	—	—
400	31	43	—	—	—	—	—
500	33	—	—	—	—	—	—
600	33	—	—	—	—	—	—

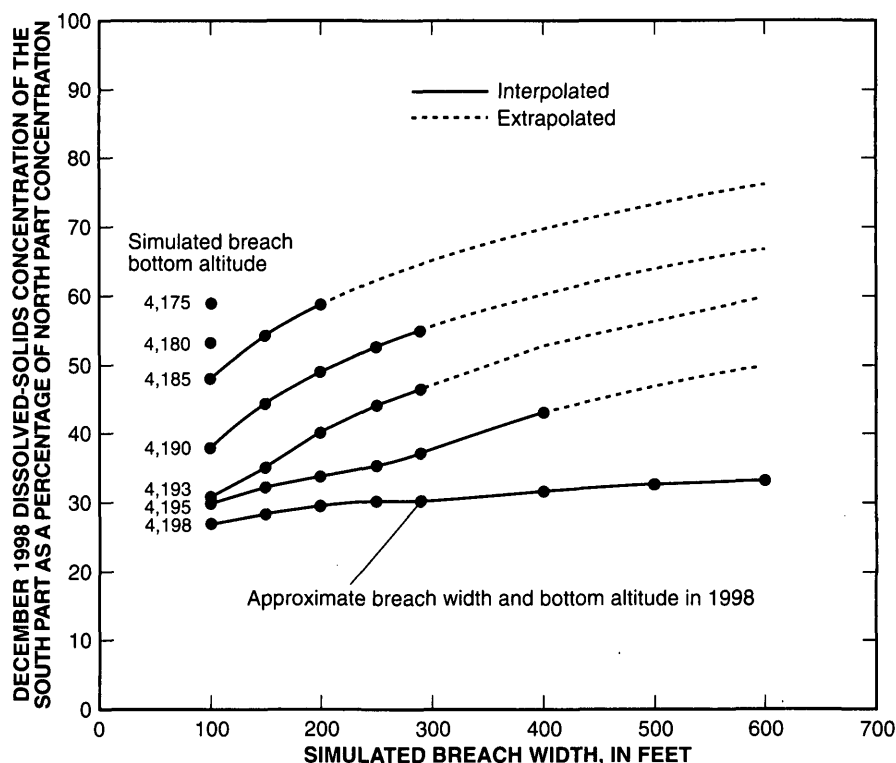
<sup>1</sup> Approximate altitude of the bottom of the breach during August 1996 through 1998; the altitude was approximately 4,200 feet August 1984 through July 1996.

<sup>2</sup> Approximate width of the top of the breach August 1984 through 1998.

**Table 3.** Results of model simulations showing comparison of salinities in Great Salt Lake, Utah, with a 290-foot-wide rectangular breach of selected bottom altitudes

[g/mL, grams per milliliter; g/L, grams per liter]

	Initial Conditions January 1987	Breach bottom altitude of 4,198 feet December 1998	Breach bottom altitude of 4,195 feet December 1998	Breach bottom altitude of 4,193 feet December 1998	Breach bottom altitude of 4,190 feet December 1998
<b>South part</b>					
Percent Salinity	7.7	9.4	11.1	12.3	13.4
Density (g/mL)	1.051	1.063	1.075	1.084	1.092
Concentration (g/L)	81	100	119	133	146
<b>North part</b>					
Percent Salinity	18.4	27.5	26.3	24.4	22.8
Density (g/mL)	1.131	1.209	1.198	1.181	1.167
Concentration (g/L)	208	332	314	287	265



**Figure 18.** Effects of selected breach widths and bottom altitudes on the dissolved-solids concentration of the south part as a percentage of that of the north part, 1987–98 hydrologic conditions, Great Salt Lake, Utah.

actual (approximately trapezoidal) shape (fig. 17a) in January 1987 to a 290-ft-wide rectangle (fig. 17b), flow through the breach would have increased and the dissolved-solids concentration of the south part of the lake would have been 97 g/L, or 29 percent of the concentration in the north part in December 1998. If the breach had been deepened from an altitude of 4,200 ft to 4,195 ft in January 1987, the December 1998 dissolved-solids concentration of the south part would have been 119 g/L, or 38 percent of the dissolved-solids concentration of the north part. Deepening the breach bottom to an altitude of 4,190 ft in January 1987 would have increased the dissolved-solids concentration of the south part to 146 g/L, or 55 percent of the north part concentration by December 1998. By comparison, widening the breach from 290 ft to 600 ft without deepening it would only have increased the dissolved-solids concentration of the south part to 110 g/L, or 33 percent of the north part concentration.

### Simulated Effects of the West Desert Pumping Project on the Salinity of the North and South Parts

The calibrated model was used to simulate effects of the WDPP on salinities of the north and south parts of the lake. Model simulations indicate that had there been no WDPP, salinity in December 1998 would have been 3 g/L or 1 percent higher in the south part, and 9 g/L or 0.3 percent higher in the north part (table 4). In addition, model simulations indicate that if there had been no WDPP, the net movement of salt from the south part to the north part during 1987–98 would have been about 0.5 billion ton instead of 0.7 billion ton.

### Sensitivity and Error Analyses

A sensitivity and error analysis was done to determine the influence of the model components on the accuracy of the water and salt balance model results. The major components of the model are the water balance; fill, breach, and culvert flows; and salt load computation. The sensitivity analyses are summa-

**Table 4.** Results of a model simulation showing comparison of salinities in Great Salt Lake, Utah, with and without the West Desert Pumping Project

[WDPP, West Desert Pumping Project; g/mL, grams per milliliter; g/L, grams per liter]

	Initial conditions January 1987	With effects of WDPP December 1998	Without effects of WDPP December 1998
<b>South part</b>			
Percent Salinity	7.7	8.8	9.8
Density (g/mL)	1.051	1.059	1.066
Concentration (g/L)	81	94	105
<b>North part</b>			
Percent Salinity	18.4	27.4	27.7
Density (g/mL)	1.131	1.209	1.211
Concentration (g/L)	208	332	335

rized below and are discussed in detail in the appendices of this report (water balance in appendix A, salt load computation in appendix B, fill flow in appendix C, culvert flow in appendix D, and breach flow in appendix E).

- Water Balance

- Most sensitive to surface-water inflow (60 percent of total inflow during 1987–98), and evaporation (100 percent of total outflow, except during the WDPP).
- Was calibrated by adjusting the estimated annual evaporation from the lake by an average of 4 percent and a maximum of 8 percent during 1987–98.
- After evaporation was calibrated in the water balance program, simulated south part water-surface altitude matched measured within an average of 0.2 ft, and with a maximum difference of 0.7 ft.

- Fill Flow

- For a specified set of boundary conditions ( $ES$ ,  $EN$ ,  $\rho_s$ ,  $\rho_n$ ), fill flow is most sensitive to hydraulic conductivity of the fill material.
- During 1987–98, the fill flow computed by the water and salt balance model averaged 611 acre-ft/d, and the fill flow computed using a theoretical equation of the water and salt balance averaged 503 acre-ft/d, or about 21 percent less than the model. The greatest differences between flows computed by the water and salt balance model and the theoretical equation of the water and salt balance occurred

during 1987–91 when the boundary conditions were rapidly changing from the decline in inflow and lake altitude.

- Breach and Culvert Flows

- Model-computed breach flow is most sensitive to head difference ( $\Delta H$ ), density difference ( $\Delta \rho$ ), and the physical dimensions of the breach.
- The standard error of estimate for computed and measured breach flow was 722 ft<sup>3</sup>/s, or 30 percent of the mean for south-to-north flow, and 294 ft<sup>3</sup>/s, or 116 percent of the mean for north-to-south flows.
- The standard error of estimate for computed and measured flow through unsubmerged culverts during 1980–83 was 12 percent of the mean for south-to-north flow, and 62 percent of the mean for north-to-south flow (Wold, Thomas, and Waddell, 1997, p. 54). Culvert flow was not computed as part of the model calibration for 1987–98 because the culverts were frequently plugged, preventing the use of theoretical equations to compute flow. The model had the capability to compute flows through both submerged and unsubmerged culverts. No measurements have been made, however, to evaluate the accuracy of model-computed flow through clean, submerged culverts.

- Water and Salt Balance Model

- The model was calibrated by reducing the causeway-fill flows by a constant factor. The model components most sensitive to this

adjustment are head difference ( $\Delta H$ ), density difference ( $\Delta \rho$ ), and precipitated load of salt in the north part (CLNP).

- After the model was calibrated, the maximum difference between simulated and measured head differences was 0.9 ft, density differences, 0.008 g/mL, and precipitated loads of salt in the north part, 0.220 billion ton.
- The calibrated model was used to simulate the effect of several breach bottom altitudes on the dissolved-solids concentration in each part of the lake. Model simulations indicate that had the breach been deepened from an altitude of 4,200 to 4,195 ft in January 1987, the December 1998 dissolved-solids concentration of the south part would have been 38 percent of the north part dissolved-solids concentration. To determine the degree of accuracy that is involved when a deeper breach is considered in the model, simulations were made deepening the breach to 4,195 ft, with breach flows increased and decreased by the standard error found between measured and simulated breach flows. The standard error for south-to-north breach flow was determined to be 30 percent, and for north-to-south flow, 116 percent (appendix E). The results of the simulations are:
  - If the south-to-north breach flows computed by the model were 30 percent too low, a breach bottom altitude of 4,196 ft, instead of 4,195 ft, would have been required to achieve a dissolved-solids concentration of the south part of 38 percent of the north part concentration in December 1998. Similarly, if the south-to-north breach flows computed by the model were 30 percent too high, a breach bottom altitude of 4,193.5 ft, instead of 4,195 ft, would have been required.
  - If the north-to-south breach flows computed by the model were 116 percent too low, a breach bottom altitude of 4,196 ft, instead of 4,195 ft, would have been required to achieve a dissolved-solids concentration of the south part of 38 percent of the north part concentration in December 1998. Similarly, if the north-to-south breach flows computed by the model were 116 percent too high, a breach bottom altitude of 4,192.5 ft, instead of 4,195 ft, would have been required.

## SUMMARY

A rock-fill causeway across Great Salt Lake was completed in 1959. The effect of the causeway was to change the water and salt balance of Great Salt Lake by creating two separate but interconnected parts of the lake, with more than 95 percent of freshwater surface inflow entering the lake south of the causeway.

The water and salt balance of Great Salt Lake depends primarily on the amount of inflow from tributary streams and the conveyance properties of the causeway that divides the lake into south and north parts. The causeway restricts circulation between the south and north parts. The conveyance properties of the causeway originally consisted of two 15-ft-wide culverts and permeable rock-fill material, but the causeway has since been modified by the addition of a breach and modifications to the causeway fill. During the 1980s, fill material was added to the causeway as lake levels rapidly rose, changing the overall dimensions of the causeway fill. In August 1984, a 290-ft-wide breach with a bottom altitude of about 4,200 ft was opened near the western end of the causeway to reduce the head difference between the two parts of the lake.

The dissolved-solids concentrations of the north and south parts were approximately equal at the time the causeway was completed in 1959, but by 1972, the concentration was about 200 g/L greater in the north part than in the south, and by December 1998, the concentration was about 250 g/L greater in the north than in the south. The theoretical concentration that would have occurred in an undivided lake in December 1998 was about 190 g/L. In 1998 the concentration in the south part was about 90 g/L, or 100 g/L less than the theoretical concentration for an undivided lake. In 1998 the concentration in the north part was about 340 g/L, or 150 g/L more than the theoretical concentration for an undivided lake.

Previous modeling of the water and salt balance incorporated the causeway conveyance properties and hydrologic conditions that existed during 1959–86. Waddell and Bolke (1973) described the effects of the causeway on the water and salt balance of Great Salt Lake and developed a model to simulate the effects of the causeway on the salt balance for variable culvert widths and tributary inflows to the lake. This original model of Waddell and Bolke was calibrated for causeway conveyance and hydrologic conditions existing during 1969–72. This model was valid until about 1981. During the 1980s, fill material was frequently added to the causeway to maintain the top of the cause-

way above the water surface. During 1983, the two 15-ft-wide culverts became submerged beneath the rising water surface and eventually filled with debris; in August 1984, a 290-ft-wide breach was opened near the western end of the causeway. Because these new conditions warranted revision of the model, Wold, Thomas, and Waddell (1997) modified the original model and recalibrated it for 1980–86.

Since 1986, additional changes in the causeway conveyance properties and withdrawals for the West Desert Pumping Project have made it necessary to revise the model of Wold, Thomas, and Waddell (1997). In this report, the U.S. Geological Survey, in cooperation with the Utah Department of Natural Resources, Division of Forestry, Fire, and State Lands, and Tooele County, Utah, modified and recalibrated the 1997 model to incorporate the changes that occurred during 1987–98.

For simulations of several hypothetical breach dimensions with 1987–98 boundary conditions, deepening the breach was more effective in reducing the difference in dissolved-solids concentration between the two parts of the lake than widening without deepening the breach. In December 1998, the dissolved-solids concentration of the south part of the lake was 94 g/L, or 28 percent of the concentration in the north part. Simulations indicate that had the altitude of the bottom of the breach been deepened from 4,200 ft to 4,195 ft in January 1987, the December 1998 dissolved-solids concentration of the south part would have been 119 g/L or 38 percent of the north part concentration. Deepening the breach bottom to 4,190 ft in January 1987 would have increased the dissolved-solids concentration of the south part to 146 g/L or 55 percent of the north part concentration by December 1998. Widening the breach from 290 ft to 600 ft without deepening it would only have increased the dissolved-solids concentration of the south part to 110 g/L, or 33 percent of the north part concentration.

During 1987–92, about 500 million tons of salt, including 17.5 million tons of magnesium and 16 million tons of potassium, were removed from the lake as part of the West Desert Pumping Project. The pumps

only operated during April 1987 to June 1989, but there was some return flow from West Pond to the lake during 1990–92. Model simulation indicated that had there been no West Desert Pumping Project, the dissolved-solids concentration in the north part would have been 3 g/L higher, and the concentration in the south part 9 g/L higher by December 1998.

## **INFORMATION NEEDED FOR MORE ACCURATE WATER AND SALT BALANCE CALCULATION**

The water and salt balance model for Great Salt Lake was calibrated with data collected during 1987–98. The accuracy of this model, and future versions of it, depend on the quantity and quality of the data used to calibrate the model. Lack of culvert-flow measurements during 1987–96 was the major limitation of the model accuracy.

To maintain accuracy of future models of the water and salt balance of Great Salt Lake, the following should be continued:

- Collect record of continuous water-surface altitude for both the north and south parts of the lake.
- Make flow measurements at the culverts and breach at least once every 3 months, on calm days.
- Collect vertical profiles of chemical samples from sampling sites in both the north and south parts of the lake, two to three times a year.

To improve the accuracy of future models of the water and salt balance of Great Salt Lake, the following should be included:

- At least one time per year, increase the number of vertical and areal sampling sites so that an accurate accounting of the load or mass of major ions can be documented.
- Develop a quality assurance plan to minimize analytical error or bias.
- Conduct tracer studies to improve estimates of the hydraulic properties of the fill.

## REFERENCES CITED

- Adams, T.C., 1934, Evaporation from the Great Salt Lake: American Meteorological Society Bulletin, v. 15, p. 35–39.
- Badon-Ghyben, W., 1888, Nota in Verband met de Voorgenomen Putboring Nabij Amsterdam (Notes on the probable results of well drilling near Amsterdam), Tijdsdar, Kon. Inst., Ing., The Hague, 1888/9, p. 8–22.
- Fenneman, N.M., 1931, Physiography of the Western United States: New York, McGraw-Hill, 534 p.
- Gwynn, J.W., and Sturm, P.A., 1987, Effects of breaching the Southern Pacific railroad causeway, Great Salt Lake, Utah—Physical and chemical changes, August 1, 1984–July 1986: Utah Geological Survey Water-Resources Bulletin 25, 25 p.
- Hahl, D.C., 1968, Dissolved-mineral inflow to Great Salt Lake and chemical characteristics of the Salt Lake brine: Summary for water years 1960, 1961, and 1964: Utah Geological Survey Water-Resources Bulletin 10, 35 p.
- Herbert, L.R., and others, 1996, Water resources data, Utah: U.S. Geological Survey Water-Data Report UT-96-1, 328 p.
- 1997, Water resources data, Utah: U.S. Geological Survey Water-Data Report UT-97-1, 328 p.
- 1998, Water resources data, Utah: U.S. Geological Survey Water-Data Report UT-98-1, 300 p.
- 1999, Water resources data, Utah: U.S. Geological Survey Water-Data Report UT-99-1, 340 p.
- Herzberg, A., 1901, Die Wasserversorgung einiger Nordseebaden (The water supply on parts of the North Sea coast in Germany), Z. Gasbeleucht, Wasserversorg, 44, p. 815–819, 824–844.
- Holley, E.R., and Waddell, K.M., 1976, Stratified flow in Great Salt Lake culvert: Journal of the Hydraulics Division, American Society of Civil Engineers, v. 102, no. HY7, Proceedings Paper 12250, July 1976, p. 969–985.
- Madison, R.J., 1970, Effects of a causeway on the chemistry of the brine in Great Salt Lake, Utah: Utah Geological Survey Water-Resources Bulletin 14, 52 p.
- Pinder, G.F., and Cooper, H.H., Jr., 1970, A numerical technique for calculating the transient position of the saltwater front: Water Resources Research, v. 6, no. 3, p. 875–882.
- ReMillard, M.D., and others, 1986, Water resources data, Utah: U.S. Geological Survey Water-Data Report UT-86-1, 404 p.
- 1987, Water resources data, Utah: U.S. Geological Survey Water-Data Report UT-87-1, 368 p.
- 1988, Water resources data, Utah: U.S. Geological Survey Water-Data Report UT-88-1, 364 p.
- 1989, Water resources data, Utah: U.S. Geological Survey Water-Data Report UT-89-1, 383 p.
- 1990, Water resources data, Utah: U.S. Geological Survey Water-Data Report UT-90-1, 383 p.
- 1991, Water resources data, Utah: U.S. Geological Survey Water-Data Report UT-91-1, 375 p.
- 1992, Water resources data, Utah: U.S. Geological Survey Water-Data Report UT-92-1, 343 p.
- 1993, Water resources data, Utah: U.S. Geological Survey Water-Data Report UT-93-1, 333 p.
- 1994, Water resources data, Utah: U.S. Geological Survey Water-Data Report UT-94-1, 329 p.
- 1995, Water resources data, Utah: U.S. Geological Survey Water-Data Report UT-95-1, 312 p.
- Sanford, W.E., and Konikow, L.F., 1985, A two-constituent solute-transport model for ground water having variable density: U.S. Geological Survey Water-Resources Investigations Report 85-4279, 88 p.
- Waddell, K.M., and Bolke, E.L., 1973, The effects of restricted circulation on the salt balance of Great Salt Lake, Utah: Utah Geological Survey Water-Resources Bulletin 18, 54 p.
- Waddell, K.M., and Fields, F.K., 1977, Model for evaluating the effects of dikes on the water and salt balance of Great Salt Lake, Utah: Utah Geological Survey Water-Resources Bulletin 21, 54 p.
- Wold, S.R., and Waddell, K.M., 1994, Salt budget for West Pond, Utah, April 1987 to June 1989: U.S. Geological Survey Water-Resources Investigations Report 93-4028, 20 p.
- Wold, S.R., Thomas, B.E., and Waddell, K.M., 1997, Water and salt balance of Great Salt Lake, Utah, and simulation of water and salt movement through the causeway: U.S. Geological Survey Water-Supply Paper 2450, 64 p.



---

---

## APPENDIXES

---

---

## APPENDIX A. WATER BALANCE AND BOUNDARY CONDITIONS

The water balance between the south and north parts of Great Salt Lake (fig. 5) consists of surface- and ground-water inflow ( $SIS$ ,  $GIS$ , and  $GIN$ ), precipitation on the lake surface ( $PIS$  and  $PIN$ ), evaporation from the lake surface ( $EOS$  and  $EON$ ), withdrawal to and return flows from West Pond ( $QWP$ ), and flow through the causeway ( $QS$  and  $QN$ ). Flow through the causeway depends on freshwater inflow to the south part of the lake, 90 percent of which is surface water, and on the conveyance properties of the causeway, and is interrelated with the boundary conditions, which consist of water-surface altitude and density of the south and north parts.

The following equations, A1 and A2, relate the change in volume of the south and north parts during a specified time interval,  $T$ , to surface- and ground-water inflow, precipitation, evaporation, exchange with West Pond, and flow through the causeway. The methods used for estimating  $SIS$ ,  $PIS$ ,  $PIN$ ,  $GIS$ ,  $GIN$ ,  $EOS$ , and  $EON$  are discussed later in this appendix. Flow through the causeway,  $QS$  and  $QN$ , consists of flow through the fill, culverts, and breach, and is discussed in appendixes C, D, and E, respectively.

$$VS(I+1) = VS(I) + [SIS + PIS + GIS - EOS + QN - QS] * T \quad (A1)$$

and

$$VN(I+1) = VN(I) + [PIN + GIN - EON - QWP + QS - QN] * T, \quad (A2)$$

where

- $VS$  = volume of south part, in acre-ft;
- $VN$  = volume of north part, in acre-ft;
- $I+1$  = next time step;
- $I$  = present time step;
- $SIS$  = surface-water inflow to south part, in acre-ft/d;
- $PIS$  = precipitation on south part, in acre-ft/d;
- $PIN$  = precipitation on north part, in acre-ft/d;
- $GIS$  = ground-water inflow to south part, in acre-ft/d;
- $GIN$  = ground-water inflow to north part, in acre-ft/d;
- $EOS$  = evaporation from south part, in acre-ft/d;
- $EON$  = evaporation from north part, in acre-ft/d;
- $QWP$  = withdrawal to (+), or return flow from (-) West Pond in acre-ft/d;

$QS$  = total flow from south-to-north through causeway, in acre-ft/d;

$QN$  = total flow from north-to-south through causeway, in acre-ft/d; and

$T$  = time interval, in days (in this case, 1.901 days).

Because the components of flow through the causeway,  $QS$  and  $QN$ , are interrelated with the differences in water-surface altitude and density, to compute  $QS$  and  $QN$ , it was necessary to use a small time interval,  $T$ , in which the boundary conditions are held constant. To minimize computation error associated with holding boundary conditions constant, the time interval can be no longer than 2 days. Total flow through the causeway,  $QS$  and  $QN$  (eqs. A3 and A4), computed for each time interval,  $T$  ( $T$  equals 1.901 days), is the sum of the fill, culvert, and breach flow.

$$QS = 1.9835(QSF + QSC + QSB) \quad (A3)$$

and

$$QN = 1.9835(QNF + QNC + QNB), \quad (A4)$$

where

$$1.9835 \text{ acre-ft/d} = 1 \text{ ft}^3/\text{s};$$

$QSF$  = south-to-north flow through fill, in  $\text{ft}^3/\text{s}$ ;

$QNF$  = north-to-south flow through fill, in  $\text{ft}^3/\text{s}$ ;

$QSC$  = south-to-north flow through culverts, in  $\text{ft}^3/\text{s}$ ;

$QNC$  = north-to-south flow through culverts, in  $\text{ft}^3/\text{s}$ ;

$QSB$  = south-to-north flow through breach, in  $\text{ft}^3/\text{s}$ ; and

$QNB$  = north-to-south flow through breach, in  $\text{ft}^3/\text{s}$ .

Equations A1 and A2 were used to compute volume,  $VS$  and  $VN$ , for the next time step ( $I+1$ ). Then, through the relations in table A1, water-surface altitudes for the south and north parts ( $ES$  and  $EN$ ) can be computed as functions of the respective volumes for the next time step. The relation between the south part water-surface altitude, surface area, and volume changed in June 1986 when a dike maintained by Magnesium Corporation of America (MagCorp) was breached by high water levels. In January 1994 the dike was repaired, restoring the original south part water-surface altitude-area-volume relation.

**Table A1.** Area and volume of Great Salt Lake, Utah, and of the Magnesium Corporation of America (MagCorp) evaporation ponds

[Data from George Pyper, U.S. Geological Survey, written commun., 1986]

Water-surface altitude, in feet	MagCorp ponds		South part		North part	
	Area, in acres	Volume, in acre-feet	Area, in acres	Volume, in acre-feet	Area, in acres	Volume, in acre-feet
4,171.0	0	0	123,900	116,100	48,010	42,100
4,171.5	0	0	131,700	180,000	53,820	67,500
4,172.0	0	0	139,500	247,800	59,640	95,900
4,172.5	0	0	147,300	319,500	65,450	127,200
4,173.0	0	0	155,100	395,100	71,260	161,400
4,173.5	0	0	162,900	474,600	77,080	198,500
4,174.0	0	0	170,700	558,000	82,890	238,500
4,174.5	0	0	178,600	645,300	88,700	281,400
4,175.0	0	0	186,400	736,500	94,520	327,200
4,175.5	0	0	194,200	831,600	100,300	375,900
4,176.0	0	0	202,000	930,600	106,100	427,500
4,176.5	0	0	209,800	1,033,500	112,000	482,000
4,177.0	0	0	217,600	1,140,300	117,800	539,400
4,177.5	0	0	225,400	1,251,000	123,600	599,700
4,178.0	0	0	233,200	1,365,600	129,400	662,900
4,178.5	0	0	241,000	1,484,100	135,200	729,000
4,179.0	0	0	248,800	1,606,500	141,000	798,000
4,179.5	0	0	256,700	1,732,900	146,800	869,900
4,180.0	0	0	264,400	1,863,200	152,600	944,700
4,180.5	0	0	269,600	1,996,700	155,600	1,021,800
4,181.0	0	0	274,700	2,132,800	158,700	1,100,400
4,181.5	0	0	279,800	2,271,400	161,700	1,180,500
4,182.0	0	0	284,900	2,412,600	164,700	1,262,100
4,182.5	0	0	290,000	2,556,300	167,700	1,345,200
4,183.0	0	0	295,100	2,702,600	170,700	1,429,800
4,183.5	0	0	300,200	2,851,400	173,800	1,515,900
4,184.0	0	0	305,400	3,002,800	176,800	1,603,600
4,184.5	0	0	310,500	3,156,800	179,800	1,692,800
4,185.0	0	0	315,600	3,313,300	182,800	1,783,500
4,185.5	0	0	320,700	3,472,400	185,800	1,875,700
4,186.0	0	0	325,800	3,634,000	188,900	1,969,400
4,186.5	0	0	330,900	3,798,200	191,900	2,064,600
4,187.0	0	0	336,000	3,964,900	194,900	2,161,300
4,187.5	0	0	341,200	4,134,200	197,900	2,259,500
4,188.0	0	0	346,300	4,306,100	200,900	2,359,200
4,188.5	0	0	351,400	4,480,500	204,000	2,460,400
4,189.0	0	0	356,500	4,657,500	207,000	2,563,200
4,189.5	0	0	361,600	4,837,000	210,000	2,667,500
4,190.0	0	0	366,700	5,019,100	213,000	2,773,300
4,190.5	0	0	372,800	5,204,000	217,100	2,880,800
4,191.0	0	0	378,900	5,391,900	221,200	2,990,400
4,191.5	0	0	384,900	5,582,900	225,300	3,102,000
4,192.0	0	0	391,000	5,776,900	229,400	3,215,700
4,192.5	0	0	397,100	5,973,900	233,500	3,331,400
4,193.0	0	0	403,200	6,174,000	237,700	3,449,200
4,193.5	0	0	414,300	6,378,400	247,500	3,570,500

**Table A1.** Area and volume of Great Salt Lake, Utah, and of the Magnesium Corporation of America (MagCorp) evaporation ponds—Continued

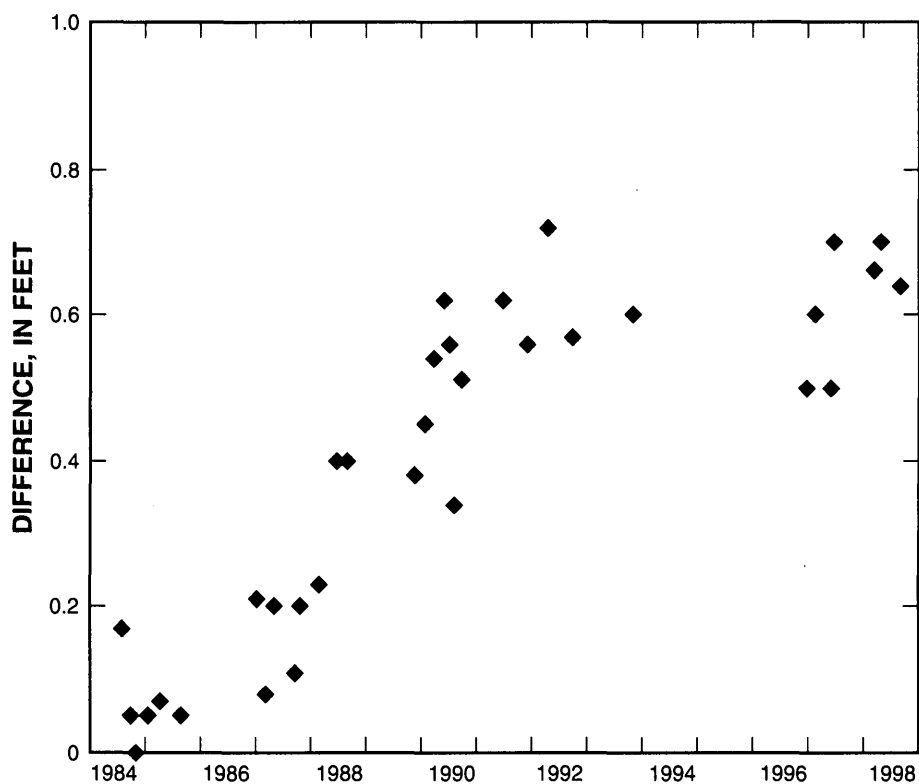
Water-surface altitude, in feet	MagCorp ponds		South part		North part	
	Area, in acres	Volume, in acre-feet	Area, in acres	Volume, in acre-feet	Area, in acres	Volume, in acre-feet
4,194.0	0	0	425,400	6,588,300	257,300	3,696,700
4,194.5	0	0	436,600	6,803,800	267,200	3,827,800
4,195.0	0	0	447,800	7,024,900	277,000	3,963,800
4,195.5	0	0	467,900	7,253,800	287,800	4,105,000
4,196.0	0	0	488,000	7,492,800	298,600	4,251,600
4,196.5	0	0	508,100	7,741,800	309,400	4,403,600
4,197.0	0	0	528,200	8,000,900	320,300	4,561,000
4,197.5	0	0	548,400	8,270,000	331,100	4,723,800
4,198.0	0	0	568,500	8,549,200	341,900	4,892,000
4,198.5	0	0	588,600	8,838,500	352,700	5,065,600
4,199.0	0	0	608,700	9,137,800	363,500	5,244,600
4,199.5	0	0	628,800	9,447,200	374,400	5,429,100
4,200.0	28,530	0	648,900	9,766,600	385,200	5,619,000
4,200.5	31,520	15,000	659,500	10,093,700	392,800	5,813,500
4,201.0	34,520	31,500	670,200	10,426,100	400,300	6,011,800
4,201.5	37,510	49,500	680,800	10,763,900	407,900	6,213,900
4,202.0	40,510	69,000	691,400	11,107,000	415,500	6,419,800
4,202.5	43,500	90,000	702,100	11,455,400	423,100	6,629,500
4,203.0	46,490	112,500	712,700	11,809,100	430,700	6,843,000
4,203.5	49,490	136,500	723,400	12,168,100	438,300	7,060,300
4,204.0	52,470	162,000	734,000	12,532,500	445,900	7,281,400
4,204.5	53,880	188,600	744,600	12,902,200	453,500	7,506,300
4,205.0	55,280	215,900	755,300	13,277,200	461,100	7,735,000
4,205.5	56,680	243,900	764,400	13,657,100	467,200	7,967,100
4,206.0	58,090	272,600	773,500	14,041,600	473,300	8,202,200
4,206.5	59,490	302,000	782,700	14,430,700	479,400	8,440,400
4,207.0	60,900	332,100	791,800	14,824,300	485,600	8,681,700
4,207.5	62,300	362,900	801,000	15,222,500	491,700	8,926,000
4,208.0	63,710	394,400	810,300	15,625,300	497,800	9,173,400
4,208.5	65,110	426,600	845,000	16,039,100	503,900	9,423,800
4,209.0	66,510	459,500	879,700	16,470,300	510,000	9,677,300
4,209.5	67,920	493,100	900,600	16,915,400	513,600	9,933,200
4,210.0	69,320	527,400	908,400	17,367,700	517,300	10,190,900
4,210.5	70,730	562,400	916,100	17,823,800	520,900	10,450,500
4,211.0	72,130	598,100	923,900	18,283,800	524,500	10,711,900
4,211.5	73,540	634,500	931,600	18,747,700	528,100	10,975,100
4,212.0	74,940	671,600	939,400	19,215,500	531,900	11,240,100
4,212.5	75,930	709,300	945,600	19,686,800	551,300	11,510,800
4,213.0	76,930	747,500	951,900	20,161,200	572,700	11,791,700
4,213.5	77,920	786,200	958,200	20,638,700	596,500	12,083,900
4,214.0	78,910	825,400	964,500	21,119,400	617,800	12,387,500
4,214.5	79,910	865,100	970,800	21,603,200	637,000	12,701,200
4,215.0	80,900	905,300	977,100	22,090,200	825,300	13,311,100
4,215.5	81,900	946,000	983,400	22,580,300	884,500	13,738,300
4,216.0	82,890	987,200	989,600	23,073,600	945,700	14,195,700

## Correction of Water-Surface Altitudes for the Boat Harbor Gage, 1987–98

During the late 1980s, rapidly rising lake levels made it necessary for the USGS to relocate the Boat Harbor gage several times. As the gage was relocated, new benchmarks had to be chosen to reference the gage's datum, because previously used benchmarks were being submerged by the rising lake. It has become apparent that during this period, some of the benchmarks had incorrect given altitudes—including National Geodetic Survey benchmark C-174 1970—which is currently used (fig. 1). As a result, there was a difference between the south part water-surface altitudes measured on calm days at the Boat Harbor gage and the altitude measured on the northern end of the south part at the breach staff gage or the Promontory Point gage. This difference, which is actually a difference between the datum of a line of benchmarks around the north part and the datums of several benchmarks near the Boat Harbor gage, steadily increased from 0.2

ft in 1987 to 0.6 ft during 1991–98 (fig. A1). Change in the magnitude of the difference over time is assumed to be the result of increasing error with each new benchmark used during 1984–88, and to the way those datum errors were applied to the water-surface altitude data. A thorough investigation of the datums used and water-surface altitudes reported is planned by the USGS in 2000, when the results of a high order GPS survey of benchmarks around Great Salt Lake are made available. (The survey was conducted in June 1999 by the USGS and Utah Department of Natural Resources in cooperation with the National Geodetic Survey.)

The USGS collected water-surface-altitude data on the southern end of the south part of Great Salt Lake at the Boat Harbor gage (10010000) and on the southern end of the north part at the Saline gage (10010100) during 1984–98. During 1997–98, additional data were collected on the northern end of the south part at the Promontory Point gage (10010050). The Promontory Point and Saline gages, which are roughly 5 mi apart on opposite sides of the causeway, are tied to the same line



**Figure A1.** Difference between datums used at the Boat Harbor gage and gages near the causeway (represented by the difference in water-surface altitudes measured on calm days at the south staff gage at the breach and the Boat Harbor gage), Great Salt Lake, Utah, 1984–98.

of levels with a stable datum (fig. 2). During the 2 years of the study period that the Promontory Point gage was operated, 1997 and 1998, head differences at the causeway can be read directly from the record at these gages. Determining accurate head differences across the causeway during 1987–96 proved more difficult.

Although it is not known whether or not the datum of the line of benchmarks around the north part is correct, it has been stable and consistently used since 1966. The line of benchmarks around the north part includes 73 FMK 1966, which is used for the Promontory Point gage; 77 FMK 1966, which is used for the Saline gage; and 120 FMK 1966, which is used to determine water-surface altitudes at the breach (fig. 2). The benchmarks are considered to be stable because levels run between them, and water-surface altitudes measured on calm days at the gages tied to them, indicate that none of them have moved over time. For this report, it is assumed that the datum of the benchmarks in the USGS FMK 1966 line is correct, and the Boat Harbor gage data for 1987–98 were corrected to this datum.

The difference in the datum used at the Boat Harbor gage and the datum used at the breach, Saline gage, and Promontory Point gage was determined by comparing south part water-surface altitudes measured on calm days at the breach to recorded values at the Boat Harbor gage at the same time (fig. A1 and eq. A4a). Monthly datum difference corrections were determined by drawing a best fit line through these measured differences during 1987–96. Monthly differences between the datum at the Boat Harbor gage and the Saline gage were subtracted from the reported Boat Harbor water-surface altitudes during 1987–96 to give Boat Harbor gage altitudes the same datum used at the Saline gage (eq. A4b).

$$\text{Correction} = \text{Reported Boat Harbor gage } WSA - \text{Breach South Staff gage } WSA \quad (A4a)$$

and

$$\text{Corrected Boat Harbor gage } WSA = \text{Reported Boat Harbor gage } WSA - \text{Correction}, \quad (A4a)$$

where

$$WSA = \text{water-surface altitude.}$$

The corrected south part water-surface altitudes are shown in table A2.

Measured water-surface altitudes of each part of the lake are needed in the water-balance program and the water and salt balance model for comparison with simulated altitudes. Measured north part water-surface altitudes are used in the water balance program to compute north part volumes and surface areas for each time step. The altitude-area-volume table (table A1) is derived from the datum of the USGS FMK 1966 benchmark line. All altitudes in this report are tied to the datum of the USGS FMK 1966 line of benchmarks

around northern Great Salt Lake, as reported by the National Geodetic Survey in 1999.

## Surface-Water Inflow

Streams and canals convey surface-water to Great Salt Lake (*SIS* in eq. A1). Most of the major streams and canals were gaged during 1987–98 (fig. 1), and measurements of monthly inflow from these sites were obtained from streamflow-gaging-station records (table A3). The other streams or canals that flow into Great Salt Lake were gaged prior to 1987. At the sites with incomplete records, empirical estimates of monthly inflow were derived using regression analysis between the sites with incomplete records and nearby sites with complete records (table A4). Monthly estimates of surface-water inflow (*SIS*) to Great Salt Lake for all streams and canals are listed in table A5.

The total annual surface-water inflow to the lake for 1987–98 ranged from 964,000 acre-ft in 1992 to 4,260,000 acre-ft in 1998 and averaged 2,060,000 acre-ft (table A6). The surface-water inflow for 1987–98 was distributed as follows: Bear River drainage system, 55 percent; Jordan River drainage system, 26 percent; Weber River drainage system, 12 percent; miscellaneous tributaries, 7 percent. Some of this inflow entered the lake as sewage effluent.

## Bear River and Weber River Basins

Monthly flow to Great Salt Lake from the Bear River Basin was estimated by combining the Bear River Basin outflow across State Highway 83 near Corinne (10127110) and outflow from Willard Bay Reservoir. Monthly flow at Bear River Basin outflow across State Highway 83 near Corinne was estimated using regression equation A5 with measured monthly flow at Bear River near Corinne (10126000) as the independent variable (table A4).

$$\text{Discharge at estimated site} = A(\text{Discharge at measured site}) + B \quad (A5)$$

Thus, to compute the estimated flow at station 10127110:

$$\text{Discharge at station 10127110} = 1.0070(\text{Discharge at station 10126000}) + 14,264.$$

Estimates of inflow to Great Salt Lake from Willard Bay Reservoir were obtained from the Weber Basin Water Conservancy District. Monthly flow to Great Salt Lake from the Weber River Basin was estimated from the record at Weber River at Plain City (10141000).

**Table A2.** South part water-surface altitude corrected to the datum used for the north part water-surface altitude, Great Salt Lake, Utah

[Datum is referenced to benchmark FMK 120 1966, fig. 2]

Year	January	February	March	April	May	June	July	August	September	October	November	December
1987	4,211.2	4,211.4	4,211.5	4,211.4	4,211.2	4,210.9	4,210.4	4,209.7	4,209.2	4,209.1	4,209.1	4,209.0
1988	4,209.0	4,209.1	4,209.0	4,209.0	4,208.6	4,208.3	4,207.6	4,207.0	4,206.4	4,206.0	4,205.9	4,205.9
1989	4,205.9	4,206.0	4,206.2	4,206.1	4,205.9	4,205.4	4,204.7	4,204.4	4,204.1	4,203.8	4,203.8	4,203.8
1990	4,203.8	4,203.9	4,204.1	4,204.0	4,203.5	4,203.2	4,202.7	4,202.2	4,201.8	4,201.7	4,201.6	4,201.6
1991	4,201.7	4,201.9	4,202.0	4,202.0	4,202.1	4,201.8	4,201.3	4,200.8	4,200.6	4,200.5	4,200.7	4,200.8
1992	4,200.9	4,201.3	4,201.3	4,201.2	4,200.7	4,200.3	4,199.9	4,199.3	4,198.8	4,198.6	4,198.6	4,198.9
1993	4,199.2	4,199.6	4,200.2	4,200.3	4,200.7	4,200.8	4,200.4	4,199.9	4,199.6	4,199.7	4,199.5	4,199.6
1994	4,199.6	4,199.8	4,200.0	4,200.2	4,200.0	4,199.5	4,198.9	4,198.1	4,197.6	4,197.5	4,197.7	4,197.9
1995	4,198.4	4,198.6	4,198.9	4,199.1	4,199.8	4,200.1	4,199.6	4,198.9	4,198.5	4,198.4	4,198.4	4,198.6
1996	4,198.9	4,199.3	4,199.8	4,200.2	4,200.2	4,200.0	4,199.4	4,198.8	4,198.4	4,198.1	4,198.4	4,198.8
1997	4,199.4	4,199.9	4,200.1	4,200.6	4,200.9	4,201.1	4,200.6	4,200.2	4,200.0	4,199.8	4,200.0	4,200.2
1998	4,200.7	4,201.3	4,201.8	4,202.3	4,202.5	4,202.9	4,202.4	4,201.9	4,201.8	4,201.9	4,202.0	4,202.2

**Table A3.** Streamflow-gaging stations used to estimate monthly surface-water inflow to Great Salt Lake, Utah, 1987–98

Station number	Station name	Period of record during 1987–98
10126000	Bear River near Corinne	Jan. 1987 to Dec. 1998
10127110	Bear River Basin outflow across State Highway 83, near Corinne	All data prior to 1987
10141000	Weber River near Plain City	Jan. 1987 to Dec. 1998
10141040	Hooper Slough near Hooper	All data prior to 1987
10141400	Howard Slough at Hooper	All data prior to 1987
10141500	Holmes Creek near Kaysville	All data prior to 1987
10142000	Farmington Creek above diversions, near Farmington	All data prior to 1987
10142500	Ricks Creek above diversions, near Centerville	All data prior to 1987
10143000	Parrish Creek above diversions, near Centerville	All data prior to 1987
10143500	Centerville Creek above diversions, near Centerville	All data prior to 1987
10144000	Stone Creek above diversions, near Bountiful	All data prior to 1987
10145000	Mill Creek at Mueller Park, near Bountiful	All data prior to 1987
10170500	Surplus Canal at Salt Lake City	Jan. 1987 to Dec. 1998
10170800	Surplus Canal at Cohen Flume, near Salt Lake City	All data prior to 1987
10171000	Jordan River at 1700 South, at Salt Lake City	Jan. 1987 to Dec. 1998
10172500	City Creek near Salt Lake City	Jan. 1987 to Dec. 1998
10172550	Jordan River at 500 North, at Salt Lake City	All data prior to 1987
10172630	Goggin Drain near Magna	All data prior to 1987
10172640	Lee Creek near Magna	Jan. 1987 to Dec. 1998
10172650	Kennecott Drain near Magna	Jan. 1987 to Dec. 1998

**Table A4.** Statistical summary of regression estimates of monthly surface-water inflow to Great Salt Lake, Utah, 1987–98

[acre-ft/month, acre-feet per month; acre-ft/year, acre-feet per year]

Site estimated (dependent variable)	Site measured for regression analysis (independent variable)	Regression units	Period of regression	Months for which regression is valid	Slope (A) <sup>1</sup>	Intercept (B) <sup>1</sup>	Correlation coefficient	Average of dependent variable, in acre-feet	Standard error of estimate	
									In acre-feet	As percentage of average of dependent variable
10127110	10126000	acre-ft/month	1972 to 1986	All months	1.0070	14,264	0.999	160,706	3,768	2
10141040	10141000	acre-ft/year	1975 to 1986	All months	.0062	8,704	.944	10,213	601	6
10141400	10141000	acre-ft/year	1972 to 1984	All months	.0171	12,985	.823	21,193	2,391	11
10141500	10172500	acre-ft/month	5/1950 to 9/1966	All months	.2434	14	.930	226	45	20
10142000	10172500	acre-ft/month	1/1950 to 10/1971	All months	1.3432	-435	.916	808	296	37
10142500	10172500	acre-ft/month	5/1950 to 9/1966	All months	.2187	-52	.937	137	37	27
10143000	10172500	acre-ft/month	1/1950 to 9/1968	All months	.1697	-53	.924	96	35	37
10143500	10172500	acre-ft/month	1/1950 to 9/1980	All months	.2177	-31	.943	183	43	24
10144000	10172500	acre-ft/month	5/1950 to 9/1966	All months	.3452	-102	.915	198	80	40
10145000	10172500	acre-ft/month	5/1950 to 9/1968	All months	.7227	-233	.953	401	123	31
10170800	10170500	acre-ft/month	10/1963 to 9/1968	Oct.-Nov.	1.1529	-2,657	.913	6,730	603	9
10170800	10170500	acre-ft/month	10/1963 to 9/1968	Dec.-Feb.	.8580	706	.976	7,092	367	5
10170800	10170500	acre-ft/month	10/1963 to 9/1968	Mar.-Jul.	.3661	2,561	.916	8,736	1,109	13
10170800	10170500	acre-ft/month	10/1963 to 9/1968	Aug.-Sep.	.3102	2,935	.329	6,935	1,833	26
10172550	10171000 +10172500	acre-ft/month	10/1974 to 9/1986	All months	1.0897	4,695	.553	16,056	5,630	35
10172630	10170500	acre-ft/month	10/1971 to 9/1984	All months	.5908	-2,535	.956	18,465	4,161	23

<sup>1</sup>Regression equation used in this table: Discharge at estimated site = A(Discharge at measured site) + B.

## Jordan River Basin

Inflow from the Jordan River Basin was separated into one part that flows into Farmington Bay and a second part that flows into the south part of Great Salt Lake. Flow from the Jordan River (10172550) and part of the flow from the Surplus Canal (10170800) enters Farmington Bay. Flow from the Jordan River at 500 North, at Salt Lake City (10172550, fig. 1) was estimated using a regression equation similar to equation A5 with the combined monthly flow at Jordan River at 1700 South, at Salt Lake City (10171000) and City

Creek near Salt Lake City (10172500) as the independent variable (table A4). The Surplus Canal at Cohen Flume, near Salt Lake City (10170800), was estimated using a regression equation with monthly flow at Surplus Canal at Salt Lake City (10170500) as the independent variable (table A4). The remainder of the Surplus Canal flow entered the main body of the south part of the lake through the Goggin Drain near Magna (10172630), and was estimated using a regression equation with monthly flow at Surplus Canal at Salt Lake City (10170500) as the independent variable (table A4).

**Table A5. Estimated monthly and annual inflow for all streams and canals to Great Salt Lake, Utah, 1987–98**

[In acre-feet; some values are estimated as described in table A4]

	JAN	FEB	MAR	APR	MAY	JUN	JUL	AUG	SEP	OCT	NOV	DEC	TOTAL
<b>10127110, Bear River Basin outflow across State Highway 83 near Corrine</b>													
1987	153,000	140,000	134,000	87,000	91,900	76,800	50,100	61,900	54,000	53,100	72,200	77,800	1,050,000
1988	84,400	77,900	82,300	105,000	53,900	22,900	21,900	20,700	29,200	54,800	53,100	59,000	665,000
1989	61,600	58,000	139,000	151,000	93,800	29,600	25,500	26,500	24,900	40,500	70,600	77,700	799,000
1990	92,600	65,400	83,400	69,300	32,600	31,800	21,900	20,800	23,900	39,100	58,300	54,400	593,000
1991	59,600	63,400	70,800	76,000	107,000	106,000	20,000	20,400	41,800	27,700	57,100	67,100	717,000
1992	58,800	60,900	72,400	52,500	18,700	18,900	19,300	17,700	18,000	20,200	54,200	53,800	465,000
1993	52,700	54,700	154,000	151,000	255,000	163,000	43,100	32,700	35,300	75,500	70,800	76,900	1,160,000
1994	84,100	79,900	115,000	110,000	40,000	22,300	18,700	18,800	20,400	49,100	51,500	47,400	658,000
1995	83,400	84,100	157,000	119,000	179,000	198,000	33,100	21,400	28,400	54,900	80,100	80,700	1,120,000
1996	75,800	97,900	129,000	181,000	180,000	164,000	30,000	22,400	40,400	57,800	79,700	143,000	1,200,000
1997	185,000	120,000	179,000	244,000	359,000	310,000	101,000	112,000	126,000	167,000	179,000	162,000	2,240,000
1998	193,000	170,000	221,000	258,000	339,000	268,000	92,800	69,000	101,000	157,000	167,000	173,000	2,210,000
<b>10141000, Weber River near Plain City</b>													
1987	28,900	20,500	52,500	26,100	9,430	6,520	3,900	4,250	5,030	6,430	6,360	5,080	175,000
1988	4,490	4,730	4,500	3,550	2,750	2,200	1,720	2,010	3,590	1,680	2,690	2,570	36,500
1989	2,170	2,270	11,900	14,600	11,400	2,610	2,030	2,790	5,090	9,190	9,970	5,110	79,100
1990	4,220	4,510	4,790	4,970	7,200	4,820	5,700	5,220	4,930	6,790	8,210	4,340	65,700
1991	3,480	3,970	4,460	4,250	8,690	20,700	3,950	5,490	10,800	9,370	11,600	10,300	97,000
1992	6,930	10,700	5,120	6,440	6,720	5,170	4,890	5,160	6,090	6,300	8,500	4,810	76,800
1993	4,540	6,410	15,300	23,700	114,000	72,600	8,630	6,520	7,860	15,900	11,100	7,310	294,000
1994	6,850	8,970	31,700	50,900	30,300	5,990	4,260	4,640	5,700	10,700	11,500	10,400	182,000
1995	10,100	11,900	58,600	36,700	81,700	121,000	33,200	7,000	8,810	11,100	11,800	19,500	412,000
1996	28,800	68,600	75,900	74,900	25,300	23,900	7,610	6,700	11,200	16,400	17,500	27,200	384,000
1997	48,700	33,600	74,900	83,700	121,000	97,200	8,780	10,700	13,400	10,200	12,200	26,300	540,000
1998	29,000	16,400	47,200	119,000	129,000	129,000	27,200	9,340	12,800	24,600	18,000	16,900	579,000
<b>10141040, Hooper Slough near Hooper</b>													
1987	507	660	946	547	1,070	1,100	1,030	1,110	1,050	705	473	586	9,790
1988	462	603	863	499	972	1,000	942	1,020	962	644	431	534	8,930
1989	476	620	889	514	1,000	1,030	970	1,050	991	663	444	550	9,200
1990	471	615	881	510	992	1,020	961	1,040	982	657	440	545	9,110
1991	482	628	900	520	1,010	1,040	981	1,060	1,000	671	449	557	9,310
1992	475	619	887	513	1,000	1,030	968	1,040	989	662	443	549	9,180
1993	545	710	1,020	589	1,150	1,180	1,110	1,200	1,130	759	508	630	10,500
1994	509	663	950	550	1,070	1,100	1,040	1,120	1,060	708	475	588	9,830
1995	583	760	1,090	630	1,230	1,260	1,190	1,280	1,210	811	544	674	11,300
1996	574	748	1,070	620	1,210	1,240	1,170	1,260	1,190	799	535	663	11,100
1997	624	813	1,170	674	1,310	1,350	1,270	1,370	1,300	868	582	721	12,100
1998	636	829	1,190	687	1,340	1,380	1,300	1,400	1,320	886	594	736	12,300
<b>10141400, Howard Slough at Hooper</b>													
1987	1,160	1,400	1,880	1,080	1,510	1,480	1,220	1,380	1,610	1,140	962	1,150	16,000
1988	990	1,190	1,600	921	1,290	1,260	1,040	1,170	1,370	972	819	978	13,600
1989	1,040	1,260	1,690	971	1,360	1,330	1,090	1,240	1,440	1,020	863	1,030	14,300
1990	1,030	1,240	1,660	955	1,330	1,310	1,080	1,220	1,420	1,010	850	1,010	14,100
1991	1,070	1,280	1,730	991	1,380	1,360	1,120	1,260	1,470	1,050	882	1,050	14,600
1992	1,040	1,250	1,690	968	1,350	1,330	1,090	1,230	1,440	1,020	861	1,030	14,300
1993	1,310	1,580	2,120	1,220	1,700	1,670	1,370	1,550	1,810	1,290	1,080	1,290	18,000
1994	1,170	1,410	1,900	1,090	1,520	1,500	1,230	1,390	1,620	1,150	969	1,160	16,100
1995	1,460	1,750	2,360	1,360	1,890	1,860	1,530	1,730	2,020	1,430	1,210	1,440	20,000
1996	1,420	1,710	2,310	1,320	1,850	1,820	1,490	1,690	1,970	1,400	1,180	1,410	19,600
1997	1,620	1,950	2,620	1,500	2,100	2,070	1,690	1,920	2,240	1,590	1,340	1,600	22,200
1998	1,670	2,000	2,700	1,550	2,160	2,130	1,740	1,970	2,300	1,640	1,380	1,650	22,900

**Table A5.** Estimated monthly and annual inflow for all streams and canals to Great Salt Lake, Utah, 1987-98—Continued

	JAN	FEB	MAR	APR	MAY	JUN	JUL	AUG	SEP	OCT	NOV	DEC	TOTAL
<b>Combined flow at streamflow-gaging stations 10141500, 10142000, 10142500, 10143000, 10143500, 10144000, and 10145000<sup>1</sup></b>													
<b>(Davis County streams)</b>													
1987	1,080	895	1,330	2,310	4,250	2,160	1,560	1,090	777	898	879	833	18,100
1988	784	660	843	1,040	2,390	1,500	771	409	308	461	507	494	10,200
1989	432	327	1,600	2,800	5,270	2,480	1,390	764	442	526	520	530	17,100
1990	445	380	598	901	1,490	1,350	823	481	354	383	402	337	7,940
1991	402	354	549	1,040	4,490	7,320	2,110	1,220	875	693	699	673	20,400
1992	820	552	833	1,150	1,630	963	608	334	275	282	282	327	8,060
1993	233	145	1,470	2,510	12,600	10,300	4,010	2,000	849	729	631	575	36,000
1994	458	285	820	2,440	5,050	2,300	1,130	526	331	389	301	468	14,500
1995	504	976	2,760	3,230	9,220	15,800	5,640	2,560	1,340	1,120	879	748	44,800
1996	673	709	1,730	3,970	10,000	6,700	2,830	1,560	986	830	777	830	31,600
1997	826	647	1,740	2,910	11,400	6,500	2,980	1,680	947	839	663	660	31,800
1998	650	504	2,120	4,360	12,500	12,300	6,440	3,130	1,690	1,740	1,100	1,170	47,700
<b>10170800, Surplus Canal at Cohen Flume, near Salt Lake City</b>													
1987	72,300	64,600	32,500	21,100	19,000	10,300	10,600	9,450	8,140	15,400	12,500	10,800	287,000
1988	11,400	9,940	7,090	7,970	11,500	7,830	7,030	7,370	7,350	10,900	9,050	9,450	107,000
1989	6,430	5,930	5,710	5,980	10,200	9,020	7,000	6,580	6,940	10,200	7,180	7,750	88,900
1990	7,610	4,750	6,070	6,480	7,660	8,780	6,410	6,240	6,440	8,460	6,730	9,200	84,800
1991	7,060	7,540	5,600	6,800	11,400	15,500	6,340	6,690	8,310	12,600	11,400	8,810	108,000
1992	7,820	8,390	5,870	5,790	8,830	7,120	6,490	5,700	5,500	6,920	10,200	9,770	88,400
1993	13,200	13,800	9,580	9,340	27,100	21,800	11,800	7,440	7,640	15,400	10,600	9,190	157,000
1994	7,350	8,100	6,270	8,660	11,000	8,970	6,610	6,800	6,250	13,000	10,000	8,250	101,000
1995	9,100	10,900	9,870	10,400	15,900	40,000	29,200	9,410	8,190	15,800	9,680	11,800	180,000
1996	32,400	44,700	26,000	25,300	26,200	26,200	9,820	7,400	8,040	11,900	9,540	19,400	247,000
1997	42,900	48,300	27,800	27,000	37,200	41,800	18,300	9,110	8,810	19,200	60,800	41,300	383,000
1998	47,700	51,500	31,000	32,800	37,400	48,700	37,300	15,800	10,700	26,700	65,800	52,300	458,000
<b>10172550, Jordan River at 500 North, at Salt Lake City</b>													
1987	15,500	13,700	14,000	16,000	14,700	13,600	14,800	14,200	14,600	13,600	12,300	12,600	170,000
1988	11,300	12,200	11,500	11,300	13,800	15,600	16,000	16,300	14,900	13,000	11,900	11,700	159,000
1989	15,500	17,400	17,700	16,400	20,800	20,300	19,200	19,100	16,300	14,900	14,000	13,900	205,000
1990	13,800	15,500	12,800	12,700	14,300	19,700	17,600	16,100	14,600	14,300	13,600	11,900	177,000
1991	13,000	12,100	13,700	12,900	17,200	24,200	19,100	19,400	17,400	16,900	15,100	14,900	196,000
1992	14,300	14,400	15,100	14,100	14,600	13,100	15,900	14,000	12,100	11,600	12,100	10,100	161,000
1993	8,700	9,070	11,500	11,900	14,400	15,100	18,100	16,600	14,700	15,500	13,200	14,500	163,000
1994	15,400	13,400	13,700	14,500	15,000	14,600	14,100	12,900	12,300	13,400	12,200	13,000	164,000
1995	13,100	12,000	13,400	11,200	15,200	13,900	14,800	13,500	14,800	13,200	12,100	10,300	158,000
1996	13,200	15,700	15,100	14,500	16,000	17,400	15,100	12,700	12,500	13,300	12,900	14,100	173,000
1997	13,800	14,400	14,700	14,500	18,300	18,400	15,900	13,900	13,700	13,700	16,200	17,100	184,000
1998	16,400	14,500	16,300	16,200	17,800	18,200	18,000	16,700	15,300	15,500	16,100	16,500	197,000
<b>10172630, Goggin Drain near Magna</b>													
1987	46,800	41,400	45,800	27,400	24,000	9,920	10,400	9,870	7,380	6,710	5,250	4,420	239,000
1988	4,820	3,820	4,780	6,200	11,900	5,960	4,680	5,910	5,870	4,400	3,460	3,490	65,200
1989	1,410	1,060	2,550	2,990	9,740	7,890	4,630	4,410	5,090	4,050	2,500	2,320	48,600
1990	2,220	248	3,130	3,790	5,700	7,510	3,680	3,750	4,140	3,160	2,270	3,310	42,900
1991	1,840	2,170	2,360	4,300	11,700	18,400	3,560	4,610	7,710	5,290	4,680	3,040	69,700
1992	2,360	2,760	2,810	2,680	7,580	4,830	3,800	2,740	2,360	2,370	4,030	3,700	42,000
1993	6,090	6,490	8,800	8,410	37,100	28,600	12,400	6,050	6,430	6,710	4,250	3,310	135,000
1994	2,040	2,560	3,450	7,310	11,100	7,800	3,990	4,830	3,780	5,460	3,980	2,660	59,000
1995	3,240	4,470	9,260	10,100	19,100	58,000	40,400	9,800	7,470	6,950	3,790	5,110	178,000
1996	19,300	27,700	35,300	34,200	35,600	35,600	9,180	5,960	7,190	4,930	3,720	10,400	229,000
1997	26,500	30,200	38,200	36,900	53,400	60,700	22,900	9,220	8,660	9,790	30,000	25,400	352,000
1998	29,800	32,500	43,300	46,200	53,700	71,900	53,500	21,900	12,300	12,500	32,600	33,000	443,000

**Table A5.** Estimated monthly and annual inflow for all streams and canals to Great Salt Lake, Utah, 1987-98—Continued

	JAN	FEB	MAR	APR	MAY	JUN	JUL	AUG	SEP	OCT	NOV	DEC	TOTAL
<b>Combined flow at streamflow-gaging stations 10172640 (Lee Creek near Magna) and 10172650 (Kennecott Drain near Magna)<sup>2</sup></b>													
1987	4,800	4,300	4,800	4,600	4,800	4,600	4,800	4,800	4,600	4,800	4,600	4,800	56,300
1988	4,800	4,300	4,800	4,600	4,800	4,600	4,800	4,800	4,600	4,800	4,600	4,800	56,300
1989	4,800	4,300	4,800	4,600	4,800	4,600	4,800	4,800	4,600	4,800	4,600	4,800	56,300
1990	4,800	4,300	4,800	4,600	4,800	4,600	4,800	4,800	4,600	4,800	4,600	4,800	56,300
1991	4,800	4,300	4,800	4,600	4,800	4,600	4,800	4,800	4,600	4,800	4,600	4,800	56,300
1992	4,800	4,300	4,800	4,600	4,800	4,600	4,800	4,800	4,600	4,800	4,600	4,800	56,300
1993	4,800	4,300	4,800	4,600	4,800	4,600	4,800	4,800	4,600	4,800	4,600	4,800	56,300
1994	4,800	4,300	4,800	4,600	4,800	4,600	4,800	4,800	4,600	4,800	4,600	4,800	56,300
1995	4,800	4,300	4,800	4,600	4,800	4,600	4,800	4,800	4,600	4,800	4,600	4,800	56,300
1996	4,800	4,300	4,800	4,600	4,800	4,600	4,800	4,800	4,600	4,800	4,600	4,800	56,300
1997	4,800	4,300	4,800	4,600	4,800	4,600	4,800	4,800	4,600	4,800	4,600	4,800	56,300
1998	4,800	4,300	4,800	4,600	4,800	4,600	4,800	4,800	4,600	4,800	4,600	4,800	56,300
<b>Outflow from Salt Lake City water-reclamation plant<sup>3</sup></b>													
1987	3,520	3,370	3,600	3,430	3,880	3,730	3,350	3,310	3,080	2,940	2,710	2,570	39,500
1988	2,850	2,960	3,070	3,390	3,460	3,460	3,340	3,330	2,880	2,720	2,570	2,410	36,500
1989	2,910	2,870	3,430	3,150	3,500	3,470	3,500	3,460	3,090	3,180	3,000	2,840	38,400
1990	2,900	2,620	3,190	3,130	3,240	3,280	3,380	3,340	2,990	3,040	2,850	2,740	36,700
1991	2,930	2,700	3,040	3,460	4,160	3,960	3,970	3,860	3,680	3,400	3,450	3,340	42,000
1992	3,190	3,240	3,400	3,210	3,290	3,170	3,210	3,220	2,870	2,820	2,850	3,000	37,500
1993	2,970	3,560	4,010	3,450	4,320	3,320	3,330	3,190	2,830	3,110	2,700	2,780	39,600
1994	2,980	2,800	3,320	3,500	3,340	3,100	3,030	3,050	2,790	3,010	3,140	3,360	37,400
1995	3,470	3,290	3,770	3,540	4,060	3,690	3,430	3,300	3,080	3,060	2,860	2,950	40,500
1996	3,160	3,640	4,280	4,030	3,720	3,320	3,400	3,220	3,030	2,970	2,980	3,250	41,000
1997	3,440	3,240	3,430	3,470	3,730	3,700	3,470	3,410	3,190	3,330	2,960	3,080	40,500
1998	3,490	3,660	5,000	4,480	3,930	4,300	3,810	3,510	3,140	3,170	3,120	3,100	44,700
<b>Outflow from Willard Bay Reservoir<sup>4</sup></b>													
1987	0	0	0	6,200	0	0	0	0	0	0	0	0	6,200
1988	0	0	0	0	0	0	0	0	0	0	0	0	0
1989	0	0	0	0	0	0	0	0	0	0	0	0	0
1990	0	0	0	0	0	0	0	0	70	234	420	434	1,160
1991	772	3,290	4,020	1,530	7,620	12,400	4,780	6,680	1,500	355	450	465	43,900
1992	403	377	403	390	430	376	372	371	330	476	480	496	4,900
1993	496	411	328	390	24,500	10,900	459	478	480	5,940	10,600	3,700	58,700
1994	10,800	336	5,550	17,300	11,100	550	558	972	1,080	1,120	918	520	50,800
1995	426	392	434	9,940	50,000	32,400	434	434	478	1,100	1,200	1,120	98,400
1996	496	464	21,200	48,400	17,100	582	768	600	508	552	582	2,790	94,100
1997	27,800	56,000	51,500	57,700	18,300	1,540	580	465	300	2,360	10,600	6,200	233,000
1998	8,480	31,400	36,000	38,600	31,100	14,800	3,550	6,270	4,440	3,290	3,040	11,200	192,000

<sup>1</sup>Based on City Creek data provided by Salt Lake City.<sup>2</sup>Reported by Kennecott Utah Copper.<sup>3</sup>Reported by Salt Lake City.<sup>4</sup>Reported by Weber Basin Conservancy District.

**Table A6.** Estimated monthly and annual surface-water inflow to Great Salt Lake, Utah, 1987–98

[In acre-feet]

	JAN	FEB	MAR	APR	MAY	JUN	JUL	AUG	SEP	OCT	NOV	DEC	TOTAL
1987	328,000	291,000	291,000	196,000	174,000	130,000	102,000	111,000	100,000	106,000	118,000	121,000	2,070,000
1988	126,000	118,000	121,000	145,000	107,000	66,300	62,300	63,100	71,000	94,300	89,100	95,400	1,160,000
1989	96,800	94,000	190,000	203,000	162,000	82,300	70,100	70,700	68,800	89,100	114,000	117,000	1,360,000
1990	130,000	99,600	121,000	107,000	79,400	84,100	66,300	63,100	64,400	81,900	98,700	93,000	1,090,000
1991	95,500	102,000	112,000	116,000	179,000	215,000	70,600	75,400	99,200	82,900	110,000	115,000	1,370,000
1992	101,000	108,000	113,000	92,300	68,900	60,600	61,400	56,200	54,500	57,400	98,500	92,500	964,000
1993	95,600	101,000	213,000	218,000	497,000	333,000	109,000	82,500	83,700	146,000	130,000	125,000	2,130,000
1994	136,000	123,000	188,000	221,000	134,000	72,800	59,500	59,900	59,900	103,000	99,600	92,600	1,350,000
1995	130,000	135,000	263,000	211,000	382,000	491,000	168,000	75,200	80,400	114,000	129,000	139,000	2,320,000
1996	181,000	266,000	317,000	393,000	321,000	285,000	86,200	68,300	91,600	116,000	134,000	228,000	2,490,000
1997	356,000	314,000	400,000	477,000	630,000	548,000	182,000	168,000	183,000	233,000	319,000	289,000	4,100,000
1998	336,000	327,000	410,000	526,000	633,000	575,000	250,000	154,000	169,000	252,000	313,000	314,000	4,260,000

**Other Surface-Water Inflow**

Monthly inflows at Hooper Slough near Hooper (10141040) and Howard Slough at Hooper (10141400) were estimated using regression equations similar to A5 with monthly flow at Weber River at Plain City (10141000) as the independent variable (table A4). Monthly flow for the seven perennial streams in Davis County (fig. 1 and table A5) between the Weber River and the Jordan River was estimated using regression equations for each stream that relate monthly flow at City Creek (10172500) to monthly flow at each stream (table A4). Most of the water in the Davis County streams is diverted for irrigation or municipal use at the point where the streams emerge from the canyons onto the benches of the East Shore area. Monthly flow used in the water balance is the estimated flow at the mouths of the canyons, before any diversions. Although most flow at the canyon mouths usually does not reach Great Salt Lake, it can be used as an estimate of the relative amount of irrigation return flow.

The Salt Lake City water-reclamation plant releases water to Great Salt Lake, and estimates of that flow were obtained from records at the plant. Monthly flows at Lee Creek near Magna (10172640) and Kennecott Drain near Magna (10172650) were provided by Kennecott Utah Copper.

**Ground-Water Inflow**

Ground-water inflow ( $GIN + GIS$ , eqs. A1 and A2) to Great Salt Lake was estimated to be 75,000 acre-ft/yr (table A7). The estimates were based on the previous water-balance study of Great Salt Lake (Waddell and Fields, 1977, p. 22). This inflow was subdivided for Farmington Bay, Bear River Bay, the shoreline extending from Bear River Bay to Syracuse, and the south and north parts of the lake.

**Table A7.** Estimated ground-water inflow to Great Salt Lake, Utah, 1987–98

(From Waddell and Fields, 1977, table 8)

Area of inflow	Monthly inflow, in acre-feet	Annual inflow, in acre-feet
Farmington Bay	2,290	27,500
Bear River Bay	1,250	15,000
Bear River Bay to Syracuse	1,000	12,000
South part of Great Salt Lake	870	10,500
North part of Great Salt Lake	830	9,960
Total monthly	6,240	
Total annual (rounded)		75,000

## Precipitation

Inflow precipitation directly on the water surface of Great Salt Lake ( $PIN + PIS$ , eqs. A1 and A2) was estimated using the method of Waddell and Fields (1977, p. 6 and 7), which was modified by Wold, Thomas, and Waddell (1997, p. 29) as follows:

1. Waddell and Fields (1977) compiled average annual precipitation data for 1931–73 from 68 sites in a large area surrounding the lake. A multiple regression equation was developed to estimate average annual precipitation as a function of latitude, longitude, and altitude. By using the equation, lines of equal average annual precipitation during 1931–73 were drawn for the lake (Waddell and Fields, 1977, fig. 3). The relative distribution of average annual precipitation for 1987–98 was assumed to be the same as for 1931–73.
2. The surface area of the lake varies with water-surface altitude, and precipitation varies areally across the lake; thus, inflow from precipitation on the lake varies according to water-surface altitude. Waddell and Fields (1977, p. 6) derived values of average annual precipitation for four altitudes ranging from 4,195 to 4,205 ft for the south and north parts of the lake. Wold, Thomas, and Waddell (1997) estimated the average annual precipitation (1931–73) for a water-surface altitude of 4,212 ft (table A7).
3. Waddell and Fields (1977, p. 6 and 7) estimated annual total precipitation on the lake for each year of the study as a fraction of average annual precipitation. Monthly precipitation for each year was estimated as a fraction of the annual total. The fraction used for each month (Waddell and Fields, 1977, fig. 4) was an average value and was the same for all years of the study.

Wold, Thomas, and Waddell (1997) found that the monthly distribution of precipitation for 1980–86 was substantially different from the average monthly distribution used by Waddell and Fields (1977, p. 7, fig. 4). Therefore, in the water balance, monthly precipitation for the lake was estimated by using an average ratio index ( $PRT$ ) determined from measured monthly precipitation at three sites around the lake (Salt Lake City

Airport, Ogden Sugar Factory, and the city of Tooele; fig. 1). This modification also was used in this report for 1987–98.

The derivation of the equation used in the water balance to estimate monthly precipitation for the south and north parts of the lake is shown in equations A6–A8. The ratio is the measured monthly precipitation at a specified precipitation site to the average annual precipitation (1931–73) at the same site.

$$PRT = [(PMSLC/PAASLC) + (PMOGSF/PAAOGSF) + (PMTOOL/PAATool)]/3, \quad (A6)$$

where

- $PRT$  = average ratio index for precipitation;
- $PMSLC$  = measured monthly precipitation at Salt Lake City Airport, in inches;
- $PAASLC$  = average annual precipitation (1931–73) at Salt Lake City Airport, in inches;
- $PMOGSF$  = measured monthly precipitation at Ogden Sugar Factory, in inches;
- $PAAOGSF$  = average annual precipitation (1931–73) at Ogden Sugar Factory, in inches;
- $PMTOOL$  = measured monthly precipitation at Tooele, in inches; and
- $PAATool$  = average annual precipitation (1931–73) at Tooele, in inches.

The equations used in the water balance to estimate monthly precipitation for the south and north parts, in acre-ft/d are

$$PIS = PRT * PAAS * CF * AS / CM \quad (A7)$$

and

$$PIN = PRT * PAAN * CF * AN / CM, \quad (A8)$$

where

- $PIS$  = precipitation on south part, in acre-ft/d;
- $PIN$  = precipitation on north part, in acre-ft/d;
- $PRT$  = average ratio index (see eq. A6);
- $PAAS$  = average annual precipitation (1931–73) for the south part of the lake, interpolated from table A8 by using water-surface altitude, in inches;
- $PAAN$  = average annual precipitation (1931–73) for the north part of the lake, interpolated from table A8 by using water-surface altitude, in inches;
- $CF$  = 1/12 (conversion between in. and ft); in ft per inch;
- $AS$  = area of south part for time step  $I$ , esti-

**Table A8.** Average annual precipitation and evaporation of freshwater for selected water-surface altitudes of Great Salt Lake, Utah, 1987–98

[PAAS: Average annual precipitation for south part; EAAS: Average annual freshwater evaporation from south part; PAAN: Average annual precipitation for north part; EAAN: Average annual freshwater evaporation from north part]

Water-surface altitude, in feet	Precipitation, in inches <sup>1</sup>	Evaporation, in inches <sup>2</sup>
<b>South part</b>	<b>PAAS</b>	<b>EAAS</b>
4,212	12.60	55.07
4,205	12.98	55.98
4,199	13.46	56.25
4,196	13.70	56.39
4,195	13.74	56.41
<b>North part</b>	<b>PAAN</b>	<b>EAAN</b>
4,212	10.67	63.14
4,205	10.66	62.72
4,199	10.80	62.09
4,196	11.08	61.48
4,195	11.13	61.32

<sup>1</sup>Average annual precipitation for 1987–98 was assumed to be the same as for 1931–73.

<sup>2</sup>Average annual evaporation for 1987–98 was assumed to be the same as for 1931–73, except for June through September evaporation.

mated from south part water-surface altitude (table A1), in acres;

$AN$  = area of north part for time step  $I$ , estimated from north part water-surface altitude (table A1), in acres; and

$CM$  = time interval (in this case, 365/12 days, about 1 month), in days.

## Evaporation

Evaporation ( $EON + EOS$ , eqs. A1, A2, A9, and A10) from Great Salt Lake was estimated with the same method used by Waddell and Fields (1977, p. 7–11). The pan-evaporation records for 1987–98 were examined for Bear River Bird Refuge, Saltair, Utah Lake at Lehi, Provo-BYU, and the IMC Kalium Bear River Bay site (fig. 1). By 1995, none of the original evaporation sites used by Waddell and Fields (1977) (Bear River Bird Refuge, Saltair, and Utah Lake at Lehi) were still in operation. To maintain continuity in the data sites used for estimation of Great Salt Lake evaporation, the original sites were related to sites with overlapping

record. The Bear River Bird Refuge site was related to the IMC Kalium Bear River Bay site with a correlation coefficient of 0.90 (11 years of overlapping record used); Saltair was related to Bear River Bird Refuge site (estimated for this period as described above) with a correlation coefficient of 0.96 (20 years of overlapping record used); and the Utah Lake at Lehi site was related to the Provo-BYU site with a correlation coefficient of 0.86 (14 years of overlapping record used). The fractions of annual evaporation for each month during 1987–98 were similar to the average fractions for 1931–73 used by Waddell and Fields (1977, fig. 4). The average fractions of June through September pan evaporation were used to estimate annual evaporation from the lake.

The following equations are used in the water balance to estimate monthly evaporation for the south and north parts, respectively, in acre-ft:

$$EOS = EAAS \cdot EAI \cdot EMI \cdot CF \cdot AS \cdot SCFS / CM \quad (A9)$$

and

$$EON = EAAN \cdot EAI \cdot EMI \cdot CF \cdot AN \cdot SCFN / CM, \quad (A10)$$

where

$EOS$  = evaporation from south part, in acre-ft/d;

$EON$  = evaporation from north part, in acre-ft/d;

$EAAS$  = average annual freshwater evaporation from south part, interpolated from table A8 by using water-surface altitude, in inches;

$EAAN$  = average annual freshwater evaporation from north part, interpolated from table A8 by using water-surface altitude, in inches;

$EAI$  = fraction of average annual evaporation (average of the three sites in table A9);

$EMI$  = fraction of average monthly evaporation, from Waddell and Fields (1977, fig. 4);

$CF$  = 1/12 (conversion between in. and ft), in ft/in;

$AS$  = area of south part for time step  $I$ , estimated from south part water-surface altitude (table A1), in acres;

$AN$  = area of north part for time step  $I$ , estimated from north part water-surface altitude (table A1), in acres;

$SCFS$  = salinity correction factor for evaporation rate in the south part;

$SCFN$  = salinity correction factor for evaporation

**Table A9.** Pan evaporation and percentage of mean pan evaporation (1931–73) for five sites near Great Salt Lake, Utah, June through September 1987–98

[Mean pan evaporation for 1931–73 was estimated by Waddell and Fields (1977, p. 7 and table 12)]

Year	Bear River Bird Refuge		Saltair		Utah Lake at Lehi		Provo-BYU <sup>1</sup>		IMC Kalium Bear River Bay site <sup>1</sup>	
	Evaporation, in inches	Percent of mean	Evaporation, in inches	Percent of mean	Evaporation, in inches	Percent of mean	Evaporation, in inches	Percent of mean	Evaporation, in inches	Percent of mean
1987	<sup>2</sup> 31.01	82	43.57	81	32.89	91	32.09	<sup>3</sup> 85	44.88	<sup>3</sup> 80
1988	<sup>2</sup> 34.77	92	50.50	94	34.88	96	34.92	<sup>3</sup> 93	51.25	<sup>3</sup> 92
1989	<sup>2</sup> 33.46	89	48.40	90	37.18	102	35.22	<sup>3</sup> 94	49.04	<sup>3</sup> 88
1990	<sup>2</sup> 34.91	93	50.72	94	33.13	91	32.51	<sup>3</sup> 87	51.48	<sup>3</sup> 92
1991	<sup>2</sup> 31.56	84	45.70	85	31.48	87	31.92	<sup>3</sup> 85	45.80	<sup>3</sup> 82
1992	<sup>2</sup> 34.08	91	<sup>2</sup> 47.80	89	30.61	84	32.67	<sup>3</sup> 87	50.09	<sup>3</sup> 90
1993	<sup>2</sup> 29.91	80	<sup>2</sup> 37.05	69	31.44	87	32.81	<sup>3</sup> 87	43.01	<sup>3</sup> 77
1994	<sup>2</sup> 35.56	95	<sup>2</sup> 56.98	106	32.55	90	36.38	<sup>3</sup> 97	52.58	<sup>3</sup> 94
1995	<sup>2</sup> 32.35	86	<sup>2</sup> 43.65	81	<sup>2</sup> 31.82	88	33.31	<sup>3</sup> 89	47.16	<sup>3</sup> 84
1996	<sup>2</sup> 33.31	89	<sup>2</sup> 47.60	88	<sup>2</sup> 32.02	88	33.58	<sup>3</sup> 89	48.76	<sup>3</sup> 87
1997	<sup>2</sup> 28.33	75	<sup>2</sup> 37.79	70	<sup>2</sup> 29.85	82	30.75	<sup>3</sup> 82	40.37	<sup>3</sup> 72
1998	<sup>2</sup> 27.41	73	<sup>2</sup> 37.30	69	<sup>2</sup> 29.74	82	30.61	<sup>3</sup> 81	49.99	<sup>3</sup> 90

<sup>1</sup> Data not collected at these sites for most or all of 1931–73; estimated June through September mean pan evaporation (1931–73) based on regression equations.

<sup>2</sup> Data estimated, based on a regression with another site.

<sup>3</sup> Average 1931–73 evaporation based on a regression with another site.

rate in the north part; and

$CM$  = time interval (in this case, 365/12 days, about 1 month), in days.

The correction factors for salinity ( $SCFS$  and  $SCFN$  in eqs. A11 and A12, respectively) were estimated for each month from measurements of dissolved-solids concentration made about twice a year. The measurements were plotted on a graph, a smooth curve was drawn through the measurements, and individual monthly salinity values were obtained from the curve. The salinity correction factors were estimated with the following equations by using data from Adams (1934) and developed by Waddell and Bolke (1973):

$$SCFS = (1 - 0.778 \text{ } CS / \rho_s) \quad (\text{A11})$$

$$SCFN = (1 - 0.778 \text{ } CN / \rho_n) \quad (\text{A12})$$

where

$SCFS$  = salinity correction factor for evaporation rate in the south part;

$SCFN$  = salinity correction factor for evaporation rate in the north part;

$CS$  = dissolved-solids concentration in the south part, in g/L;

$CN$  = dissolved-solids concentration in the north part, in g/L;

$\rho_s$  = density of brine in south part at any temperature, in g/mL; and

$\rho_n$  = density of brine in north part at any temperature, in g/mL.

## West Desert Pumping Project

From April 10, 1987, to June 30, 1989, water was pumped from the north part of the lake into West Pond in an effort to lower lake levels during a period of substantially higher than normal inflow. The West Desert Pumping Project removed more than 2.5 million acre-ft of water and 695 million tons of salt from the lake during a 27-month period (Wold and Waddell, 1994). From January 1990 to June 1992, 200,000 acre-ft of water and 94 million tons of salt returned to the lake from West Pond.

## Calibration

A water balance between the south and north parts of Great Salt Lake was calibrated for 1987–98 by using monthly surface- and ground-water inflow (*SIS*, *GIS*, and *GIN*), precipitation (*PIS* and *PIN*), evaporation (*EOS* and *EON*), losses to and gains from West Pond (*QWP*), and net flow through the causeway (*QS* - *QN*). The water balance is used to test the independent estimates of monthly inflow, precipitation, and evaporation so that simulated water-surface altitudes for the south part reasonably match measured water-surface altitudes. By estimating the volume of the north part (*VN*) from the measured water-surface altitude of the north part (*EN*), all the error in the water balance simulations (from both the south and north parts) appeared as error in the simulations of the volume of the south part (*VS*) and the subsequent water-surface altitude of the south part (*ES*).

Change in volume of the north part ( $\Delta VN$ ) was estimated from the difference in measured water-surface altitude in the north part from the beginning to the end of the time interval (*CM*) by using the altitude-area-volume relations (table A1). After the change in volume of the north part ( $\Delta VN$ ), ground-water inflow (*GIN*), precipitation (*PIN*), West Pond exchange (*QWP*), and evaporation (*EON*) for the north part were estimated, equation A13 (rearranged from eq. A2) was used to solve for net flow through the causeway (*QS* - *QN*), in acre-ft/d.

$$(QS - QN) = \Delta VN / CM - PIN - GIN + EON + QWP \quad (A13)$$

where

- QS* = total flow from south-to-north through causeway, in acre-ft/d;
- QN* = total flow from north-to-south through causeway, in acre-ft/d;
- $\Delta VN$  =  $VN(I+1) - VN(I)$  = change in volume of north part, in acre-ft;
- CM* = time interval (in this case, 365/12 days, about 1 month), in days;
- PIN* = precipitation on north part, in acre-ft/d;
- GIN* = ground-water inflow to north part, in acre-ft/d;
- EON* = evaporation from north part, in acre-ft/d; and
- QWP* = discharge to (+), or return flow from (-) West Pond in acre-ft/d.

Net flow through the causeway (*QS* - *QN*) is the difference between total flow through the causeway from south to north (*QS*) and total flow through the causeway from north to south (*QN*). To simulate the water-surface altitude of the south part, only the difference between *QS* and *QN* needs to be known. For convenience, net flow through the causeway was always assumed to be a positive value of south-to-north flow. After the net flow through the causeway (*QS* - *QN*) and the surface- and ground-water inflow (*SIS* and *GIS*), precipitation (*PIS*), and evaporation (*EOS*) for the south part were estimated, equation A14 (rearranged from eq. A1) was used to compute change in volume of the south part,  $\Delta VS$ , in acre-ft, as follows:

$$\Delta VS = [SIS + PIS + GIS - EOS - (QS - QN)]CM \quad (A14)$$

where

- $\Delta VS$  =  $VS(I+1) - VS(I)$  = change in volume of south part, in acre-ft;
- SIS* = surface-water inflow to south part, in acre-ft/d;
- PIS* = precipitation on south part, in acre-ft/d;
- GIS* = ground-water inflow to south part, in acre-ft/d;
- EOS* = evaporation from south part, in acre-ft/d; and
- CM* = time interval (in this case, 365/12 days, about 1 month), in days.

Initial estimates of inflow and outflow resulted in simulated water-surface altitudes that were a maximum of about 2 ft higher than measured water-surface altitudes (fig. A2); thus, the water balance included either too much inflow or too little outflow (evaporation). Because evaporation is determined indirectly from pan evaporation and has potentially greater error than inflow, calibration of the water balance was achieved by adjusting the evaporation rate each year and then comparing simulated and measured water-surface altitudes of the south part. Evaporation rate adjustments ranged from -6 percent to +8 percent of the annual values estimated from pan-evaporation records, with 3 years requiring no adjustment (fig. A2). The simulated water-surface altitudes reasonably matched measured water-surface altitudes in all years of the calibration period (fig. A3).

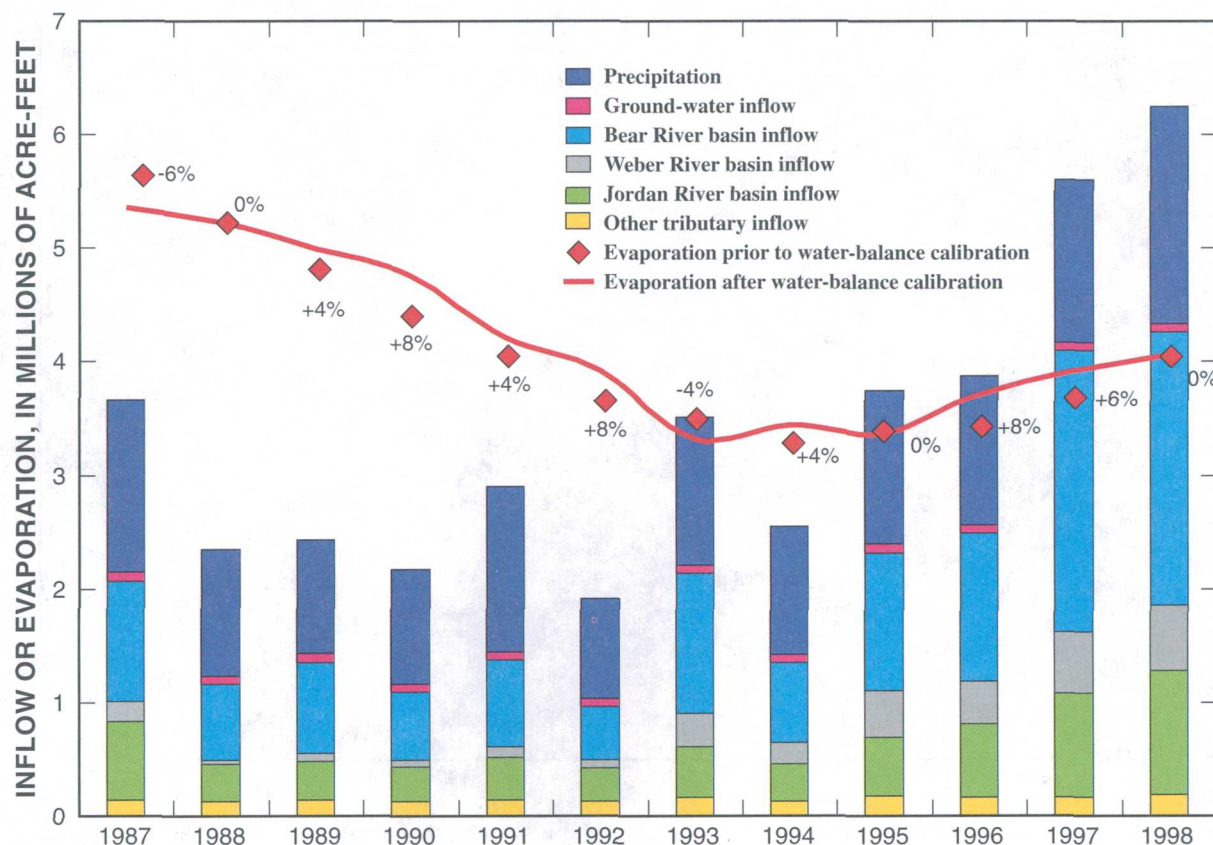


Figure A2. Inflow and evaporation for Great Salt Lake, Utah, 1987–98.

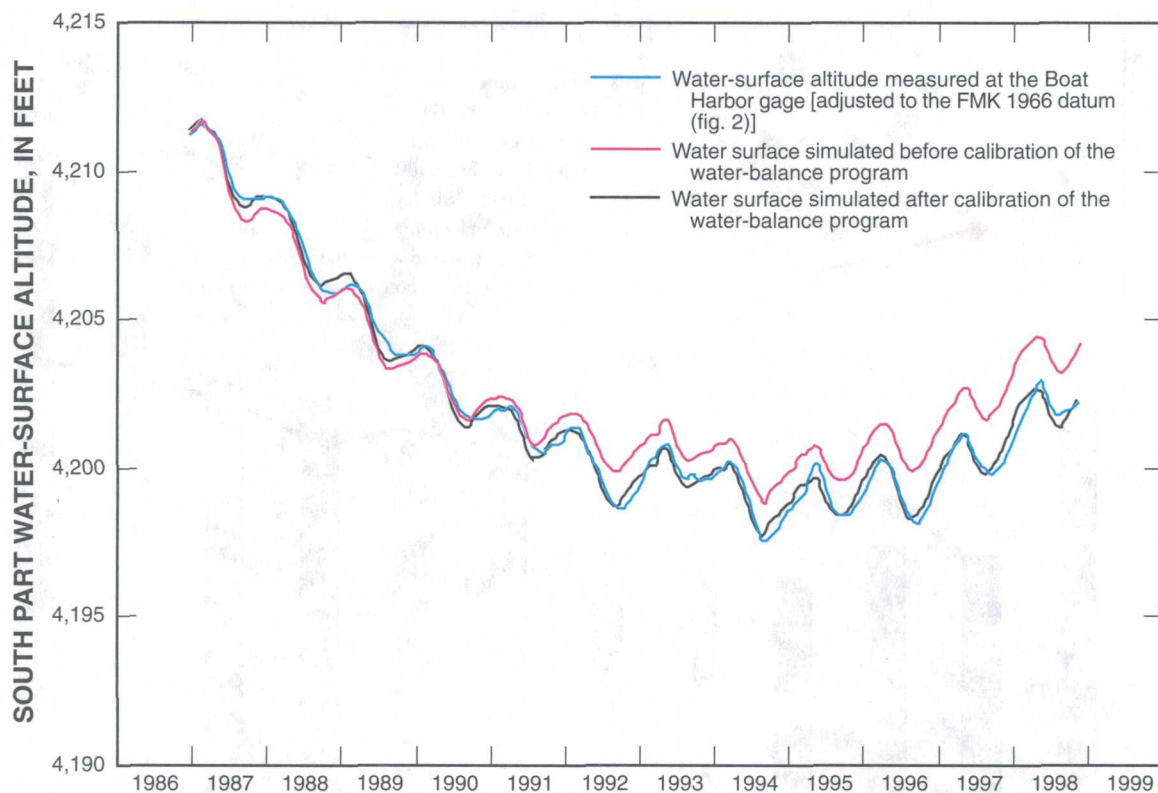
## Sensitivity and Error Analysis

A sensitivity and error analysis was performed to determine which model parameters have the most influence on accuracy of the model results. The critical parameters used to calibrate the water balance ( $\Delta V_N$ ,  $SIS$ ,  $GIS$ ,  $GIN$ ,  $PIS$ ,  $PIN$ ,  $EOS$ ,  $EON$ , and  $QWP$ ) can be found in equations A13 and A14. To determine the sensitivity of the water-balance program to these parameters, simulations of south part water-surface altitude were run with the maximum positive and negative error for each parameter (the program uses measured north part altitudes). Comparison of measured south part water-surface altitudes with these simulated altitudes indicates the potential errors for each of the critical parameters (figs. A4–A11).

For example, about 70 percent of the total surface-water inflow ( $SIS$ ) is measured. Measured surface-water inflow has an error of about 10 percent. The

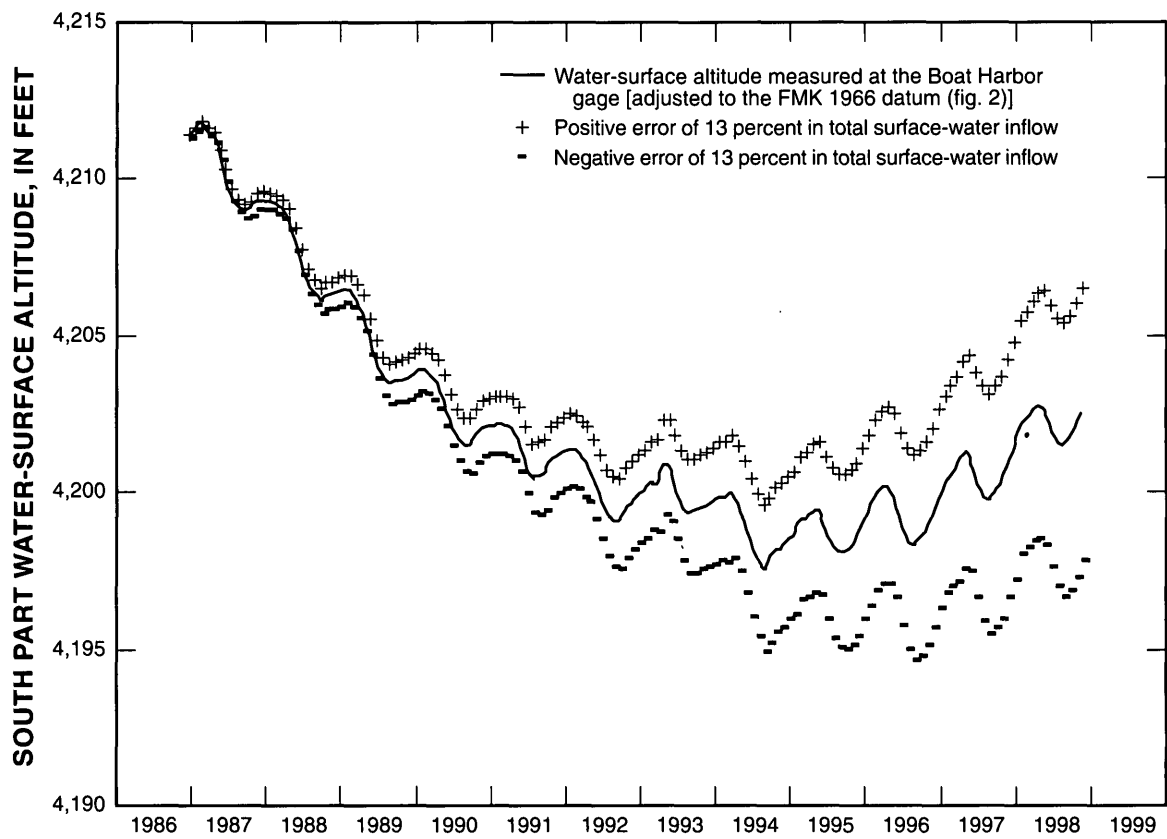
other 30 percent of surface-water inflow is estimated from correlations with other sites and is considered to have an error of 20 percent. The combined measured and estimated total surface-water inflow is calculated to have an error of 13 percent. The water-balance program was run with the measured and estimated monthly total surface-water inflow increased by 13 percent and decreased by 13 percent. The resultant south part water-surface altitudes computed by the program show the maximum effect that a 13-percent error in the total surface-water inflow data could have (fig. A4).

Parameter errors are based on oral communications with individuals considered experts on each type of data: surface-water inflow and West Pond outflow—James Kolva, USGS, Utah District Surface-Water Specialist; ground-water inflow—Walter Holmes, USGS, Utah District Investigations Chief; and precipitation and evaporation—Donald Jensen, Utah State Climatologist.

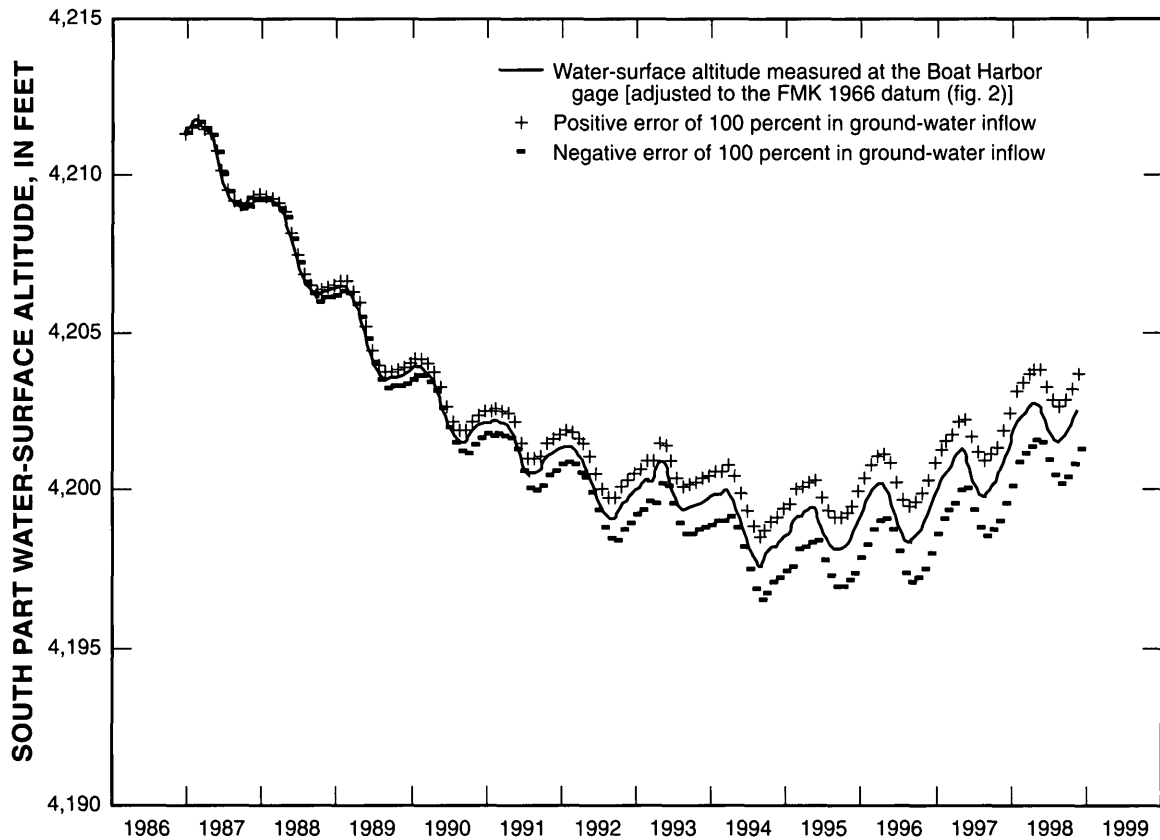


**Figure A3.** Simulated and measured water-surface altitude of the south part of Great Salt Lake, Utah, before and after calibration of water balance, 1987–98.

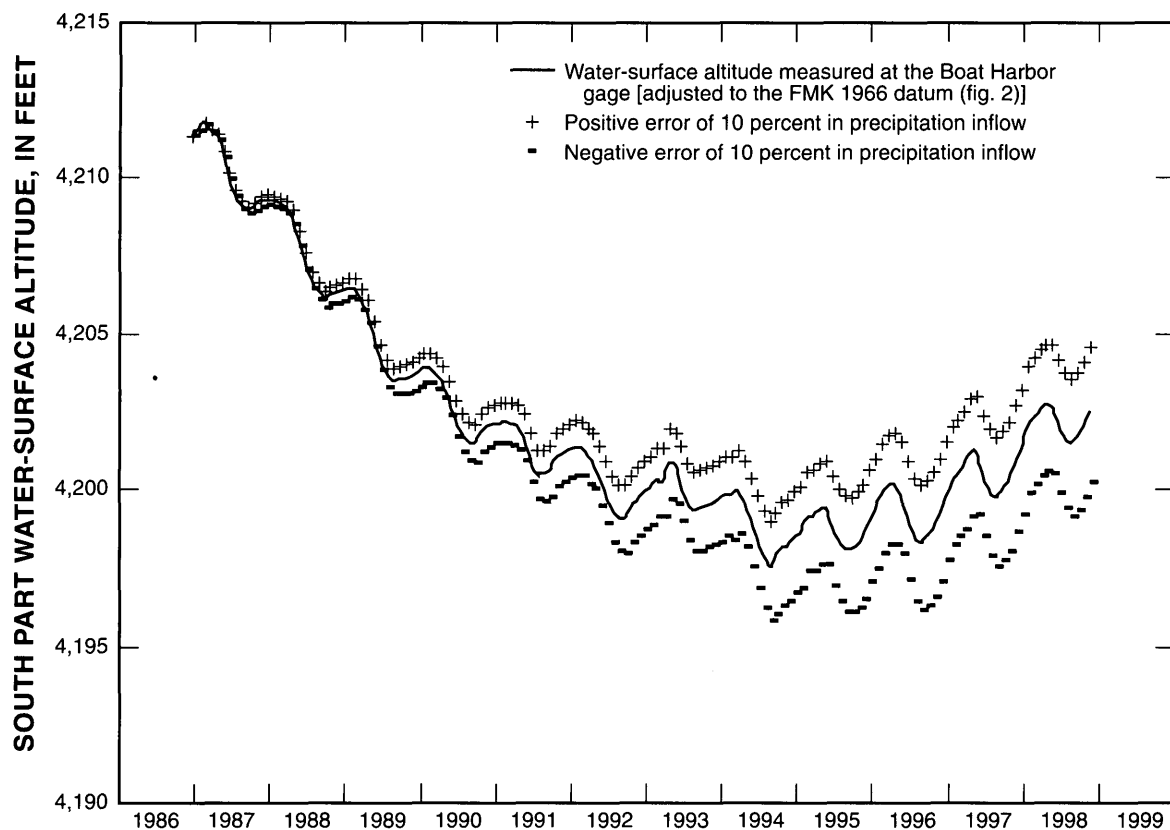
The analysis showed that the model is most sensitive to surface-water inflow, which is mostly measured (fig. A4), and evaporation, which is indexed with pan-evaporation data from sites near the lake (fig. A10). The model is least sensitive to change in north part volume (fig. A8), and outflow to and return flow from West Pond (fig. A9).



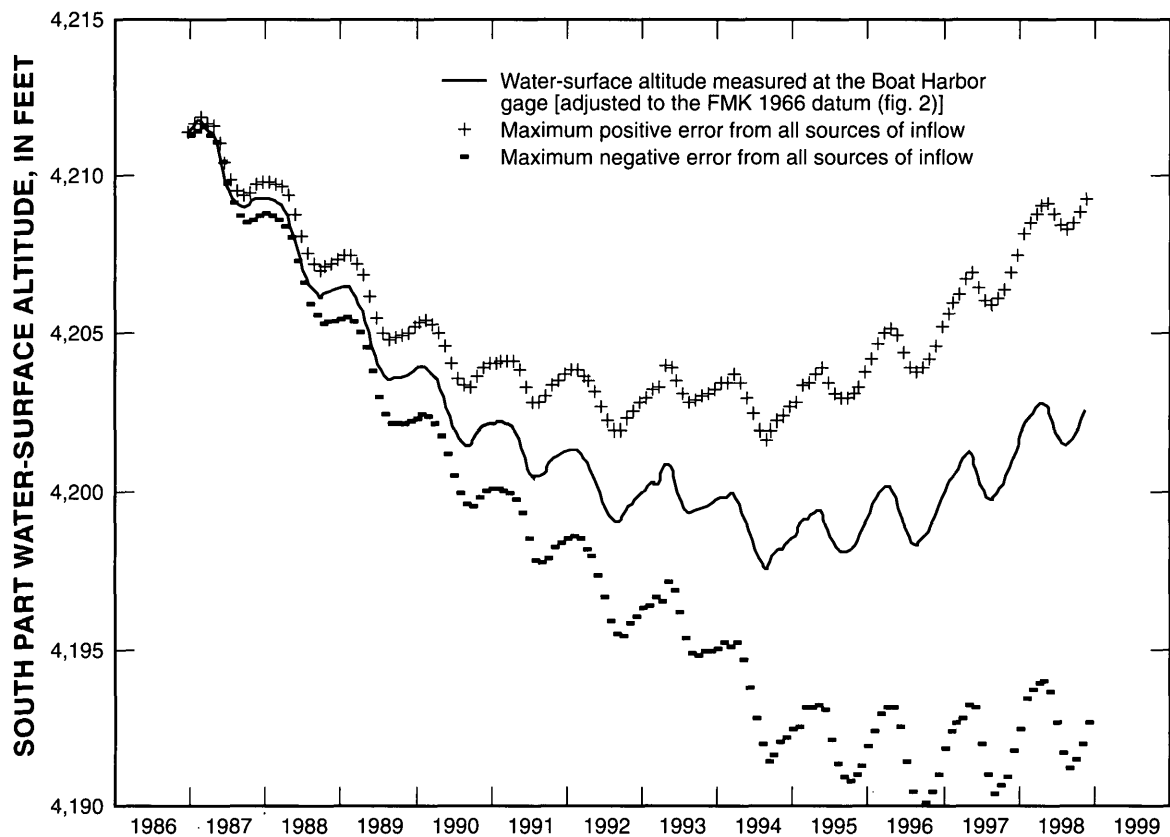
**Figure A4.** Simulations showing sensitivity of the south part water-surface altitude to a 13-percent error in the surface-water inflow, Great Salt Lake, Utah.



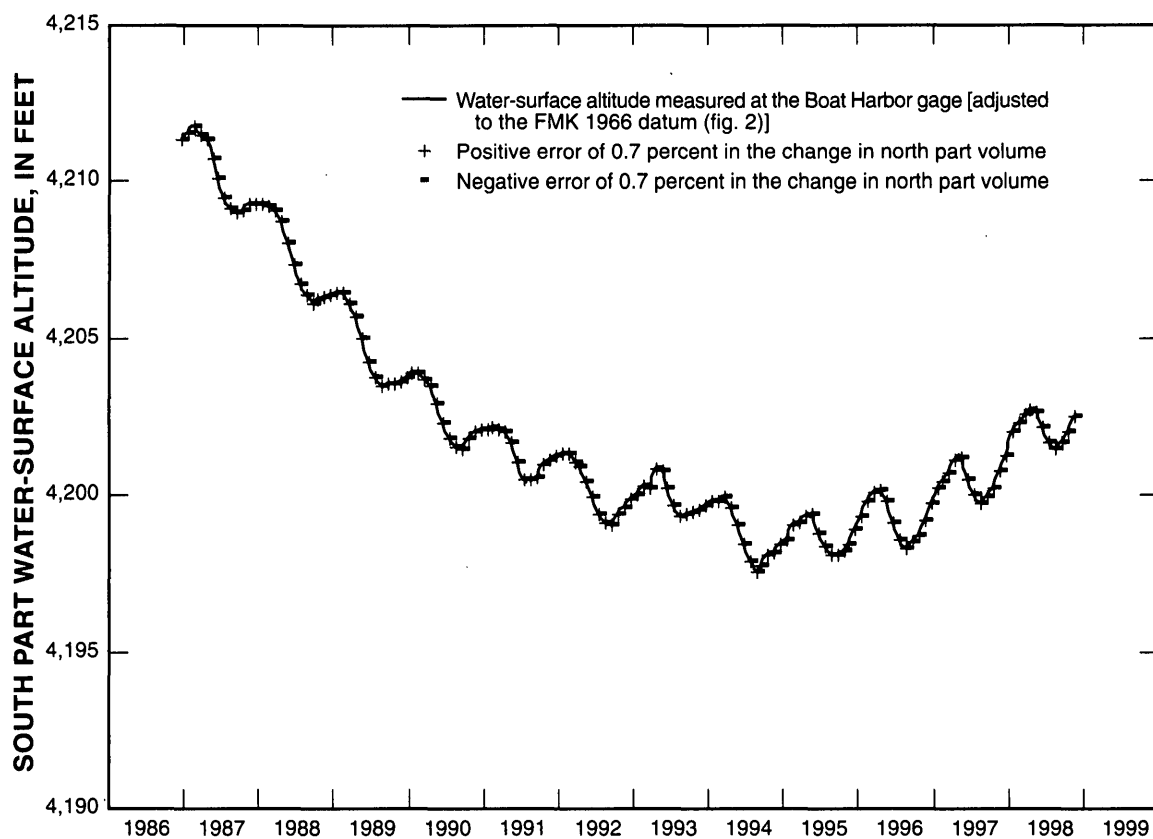
**Figure A5.** Simulations showing sensitivity of the south part water-surface altitude to a 100-percent error in ground-water inflow, Great Salt Lake, Utah.



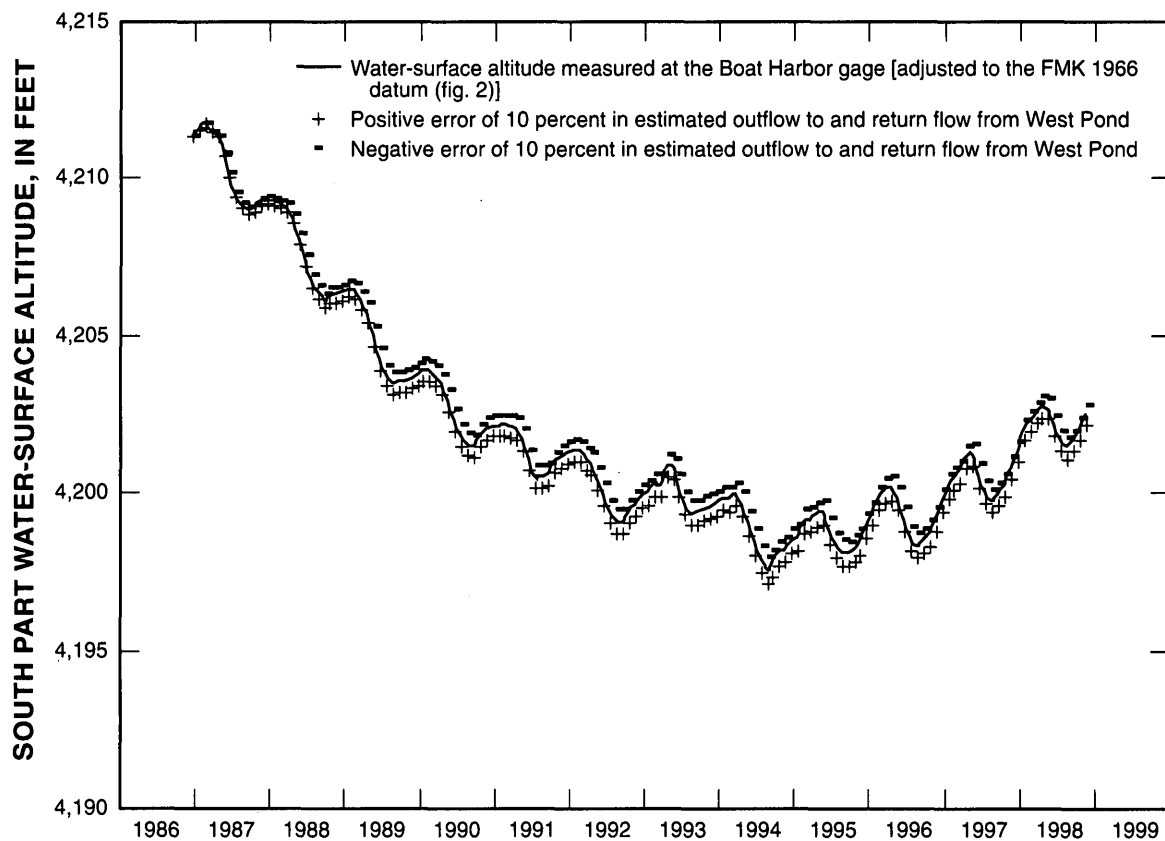
**Figure A6.** Simulations showing sensitivity of the south part water-surface altitude to a 10-percent error in precipitation, Great Salt Lake, Utah.



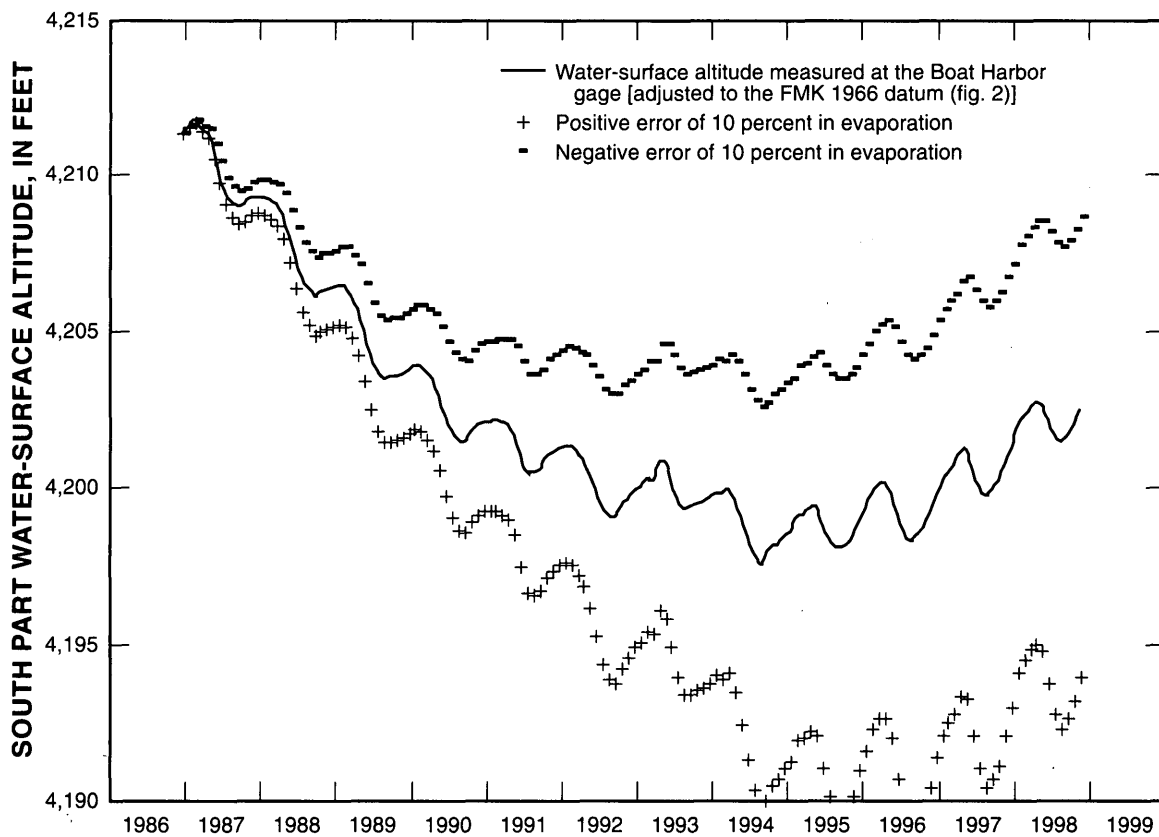
**Figure A7.** Simulations showing sensitivity of the south part water-surface altitude to the maximum positive and negative errors from all sources of inflow, Great Salt Lake, Utah.



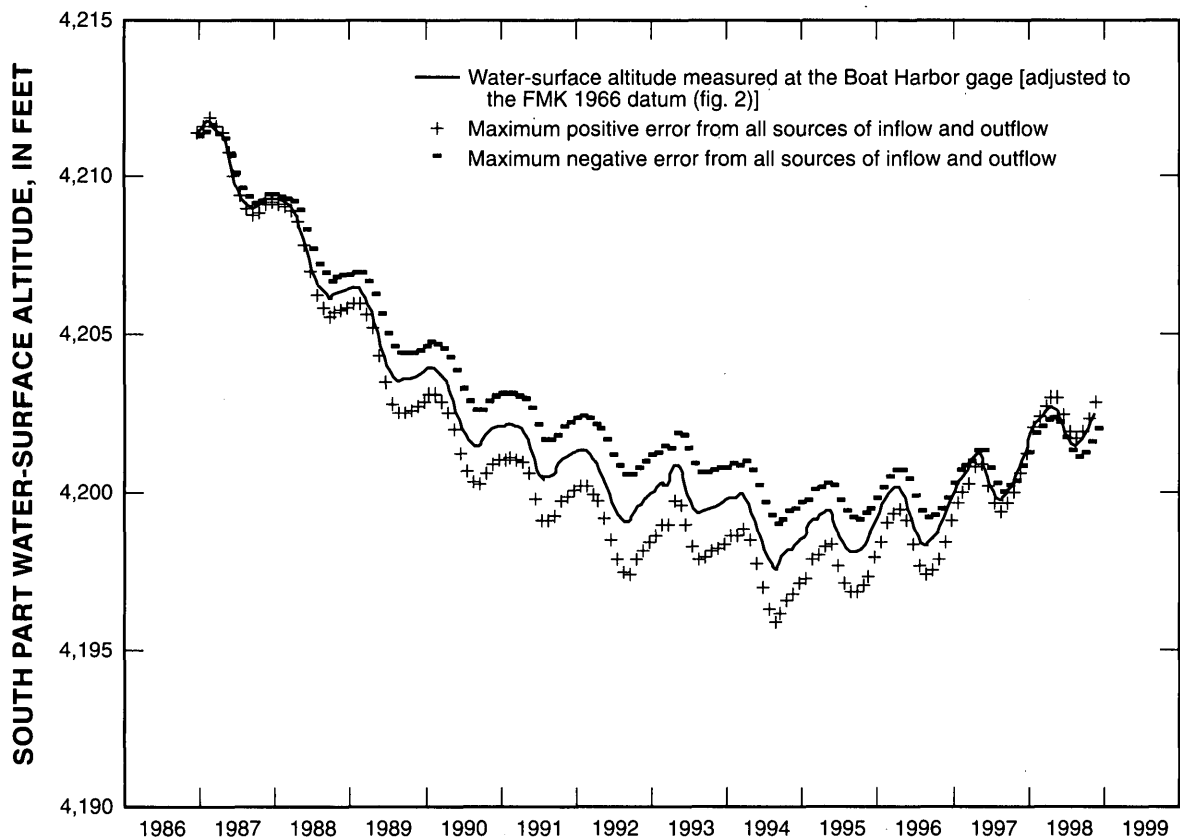
**Figure A8.** Simulations showing the sensitivity of south part water-surface altitude to 0.7-percent error in change in north part volume, Great Salt Lake, Utah.



**Figure A9.** Simulations showing sensitivity of the south part water-surface altitude to a 10-percent error in estimates of outflow to and return flow from West Pond, Great Salt Lake, Utah.



**Figure A10.** Simulations showing sensitivity of the south part water-surface altitude to a 10-percent error in evaporation, Great Salt Lake, Utah.



**Figure A11.** Simulations showing sensitivity of the south part water-surface altitude to the maximum positive and negative errors from all sources of inflow and outflow, Great Salt Lake, Utah.

## APPENDIX B. SALT BALANCE

A schematic diagram of the salt balance for the south and north parts of Great Salt Lake is shown in figure 6. Dissolved-solids concentration, density, and density difference were computed from the salt balance by using the same procedure as in Waddell and Bolke (1973, p. 34). Total salt load in the lake for 1987–98 is represented by:

$$LT = LS + LSL + CLSP + LN + CLNP - LWP, \quad (B1)$$

where

- $LT$  = total salt load in lake, in tons;
- $LS$  = dissolved salt load in south part, in tons;
- $LSL$  = dissolved salt load in deep brine layer in south part, in tons;
- $CLSP$  = precipitated salt load in south part, in tons;
- $LN$  = dissolved salt load in north part, in tons;
- $CLNP$  = precipitated salt load in north part, in tons; and
- $LWP$  = load lost to (+), or returned from (-) West Pond in tons.

The dissolved salt load in the south part ( $LS$ ) at any time step ( $I$ ) can be represented by:

$$LS(I) = LS(I-1) - QS(LS(I-1))T/VS(I-1) + QN(LN(I-1))T/VN(I-1) + LSD(I) - CLSP(I) \quad (B2)$$

where

- $LS(I)$  = dissolved salt load in south part at time step  $I$ , in tons;
- $I$  = present time step;
- $LS(I-1)$  = initial dissolved salt load in south part, in tons;
- $I-1$  = previous time step;
- $QS(LS(I-1))T/VS(I-1)$  = outflow load from south part, in tons;
- $QN(LN(I-1))T/VN(I-1)$  = inflow load from north part, in tons;
- $LSD(I)$  = redissolved salt in south part, in tons;
- $CLSP(I)$  = precipitated salt load in south part, in tons;
- $VS$  = volume of south part, in acre-ft; and
- $T$  = one time step (1.901 days).

Salt re-solution ( $LSD(I)$ ) and salt precipitation ( $CLSP(I)$ ) cannot occur in the same time step. Similarly,

the dissolved load in the north part ( $LN$ ), in tons, can be represented by:

$$LN(I) = LN(I-1) + QS(LS(I-1))T/VS(I-1) - QN(LN(I-1))T/VN(I-1) + LND(I) - CLNP(I) - LWP(I) \quad (B3)$$

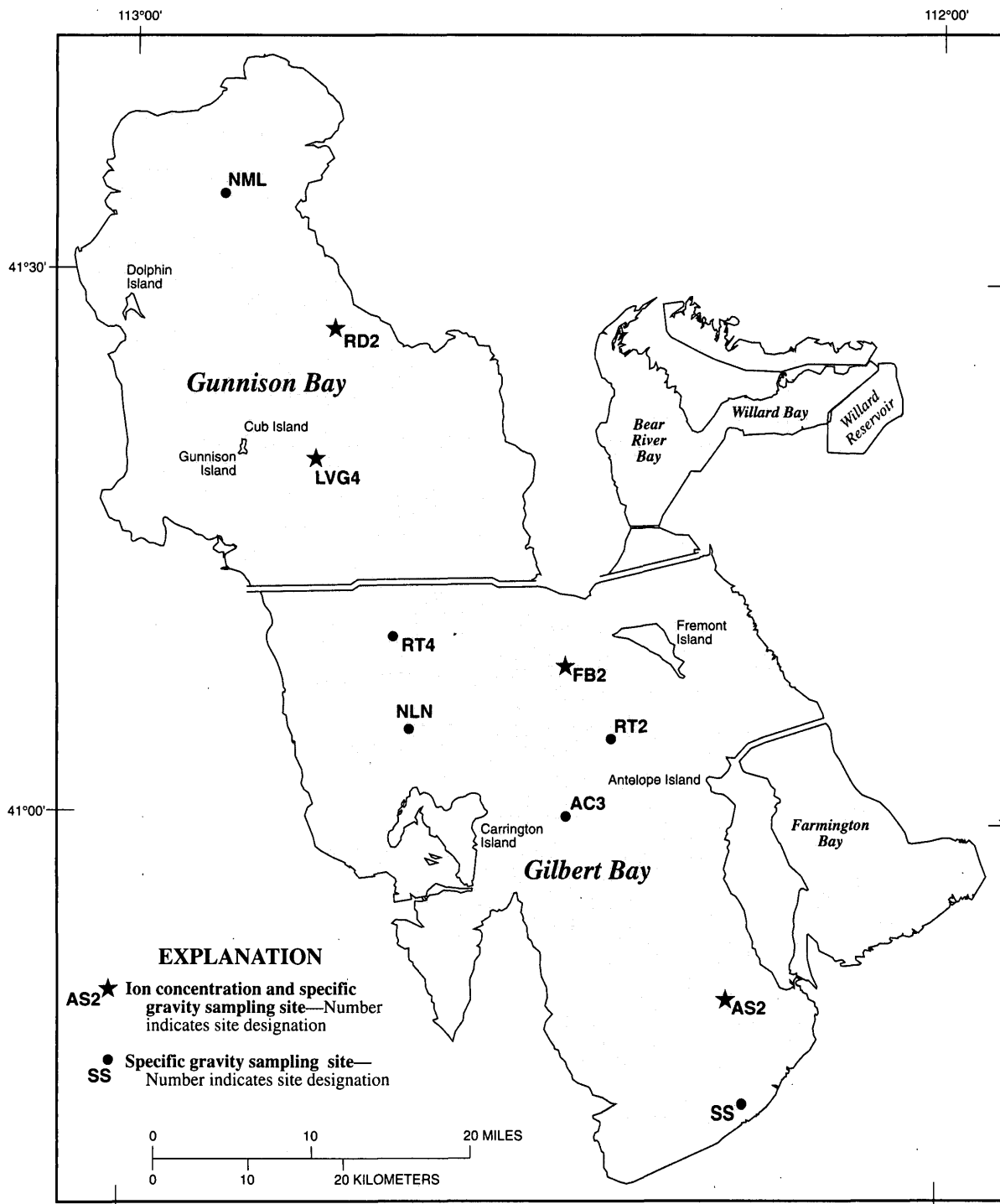
where

- $LN(I)$  = dissolved salt load in north part at time step  $I$ , in tons;
- $LN(I-1)$  = initial dissolved salt load in north part, in tons;
- $QS(LS(I-1))T/VS(I-1)$  = inflow load from south part, in tons;
- $QN(LN(I-1))T/VN(I-1)$  = outflow load from north part, in tons;
- $LND(I)$  = redissolved salt in north part, in tons;
- $CLNP(I)$  = precipitated salt load in north part, in tons; and
- $LWP(I)$  = load lost to (+), or returned from (-) West Pond, in tons.

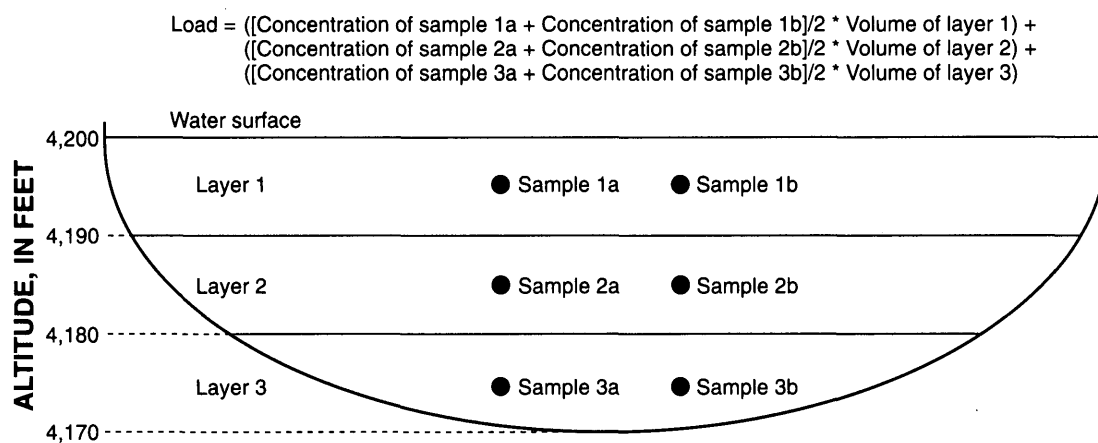
### Computation of Salt Load

The term load, as applied to hydrology, is the mass of a constituent within a solution (concentration \* volume or flow rate). In Great Salt Lake, load calculations are complicated by stratification, or the variation of dissolved-solids concentration with depth. Load is used to quantify the mass of individual ions and total amount of dissolved solids in each part of the lake.

Measured loads of dissolved solids, which were used to determine initial conditions and calibrate the model, were computed in the following manner. During 1966–99, the Utah Geological Survey collected brine samples in vertical profiles of 1- to 5-ft-depth increments at three to eight sites in each part of the lake (fig. B1). Measured specific-gravity values of all samples collected in the north or south part of the lake for a specified day were averaged to obtain a mean value for each 1- to 5-ft-deep vertical layer of that part of the lake. Mean specific-gravity values (density at 20° C) for each layer were then converted to dissolved-solids concentrations with the following empirical relation described by Waddell and Bolke (1973, p. 35):



**Figure B1.** Sites where chemical samples have been collected from Great Salt Lake by the Utah Geological Survey.



**Figure B2.** Diagram of a load calculation for a hypothetical lake divided into 10-foot-thick layers with two sampling sites.

$$C = \frac{(\rho - 1)(1,000)}{0.63}$$

where

C = dissolved-solids concentration, in g/mL;  
and

$\rho$  = density at 20° C, in g/L.

Multiplying the concentration of each layer by the volume of that layer yields the load for each individual layer. The sum of the loads of all the layers is the total load for that part of the lake (fig. B2). Measured loads of individual ions were computed in much the same way, except that the number of sampling sites in each part of the lake was fewer, typically consisting of one or two sites in each part.

## Salt Precipitation and Re-resolution

The following is a synopsis of a description of the lake dynamics governing salt precipitation and re-resolution by Waddell and Bolke (1973):

Most salt precipitation in the north part occurs during summer and fall when the water surface is falling, and re-resolution generally occurs during winter and spring when the water surface is rising. When the water surface is falling, water loss from evaporation in the north part may exceed the net gain of water to the north part; therefore, the concentration of dissolved solids increases in the north part, and if saturation concentration is attained (355 g/L), sodium chloride may precipitate. When the water surface is rising, the net gain of water in the north part may exceed water loss from evaporation and the concentrations in the north part may be diluted below saturation concentration. If dilution

occurs, then conditions are conducive to re-resolution of salt. Whether there is a net increase of salt precipitation or re-resolution in the north part depends upon the magnitude of salt gain relative to net water gain from flow through the causeway.

The addition of total dissolved salts from inflow into Great Salt Lake is roughly equal to the amount of total salts mined from the lake (J.W. Gwynn, Utah Geological Survey, oral commun., 2000) and over periods of a few years is negligible compared with the total salt load of the lake. In the lake, salt can be either dissolved (*LS*, *LN*, and *LSL*) (fig. 6) or be present in its precipitated form (*CLSP* and *CLNP*). Salt precipitation has not been observed in the south part (*CLSP*) since at least 1970 (Wold, Thomas, and Waddell, 1997, p. 35).

During 1987–98, the amount of salt deposition or re-resolution in the lake was estimated from changes in total dissolved salt load for the lake. Except for during the WDPP (1987–90), precipitation of salt is indicated when the total load of dissolved salt decreases, and re-resolution of salt is indicated when the total load of salt increases (fig. 7). During the WDPP, precipitation of salt is indicated when the total load of dissolved salt minus the loss of salt to West Pond decreases, and re-resolution of salt is indicated when the total load of dissolved salt minus the loss of salt to West Pond increases (fig. 7). The dissolved-solids concentration in the north part was at or near saturation of about 355 g/L during 1970–85 and 1994–98 (fig. 4). During 1986–93, lake volume was large enough to dissolve most if not all of the precipitated salt in the north part (figs. 4 and 7).

Re-resolution of salt in either the south (*LSD*) or north part (*LND*) is represented by the equations revised from Waddell and Bolke (1973) as follows:

$$LSD = T[483(VS) - LS(I)](5.25 \times 10^{-3}) \quad (B4)$$

$$LND = T[483(VN) - LN(I)](5.25 \times 10^{-3}) \quad (B5)$$

where

*LSD* = redissolved salt in south part, in tons;

*LND* = redissolved salt in north part, in tons;  
and

*T* = time interval (1.901 days), in days.

The value 483 is an empirical constant associated with the limiting salt load in either part of the lake for a specified volume, in tons/acre-ft. The constant is the product of the saturation concentration of sodium chloride (355 g/L) and a factor for converting from g/L to tons/acre-ft ( $355 \times 1.36 = 483$ );

*VS* = volume of south part, in acre-ft;

*VN* = volume of north part, in acre-ft;

*LS* = dissolved salt load in south part at time step *I*, in tons;

*LN* = dissolved salt load in north part at time step *I*, in tons;

*I* = present time step; and

$5.25 \times 10^{-3}$  is an empirical constant, determined by Waddell and Bolke (1973, p. 34), for re-resolution rate per day, in tons per day per total tons of salt deposited in north or south part.

Salt precipitation that occurred during one time step in the north part (*LNP*) was computed the same way in the model as was done by Waddell and Bolke (1973, p. 34) with the equation:

$$LNP = LN - 483(VN) \quad (B6)$$

where

*LNP* = load of salt precipitated during one time step in the north part, in tons.

The amount of salt precipitation that might occur in the future depends on inflow conditions and changes in the conveyance properties of the causeway. A decrease in inflow causes a decrease in lake volume, which can cause salt precipitation in the south and north parts. The distribution of salt precipitation between the

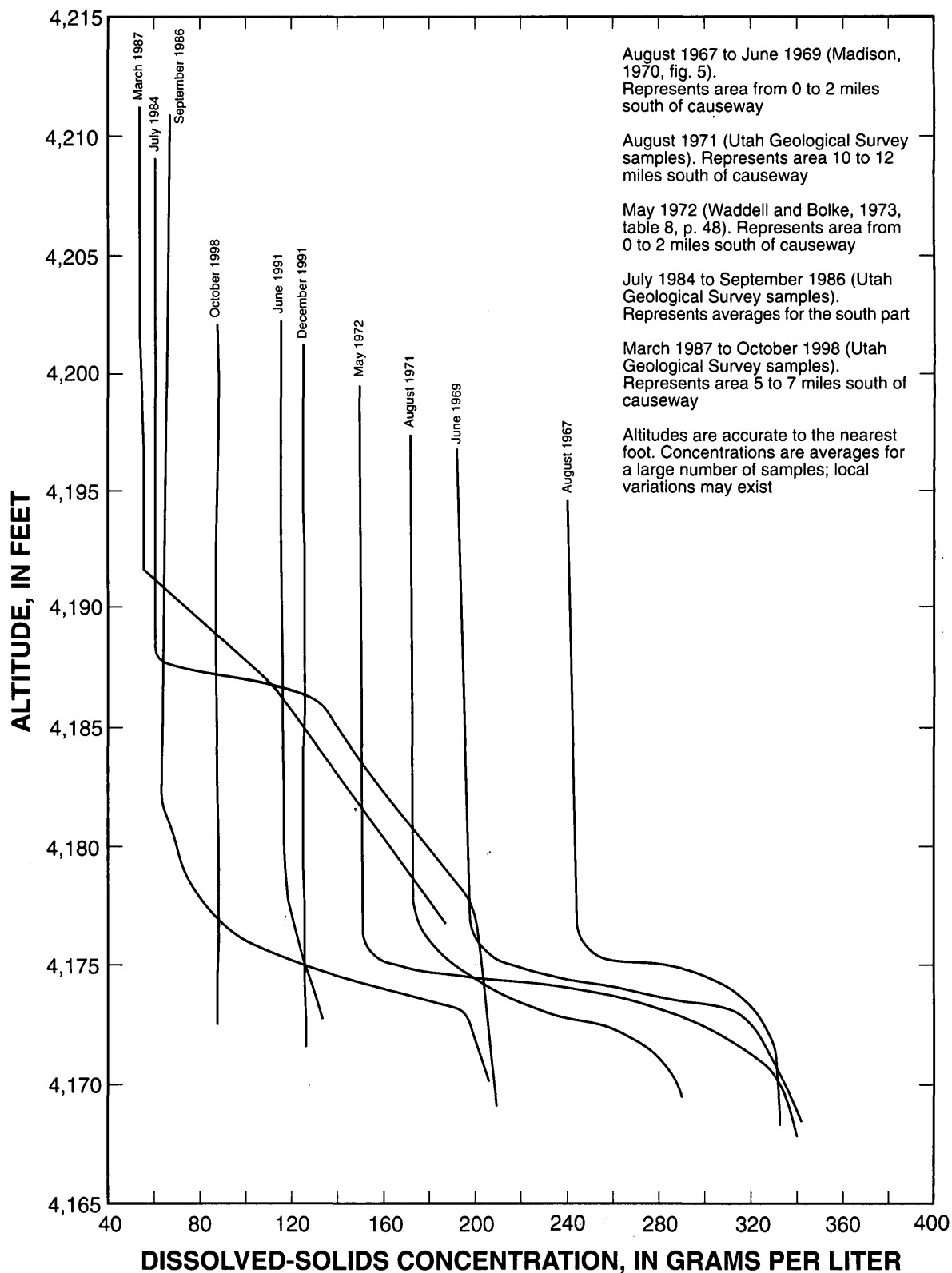
south and north parts also is affected by the conveyance properties of the causeway. For a specified volume, the smaller the openings in the causeway, the more likely precipitation of salt is to occur in the north part as a result of restricted circulation.

## Stratification in Great Salt Lake

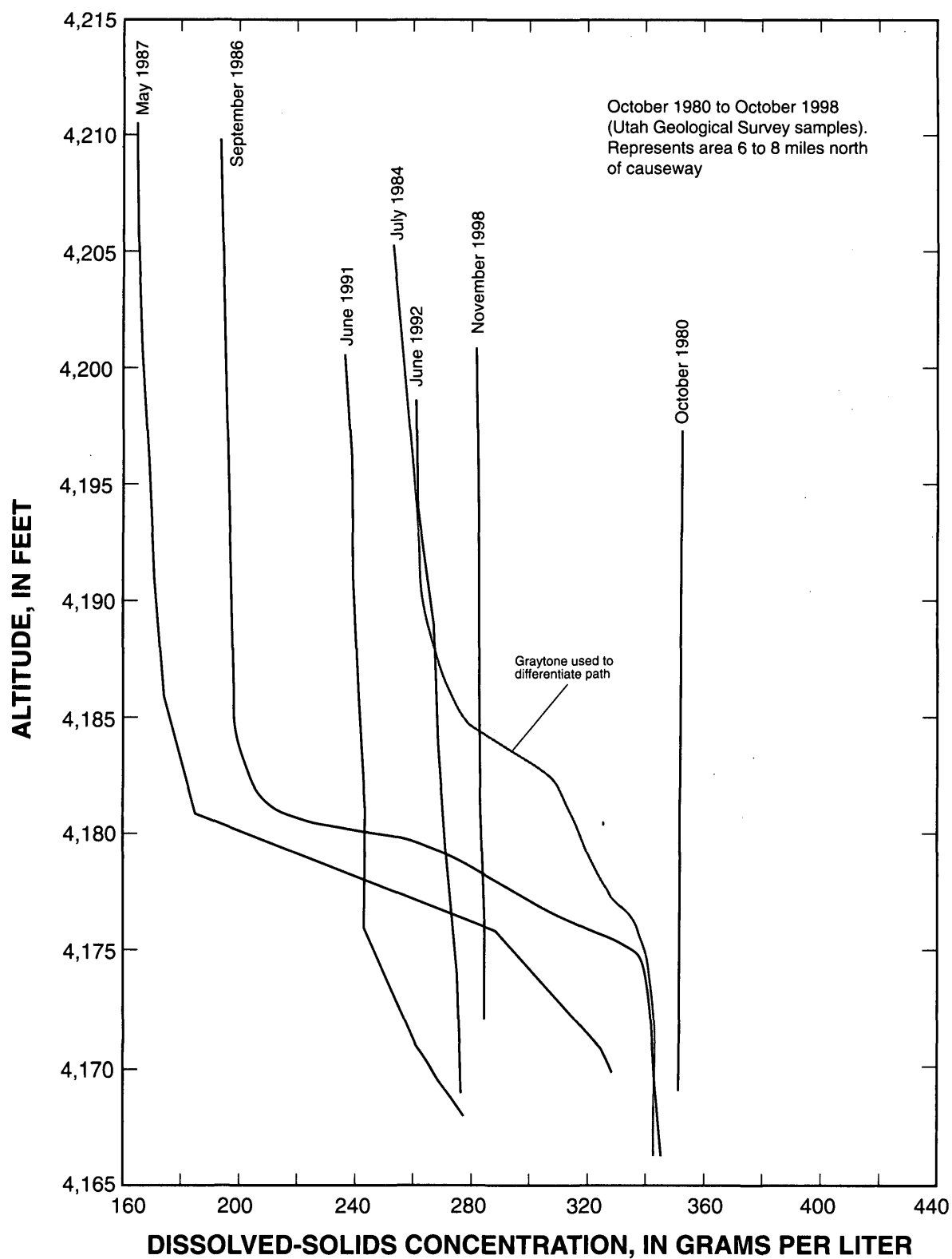
During and after completion of the causeway, data were collected (Madison, 1970; Waddell and Bolke, 1973; and Gwynn and Sturm, 1987) to define the stratification in the south and north parts of the lake. Madison (1970, p. 12) observed that a lower layer of dense brine (*LSL*, fig. 6) occurred in the south part of the lake below 4,175 ft (fig. B3, August 1967 to June 1969 density profiles). Madison further noted that the volume of the lower layer of brine remained relatively constant and that this apparent stability is the result of equilibrium between the amount of dense brine moving from the north part of the lake to the south through the causeway and the amount of mixing that took place at the interface. Waddell and Bolke (1973) collected additional data in the south part during 1971–72 (fig. B3, August 1971 to May 1972 dissolved-solids concentration profiles) that indicated that this volume was about the same as during the study by Madison (1970).

Gwynn and Sturm (1987) observed changes in stratification during 1984 that indicated that the interface in the south part became more diffused than in preceding years (fig. B3, July 1984 density profiles) as a result of record surface-water inflow during 1983–84. By September 1986, the interface in the south part had become less diffused because of increased circulation and mixing following the opening of the breach during August 1984 (fig. B3, September 1986 dissolved-solids concentration profiles). The transition from no stratification to gradual stratification in the north part (fig. B4, October 1980 to September 1986 dissolved-solids concentration profiles) resulted from high inflow, the rapid rise of the water-surface altitude, and increased flow to the north part after the breach was opened (Gwynn and Sturm, 1987).

As lake levels started an 8-year decline in 1987, flow through the causeway was reduced and the density stratification in each part of the lake again began to slowly disappear. There was no stratification in the south part by December 1991, or in the north part by June 1992 (fig. B3, dissolved-solids concentration profiles in 1987 and 1991; fig. B4, dissolved-solids concentration profiles in 1987 and 1992). Dissolved-solids concentrations indicate that both parts remained



**Figure B3.** Approximate dissolved-solids concentration gradients for south part of Great Salt Lake, Utah, on selected dates, 1967–98.



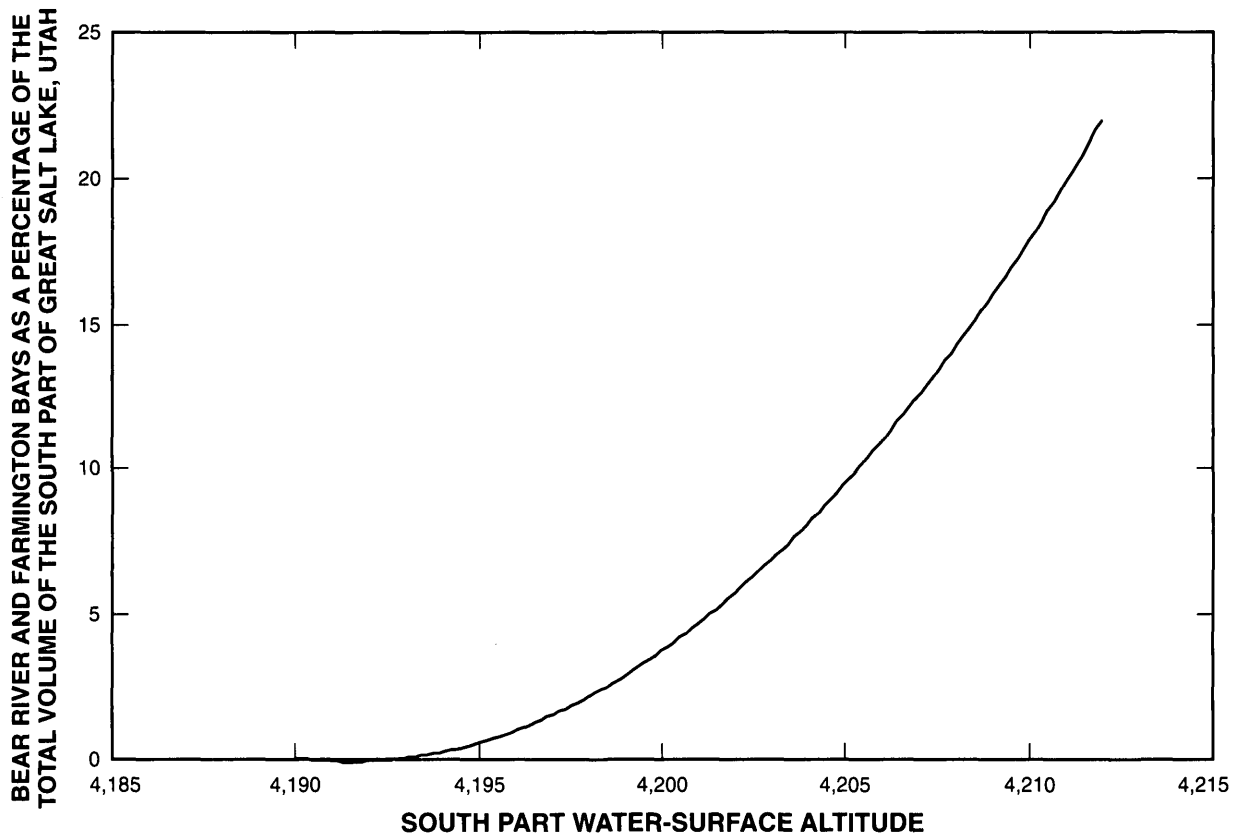
**Figure B4.** Approximate dissolved-solids concentration gradients for north part of Great Salt Lake, Utah, on selected dates, 1980–98.

unstratified during 1993–98 (fig. B3, dissolved-solids concentration profiles in 1991 and 1998; fig. B4, dissolved-solids concentration profiles in 1992 and 1998). In October 1998, samples were collected only to a depth of 4,172.5 ft, and stratification below this depth would not have been detected.

### Effects of Bear River and Farmington Bays on Salt Load Computations

The altitude-area-volume table used in the model incorporates Bear River Bay and Farmington Bay into the main body of the south part of the lake (also referred to as Gilbert Bay). The bays are assumed in the model as continuous with the main body of the south part (fig. 1) and are assumed to have the same average concentration of individual ions and dissolved solids as the main body of the south part. This assumption is not correct for the entire range of lake levels, which creates an error

in computed salt loads for the south part. This error however, is very small when compared to the total load of the south part of the lake. Neither of the bays is completely fresh; both are brackish as a result of exchange through breaches in the causeways that separate them from the main body of the south part. As south part water-surface altitude increases above 4,201 ft, the salinity in the bays increases and the salinity in the main body of the south part decreases, reducing the salinity differences between them. Where south part water-surface altitudes are below 4,201 ft, the bays represent less than 5 percent of the total volume of water in the south part (fig. B5). Where the south part water surface reaches an altitude of about 4,207 ft, the causeways that separate Farmington Bay from the rest of the lake are submerged and the bay becomes part of the main body of the south part of the lake.



**Figure B5.** Percentage of total south part volume contained in the Bear River and Farmington Bays, Great Salt Lake, Utah.



## APPENDIX C. FLOW THROUGH THE CAUSEWAY FILL

### Causeway Properties

The causeway properties have undergone major changes and modifications since the first construction in the early 1900s. The history of construction and modification through 1987 were summarized by Wold, Thomas, and Waddell (1997, p. 38).

In the early 1900s, fill material was used to form approaches to a railroad trestle that crossed Great Salt Lake. The approaches and trestle traversed the lake in an east-west direction from Promontory Point to Lakeside (fig. 1) where the lake is about 18 mi wide. The approaches have a combined length of about 6 mi and now abut either end of the causeway that was constructed during 1957–59 (fig. 2) to replace the trestle. The causeway was constructed across the remaining distance of 12.21 mi (Madison, 1970, p. 7) to support the railroad track above the surface of Great Salt Lake.

Construction of the causeway began by dredging a channel 25 to 40 ft deep and 150 to 500 ft wide. The channel was backfilled with sand and gravel, and quarry rock was used as fill to raise the top of the causeway above the surface of the lake. The causeway was completed with riprap that varied in size from 1-ton capstone 15 ft below the surface to 3-ton capstone at the top. The causeway is permeable, which allows flow through the fill material. It also was breached by two culverts, each 15 ft wide by 23 ft high, that allow brine to flow through channels. Prior to causeway construction, circulation was unimpeded through the trestle, but the causeway restricted circulation in the lake.

Since 1970, sand, gravel, and rock have been added periodically to the causeway to maintain its height as it settles and to replace material removed by erosion from wave action. During 1982–84 when the lake surface altitude rose almost 11 ft, a large amount of fill material was added to keep the causeway surface above water. Fill material also was added parallel to the causeway to compensate for settling of the causeway into the lake-bottom muds. From 1970 to 1987, the height of the fill increased by an average of about 7 ft and width increased about 10 to 20 ft. During 1987–98 the causeway surface was not raised, but continuous maintenance has been required to replace material eroded by storms and to maintain the height because of continued settling.

The physical conditions of the causeway affect the rate of movement of brine through the causeway

fill. Waddell and Bolke (1973, table 4) determined that water moves through the center 12.21 mi of the causeway. The original fill that was used to form approaches to the railroad trestle is virtually impermeable relative to the more recent fill, and no water is assumed to move through this original fill. Two-way flow of brine occurs through the causeway fill (fig. 3) because of head and density differences between the south and north parts of the lake ( $\Delta H$  and  $\Delta \rho$ ). South-to-north flow ( $Q_{SF}$ ) through the upper part of the fill is caused by a positive head difference ( $\Delta H$ ) at the causeway. A positive density difference ( $\Delta \rho$ ) between the north and south parts creates the potential for north-to-south flow ( $Q_{NF}$ ) through the lower part of the fill.

### Modeling of the Fill Flow

During the Waddell and Bolke (1973) study of Great Salt Lake, a model developed by Pinder and Cooper (1970) was calibrated and used to simulate flow through the causeway fill for a wide range of boundary conditions. During the Wold, Thomas, and Waddell (1997) study, a more efficient steady-state, cross-sectional, finite-difference, solute-transport model (referred to here as the fill-flow model) for density-dependent flow (Sanford and Konikow, 1985) was calibrated for a larger range of boundary conditions, a larger grid size, and a larger amount of input data. The changed boundary conditions were larger dimensions of the fill, a larger head difference, higher water-surface altitudes, and a different density profile as a function of depth for both parts of the lake.

### Hydraulic Properties

Hydraulic properties of the fill that influence flow of water and solutes are intrinsic permeability, dispersivity, effective porosity, molecular diffusivity, and anisotropy for permeability and dispersivity. Hydraulic conductivity and effective porosity of the fill were estimated in a previous study of flow through the causeway fill (Waddell and Bolke, 1973, table 3). Those estimates were made from dye-injection studies in 10 wells drilled into the causeway fill. Hydraulic conductivity was estimated to range from 0.08 to 2.10 ft/s. That range of hydraulic-conductivity values converts to a range of intrinsic permeability from  $2.68 \times 10^{-8}$  to  $70.4 \times 10^{-8}$  ft<sup>2</sup>. Effective porosity was estimated to be a uniform value of 0.3 for the entire causeway.

The fill was simulated in a two-dimensional cross section. The areal distribution of permeability was var-

ied within the cross section; however, the 12.21 mi of causeway fill was assumed to have the same cross-sectional permeability along its entire length. The magnitude and distribution of intrinsic permeability for the cross section used in the fill-flow model was the same as that used in the Pinder and Cooper (1970) model. The only difference is that the height and width of the fill cross section is slightly larger in the fill-flow model than in the Pinder and Cooper model. The new material on the sides and above the old core of the fill was assigned the permeability values used on the outside of the fill in the Pinder and Cooper model. The hydraulic-conductivity values in the Pinder and Cooper model were 0.39, 0.79, and 1.57 ft/s. These values were converted to intrinsic permeability values of  $1.3 \times 10^{-7}$ ,  $2.6 \times 10^{-7}$ , and  $5.3 \times 10^{-7}$  ft<sup>2</sup> in the fill-flow model:  $5.3 \times 10^{-7}$  ft<sup>2</sup> forming the outer layer of the fill about 10 ft thick,  $2.6 \times 10^{-7}$  ft<sup>2</sup> forming the middle layer about 15 ft thick, and  $1.3 \times 10^{-7}$  ft<sup>2</sup> forming the inner core. The inner core of lower permeability ranges through widths of 35 ft at an altitude of 4,210 ft, 60 ft at an altitude of 4,200 ft, and 130 ft at an altitude of 4,180 ft.

### Selected Causeway-Fill Flows

Wold, Thomas, and Waddell (1997) used the fill-flow model to compute selected fill flows for a range of boundary conditions, and the relations between the fill flows and boundary conditions were used in the causeway model. Flow was computed by the fill-flow model as an average of the flow through columns 16–20 of the finite-difference grid (fig. C1). Flow through the causeway fill (tables C1–C3) was computed for the head difference ( $\Delta H$ ) at the causeway from 0.10 to 3.9 ft, density difference ( $\Delta \rho$ ) from 0.02 to 0.15 g/mL, and water-surface altitude of the north part ( $EN$ ) from 4,191 to 4,211 ft.

### Methods Used to Compute Causeway-Fill Flow

For this study, the methods used by Wold, Thomas, and Waddell (1997) to compute fill flow were used with some modifications to the hydraulic conductivity (intrinsic permeability) of the causeway fill. A change of the hydraulic conductivity is directly proportional to the change in discharge through the fill material. The algorithms provided by Wold, Thomas, and Waddell to compute discharge to the north and south parts were modified by two constant factors that were determined through calibration of the water and salt

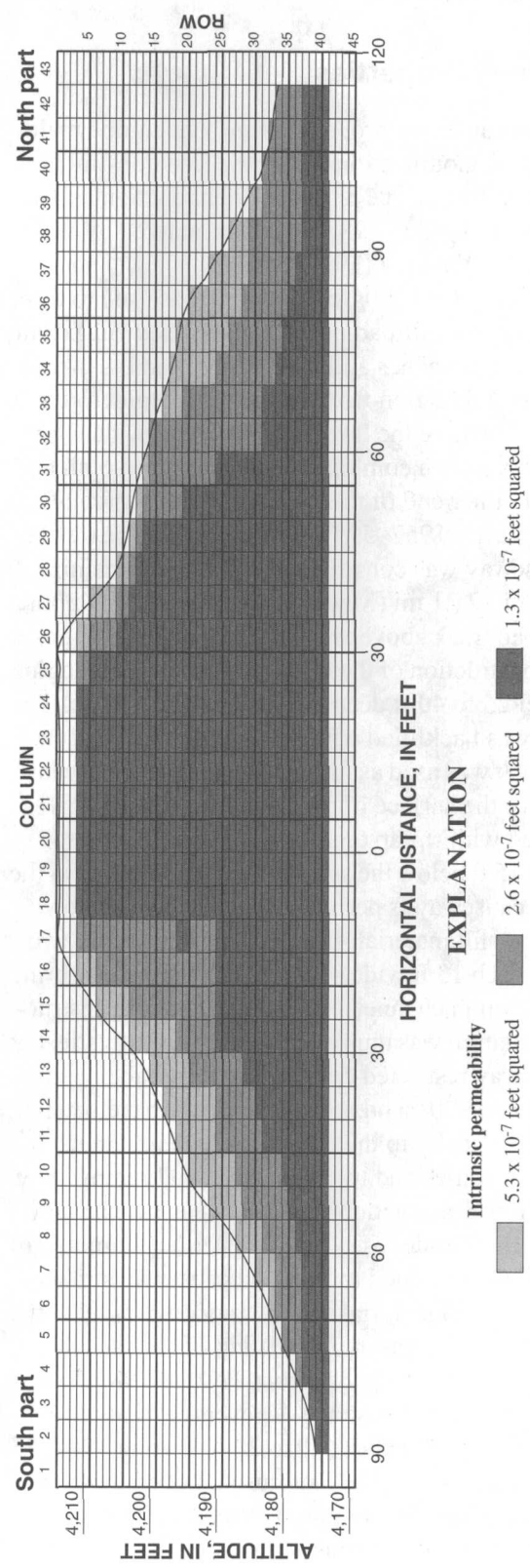


Figure C1. Model grid of the cross section of causeway fill across Great Salt Lake, Utah, showing intrinsic permeability values of cells.

**Table C1.** South-to-north flow through the causeway fill as computed by the fill-flow model, Great Salt Lake, Utah

[EN, water-surface altitude of north part; flow in cubic feet per second; density of north part is 1.210 grams per milliliter except where noted; —, no data]

Density difference ( $\Delta\rho$ ), in grams per milliliter	EN, in feet	Head difference at the causeway ( $\Delta H$ ), in feet										
		0.10	0.25	0.50	0.75	1.00	1.50	1.75	2.00	2.50	3.00	3.50
0.02	4,191	59	—	1,086	—	2,590	4,677	—	6,063	—	—	—
.02	4,194	87	—	1,264	—	3,129	5,487	—	7,449	—	—	—
.02	4,199	112	528	1,653	—	4,390	7,406	8,765	10,367	13,232	18,010	—
.02	4,204	134	—	2,273	—	6,398	11,290	—	15,920	—	—	—
.06	4,191	3	—	561	—	1,813	4,292	—	5,908	—	—	—
.06	4,194	13	—	653	—	2,002	4,817	—	7,046	—	—	—
.06	4,199	92	327	856	1,577	2,465	6,046	7,470	9,203	12,600	17,930	—
.06	4,204	168	—	1,295	—	3,599	8,419	—	13,490	—	—	—
.10	4,191	9	—	447	—	1,284	3,684	—	5,320	—	—	—
.10	4,194	71	—	568	—	1,472	4,093	—	6,059	—	—	—
.10	4,199	142	303	729	—	1,976	4,901	5,908	7,327	10,850	16,760	—
.10	4,204	172	—	1,102	—	<sup>1</sup> 2,128	—	—	<sup>1</sup> 11,550	16,050	22,360	27,570
						<sup>1</sup> 2,925	7,027		<sup>1</sup> 17,110			
						<sup>1</sup> 3,181	—		—			
.124	4,191	9	—	418	—	1,195	3,403	—	4,914	—	—	—
.124	4,194	60	—	505	—	1,374	3,759	—	5,466	—	—	—
.124	4,199	141	313	737	—	1,873	4,683	5,524	6,739	9,772	15,580	—
.124	4,204	184	—	1,125	—	<sup>2</sup> 2,009	6,782	—	<sup>2</sup> 10,500	15,000	20,590	25,520
						<sup>2</sup> 2,799			<sup>2</sup> 16,110			
						<sup>2</sup> 3,041			—			

<sup>1</sup>Flow computed with lower absolute density. Density of brine in south part ( $\rho_s$ ) = 1.063 grams per milliliter; density of brine in north part ( $\rho_n$ ) = 1.163 grams per milliliter.<sup>2</sup>Flow computed with lower absolute density. Density of brine in south part ( $\rho_s$ ) = 1.039 grams per milliliter; density of brine in north part ( $\rho_n$ ) = 1.163 grams per milliliter.

balance model for 1987–98. One factor was applied to flows through the new fill (above 4,200 ft), and the other factor was applied to the old fill (below 4,200 ft).

To facilitate computational time, functional relations between fill flow and principal variables were used in the causeway model in place of interactive computations with the fill-flow model. The following estimates of  $QSF$  and  $QNF$  were made with the density of the north part equal to 1.210 g/mL. Estimated flow is valid for the range of observed density in the north part (from 1.120 g/mL to saturation, 1.223 g/mL) within the inaccuracies of the hydraulic-conductivity values used in the fill-flow model.

## South-to-North Flow

South-to-north flow through the fill ( $QSF$ ) was computed in terms of head difference ( $\Delta H$ ) at the causeway, density of the south part ( $\rho_s$ ), average thickness of the upper-brine layer, and length of permeable fill (12.21 mi). Wold, Thomas, and Waddell (1997, p. 48) used the average thickness of the upper brine layer in conjunction with the velocities computed by the fill-

flow model to compute the flows for the head and density differences ( $\Delta H$  and  $\Delta\rho$ ) (table C4). The flow was then computed by linearly interpolating between discrete boundary conditions ( $\Delta H$ ,  $\Delta\rho$ , and  $EN$ ) for flow computed by the fill-flow model when the density of the north part ( $\rho_n$ ) was 1.210 g/mL (table C4).

The following calculation illustrates how south-to-north flow ( $QSF$ ), which varies with  $\Delta H$ ,  $EN$ , and  $\Delta\rho$ , was interpolated from data in table C4 for a specific set of boundary conditions (table C5). The boundary conditions for the calculation are  $\Delta H = 0.30$  ft,  $\Delta\rho = 0.050$  g/mL, and  $EN = 4,200$  ft.

The interpolation necessary for  $QSF_{\Delta H}$  is:

$$QSF_{0.30} = (QSF_{0.50} - QSF_{0.25}) * (0.30 - 0.25) / (0.50 - 0.25) + QSF_{0.25} \quad (C1)$$

Equation C1 is used to interpolate the following flows for  $\Delta H = 0.30$  ft and their respective  $EN$  and  $\Delta\rho$ .

For  $EN = 4,199$  ft and  $\Delta\rho = 0.02$  g/mL:  $753 = (1,653 - 528)0.2 + 528$ .

For  $EN = 4,204$  ft and  $\Delta\rho = 0.02$  g/mL:  $1,135 = (2,273 - 850)0.2 + 850$ .

**Table C2.** North-to-south flow through the causeway fill as computed by the fill-flow model, Great Salt Lake, Utah

[g/mL, grams per milliliter; EN, water-surface altitude of north part; flow in cubic feet per second; density of north part is 1.210 grams per milliliter except where noted; —, no data]

Density difference ( $\Delta\rho$ ), in g/mL	EN, in feet	Head difference at the causeway ( $\Delta H$ ), in feet										
		0.10	0.25	0.50	0.75	1.00	1.50	1.75	2.00	2.50	3.00	3.50
0.02	4,191	154	—	0	—	0	0	—	0	—	—	—
.02	4,194	262	—	0	—	0	0	—	0	—	—	—
.02	4,199	494	141	0	—	0	0	—	0	0	0	—
.02	4,204	830	—	0	—	0	0	—	0	—	—	—
.06	4,191	831		195	—	0	0	—	0	—	—	—
.06	4,194	1,202		409	—	0	0	—	0	—	—	—
.06	4,199	2,110	1,505	918	441	94	0	0	0	0	0	—
.06	4,204	3,434		1,691	—	495	0	—	0	—	—	—
.10	4,191	1,532		742	—	188	0	—	0	—	—	—
.10	4,194	2,212		1,248	—	474	6	—	0	—	—	—
.10	4,199	3,720	2,960	2,280	—	1,202	450	170	0	0	0	—
.10	4,204	6,009		3,916	—	<sup>1</sup> 1,465 <sup>1</sup> 2,403 <sup>1</sup> 2,806	1,259	—	466	<sup>1</sup> 0 44 <sup>1</sup> 106	0	0
.124	4,191	1,977	—	1,117	—	498	61	—	0	—	—	—
.124	4,194	2,841	—	1,748	—	946	360	—	0	—	—	—
.124	4,199	4,719	3,865	3,182	—	2,042	1,134	777	433	29	0	—
.124	4,204	7,584	—	5,349	—	<sup>2</sup> 2,383 3,720 <sup>2</sup> 4,271	2,420	—	1,384	<sup>2</sup> 134 687 <sup>2</sup> 901	147	0

<sup>1</sup>Flow computed with lower absolute density. Density of brine in south part ( $\rho_s$ ) = 1.063 grams per milliliter; density of brine in north part ( $\rho_n$ ) = 1.163 grams per milliliter.

<sup>2</sup>Flow computed with lower absolute density. Density of brine in south part ( $\rho_s$ ) = 1.039 grams per milliliter; density of brine in north part ( $\rho_n$ ) = 1.163 grams per milliliter.

For  $EN = 4,199$  ft and  $\Delta\rho = 0.06$  g/mL:  $433 = (856 - 327)0.2 + 327$ .

For  $EN = 4,204$  ft and  $\Delta\rho = 0.06$  g/mL:  $711 = (1,295 - 565)0.2 + 565$ .

The interpolation necessary for  $QSF_{EN}$  is shown in equation C2.

$$QSF_{4,200} = (QSF_{4,204} - QSF_{4,199})(4,200 - 4,199)/(4,204 - 4,199) + QSF_{4,199} \quad (C2)$$

Equation C2 is used to interpolate the following flows for  $\Delta H = 0.30$  ft,  $EN = 4,200$  ft, and the respective  $\Delta\rho$ .

For  $\Delta\rho = 0.02$  g/mL:  $QSF_{4,200} = (1,135 - 753)0.2 + 753 = 829$ .

For  $\Delta\rho = 0.06$  g/mL:  $QSF_{4,200} = (711 - 433)0.2 + 433 = 488$ .

The interpolation necessary for  $QSF_{\Delta\rho}$  is shown in equation C3.

$$QSF_{0.05} = (QSF_{0.06} - QSF_{0.02})(0.05 - 0.02)/(0.06 - 0.02) + QSF_{0.02} \quad (C3)$$

Equation C3 is used to interpolate final flow,  $QSF$ .

For  $\Delta H = 0.30$  ft,  $EN = 4,200$  ft, and  $\Delta\rho = 0.05$  g/mL:

$$QSF = (488 - 829)0.75 + 829 = 574 \text{ ft}^3/\text{s}.$$

### North-to-South Flow

Wold, Thomas, and Waddell (1997, p. 46) developed an empirical equation to compute north-to-south flow ( $QNF$ ) using the Ghyben-Herzberg principle (Badon-Ghyben, 1888; and Herzberg, 1901) and north-to-south flows computed by the fill-flow model. Based

**Table C3.** Post-breach flow through the causeway fill as computed by the fill-flow model, Great Salt Lake, Utah

[g/mL, grams per milliliter; ft<sup>3</sup>/s, cubic feet per second]

Density of upper layer		Density difference <sup>1</sup> ( $\Delta\rho$ ), in g/mL	Head difference ( $\Delta H$ ), in feet	Water-surface altitude of north part (EN), in feet	Flow	
South part, in g/mL	North part, in g/mL				South to north (QSF), in ft <sup>3</sup> /s	North to south (QNF), in ft <sup>3</sup> /s
1.035	1.120	0.085	0.5	4,206	1,307	4,107
1.035	1.120	.085	1.0	4,206	3,489	1,869
1.035	1.120	.085	.5	4,211	1,564	6,953
1.035	1.120	.085	1.0	4,211	4,161	3,863
1.045	1.100	.055	.5	4,206	1,508	1,942
1.045	1.100	.055	1.0	4,206	4,467	383
1.045	1.100	.055	.5	4,211	1,807	3,512
1.045	1.100	.055	1.0	4,211	5,234	1,039
1.055	1.080	.025	.5	4,206	2,387	322
1.055	1.080	.025	1.0	4,206	6,873	47
1.055	1.080	.025	.5	4,211	2,737	500
1.055	1.080	.025	1.0	4,211	8,547	94

<sup>1</sup> Three density differences were used in the post-breach flow computations. Density differences in the post-breach flow computations were computed as the difference between the upper layers of uniform density in the south and north parts. The lower layers of greater density in both parts were kept constant in all post-breach flow computations.

on the Ghyben-Herzberg principle, equation C4 is used to estimate the thickness of the lower brine layer (*YNF*), which flows from north to south.

$$YNF = EN - 4,175 - \Delta H (\rho_s / \Delta \rho) \quad (C4)$$

where

- YNF* = thickness of the lower layer of brine flowing through fill from north to south where it exits on the south side of fill, in ft;
- EN* = water-surface altitude of north part, in ft; and
- 4,175 = water-surface altitude of lower boundary of fill flow, in ft.

Equation C5 was developed for *QNF* relating the boundary conditions  $\Delta\rho$  and *YNF*.

$$QNF = a * \Delta\rho * (YNF)^2 + b \quad (C5)$$

where

- QNF* = north-to-south flow through the fill, in ft<sup>3</sup>/s,
- a* = 73.401 for *QNF* less than or equal to 4,300 ft<sup>3</sup>/s or 84.401 for *QNF* greater than 4,300 ft<sup>3</sup>/s, and
- b* = 0.0 for *QNF* less than or equal to 4,300

ft<sup>3</sup>/s or -516.54 for *QNF* greater than 4,300 ft<sup>3</sup>/s.

The fill flow model-computed north-to-south flow and regression-computed north-to-south flow are shown in tables C2 and C3.

## Fill-Flow Calibration

During calibration of the model for 1980–86, Wold, Thomas, and Waddell (1997) reduced the hydraulic conductivity of the causeway fill by 40 percent of that determined by Waddell and Bolke (1973). During calibration for 1987–98 conditions, the hydraulic-conductivity reduction was 90 percent of that determined by Waddell and Bolke for the fill below an altitude of 4,200 ft (original fill), and there was no reduction for flows in the fill above an altitude of 4,200 ft (new fill, fig. C2). It was assumed that the fill that was added during the mid-1980s had a conductivity near that of the original fill emplaced in 1957–59. The 4,200-ft altitude is not a precise interface between the old and new fill, but was estimated as an average during calibration of the water and salt balance model. The causeway, which was raised about 7 ft during 1986–87 to an approximate altitude of 4,220 ft, also had fill

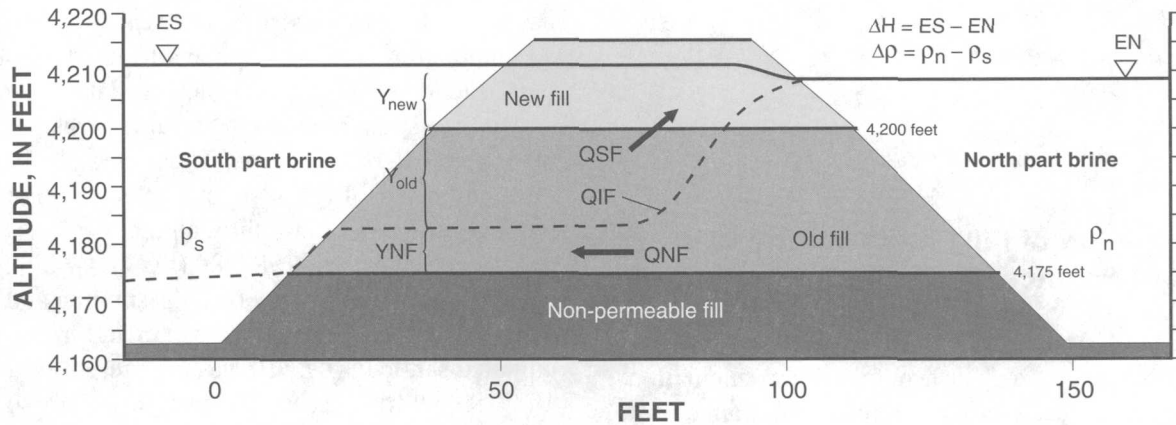
**Table C4.** Interpolation matrix for south-to-north flow through the causeway fill, Great Salt Lake, Utah

Density difference ( $\Delta\rho$ ), in grams per milliliter	Water-surface altitude of north part (EN), in feet	Flow in cubic feet per second for indicated head difference ( $\Delta H$ ), in feet															
		0.00	0.10	0.25	0.50	0.75	1.00	1.25	1.50	1.75	2.00	2.25	2.50	2.75	3.00	3.25	3.50
0.020	4,191	0.00	59	465	1,086	1,770	2,590	3,700	4,677	5,430	6,063	6,900	8,150	10,190	12,280	13,810	15,060
.020	4,194	.00	87	500	1,264	2,135	3,129	4,330	5,487	6,570	7,449	8,480	9,900	12,100	14,260	15,900	17,210
.020	4,199	.00	112	528	1,653	2,990	4,390	5,970	7,406	8,765	10,367	11,700	13,232	15,750	18,010	19,810	21,340
.020	4,204	.00	134	850	2,273	4,170	6,398	8,870	11,290	13,630	15,920	18,290	20,770	23,140	25,600	27,330	29,220
.020	4,211	.00	135	1,149	2,576	4,885	8,052	11,070	14,457	17,804	20,536	22,425	25,185	27,749	30,354	32,039	33,861
.060	4,191	.00	3	200	561	1,025	1,813	3,050	4,292	5,225	5,908	6,710	8,120	10,050	12,250	13,760	15,030
.060	4,194	.00	13	230	653	1,150	2,002	3,330	4,817	6,050	7,046	8,140	9,750	11,860	14,170	15,810	17,170
.060	4,199	.00	92	327	856	1,577	2,465	4,190	6,046	7,470	9,203	10,750	12,600	15,100	17,930	19,670	21,010
.060	4,204	.00	168	565	1,295	2,200	3,599	5,775	8,419	11,000	13,490	16,190	19,130	21,670	24,330	26,330	28,450
.060	4,211	.00	245	779	1,495	2,449	4,317	6,352	9,355	12,926	15,780	18,003	21,039	23,569	26,165	27,996	29,902
.100	4,191	.00	9	146	447	700	1,284	2,430	3,684	4,600	5,320	6,290	7,870	10,000	12,160	13,620	15,000
.100	4,194	.00	71	248	568	820	1,472	2,700	4,093	5,200	6,059	7,140	8,960	11,430	13,840	15,570	17,070
.100	4,199	.00	142	303	729	1,240	1,976	3,095	4,901	5,908	7,327	8,880	10,850	13,700	16,760	18,860	20,680
.100	4,204	.00	172	520	1,102	1,780	2,925	4,850	7,027	9,000	10,830	13,300	16,050	19,200	22,360	25,000	27,570
.100	4,211	.00	215	645	1,353	2,164	3,519	5,774	8,278	10,490	12,487	15,169	18,104	21,418	24,663	27,263	29,720
.124	4,191	.00	9	160	418	680	1,195	2,240	3,403	4,260	4,914	5,710	7,120	9,240	11,350	12,860	14,080
.124	4,194	.00	60	200	505	780	1,374	2,500	3,759	4,720	5,466	6,380	7,920	10,290	12,630	14,290	15,660
.124	4,199	.00	141	313	737	1,120	1,873	3,280	4,683	5,524	6,739	8,000	9,772	12,500	15,580	17,620	19,320
.124	4,204	.00	184	560	1,125	1,720	2,799	4,680	6,782	8,600	10,210	12,390	15,000	17,800	20,590	23,050	25,520
.124	4,211	.00	221	670	1,334	2,023	3,264	5,410	7,772	9,770	11,496	13,827	16,590	19,509	22,361	24,802	27,204

**Table C5.** Summary of intermediate and final interpolated south-to-north flow for selected boundary conditions, Great Salt Lake, Utah

[In this example  $\Delta H = 0.30$  foot,  $\Delta\rho = 0.050$  gram per milliliter, and  $EN = 4,200$  feet. Values in brackets [] are interpolated values or boundary conditions; all other values are calculated values listed in table C4]

Density difference ( $\Delta\rho$ ), in grams per milliliter	Water-surface altitude of north part (EN), in feet	Flow in cubic feet per second for indicated head difference ( $\Delta H$ ), in feet		
		0.25	[0.30]	0.50
0.020	4,199	528	753	1,653
.020	[4,200]		[829]	
.020	4,204	850	1,135	2,273
[.050]	[4,200]		[574]	
.060	4,199	327	433	856
.060	[4,200]		[488]	
.060	4,204	565	711	1,295



#### EXPLANATION

ES	Water-surface altitude of the south part	$Y_{old}$	Thickness of QSF flow through the old fill
EN	Water-surface altitude of the north part	$\rho_s$	Density of south part
QIF	Altitude of the interface between QSF and QNF	$\rho_n$	Density of north part
YNF	Thickness of the north-to-south fill-flow layer at the south end of the causeway	QSF	South-to-north flow through causeway fill
$Y_{new}$	Thickness of QSF flow through the new fill	QNF	North-to-south flow through causeway fill
		←	Direction of flow

**Figure C2.** Schematic diagram of flow through a cross section of the causeway fill; interfaces between new, old, and non-permeable fill; and the relation of the new and old fill interface to the south and north flows through the fill, Great Salt Lake, Utah.

added during 1988–98 to maintain height due to settling.

Because the fill material was considered to have a different hydraulic-conductivity value above and below 4,200 ft during 1987–98, an algorithm was developed to compute a weighted conductivity coefficient for flow layers that span the two different layers of fill. For this to be done, the percentage of each flow layer located above and below 4,200 ft must be determined. The location within a cross section of the causeway fill where the altitudes of the top of each fill-flow layer are best known is at the southern end of the causeway where  $YNF$  is computed (fig. C2). At this location, the top of the south-to-north fill-flow layer is the south part water-surface altitude ( $ES$ ). The interface between the layers of fill flow ( $QIF$ ), which is the bottom of the south-to-north fill-flow layer and the top of the north-to-south fill-flow layer, is computed as the sum of the thickness of the north-to-south flow layer ( $YNF$ , eq. C4) and the altitude below which the fill is nonpermeable (4,175 ft):

$$QIF = YNF + 4,175.$$

For the condition where the  $QIF$  is located in the old fill, below 4,200 ft, the thickness of the  $QSF$  flow layer in the old fill ( $Y_{old}$ , fig. C2) is represented by:

$$Y_{old} = 4,200 - QIF,$$

and in the new fill ( $Y_{new}$ , fig. C2) by:

$$Y_{new} = ES - 4,200.$$

The weighted hydraulic-conductivity coefficient for the  $QSF$  flow layer ( $WKS$ ) is then:

$$WKS = (Y_{new} * K_{new} + Y_{old} * K_{old}) / (Y_{new} + Y_{old}) \quad (C6)$$

where

- $K_{new}$  = hydraulic-conductivity coefficient assigned to the new fill layer; and
- $K_{old}$  = hydraulic-conductivity coefficient assigned to the old fill layer.

In this case, the hydraulic-conductivity coefficient ( $WKN$ ) of the north-to-south flow layer would equal  $K_{old}$ .

Similarly, if the interface ( $QIF$ ) is in the new fill, a weighted hydraulic-conductivity coefficient ( $WKN$ ) must be computed for the north-to-south fill flow which would extend from the top of the non-permeable layer of fill (4,175 ft) up to  $QIF$ :

$$WKN = \frac{(QIF - 4200)K_{new} + (4200 - 4175)K_{old}}{QIF - 4175}. \quad (C7)$$

In this case, the hydraulic conductivity ( $WKS$ ) of the south-to-north layer of flow would equal  $K_{new}$ .

With equations C6 and C7, the fill-flow discharges determined earlier ( $QSF$  and  $QNF$ , see sections “South-to-north flow” and “North-to-south flow”) can

now be corrected for the new hydraulic-conductivity values,  $WKS$  and  $WKN$ , where  $Q_{cor}$  and  $QNF_{cor}$  are the corrected discharges:

$$QSF_{cor} = QSF_{uncor} * WKS, \text{ and}$$

$$QNF_{cor} = QNF_{uncor} * WKN.$$

## Computation of Fill Flow With the Water and Salt Balance Model

The fill flows were calculated with the water and salt balance equations. The accuracy of the calculation, however, is subject to how well the other parameters in the water and salt balance can be either measured or estimated. An equation for north-to-south flow was developed, and flows computed with this equation were compared to those computed with the algorithms described previously. The net flow north-to-south through the causeway ( $QN$ ) is described in equation 5 as:

$$QN = \frac{CS}{CN-CS} \left[ \Delta VN - PIN - GIN + EON + QWP - \frac{\Delta LN}{CS} - \frac{\Delta CLNP}{CS} - \frac{LWP}{CS} \right]$$

and in equation A4, where  $QNF$ ,  $QNC$ , and  $QNB$  are the north-to-south flows through the fill, culverts, and breach, respectively, in acre-ft, as:

$$QN = QNF + QNC + QNB.$$

Combining equations 5 and A4, to solve for  $QNF$ :

$$QNF = \frac{CS}{CN-CS} \left[ \Delta VN - PIN - GIN + EON + QWP - \frac{\Delta LN}{CS} - \frac{\Delta CLNP}{CS} - \frac{LWP}{CS} \right] - QNB - QNC \quad (C8)$$

## Sensitivity and Error Analysis

All parameters on the right side of equation C8 can be either measured or estimated with some degree of accuracy. With equation C8,  $QNF$  was calculated for 1987–98 and compared to the flow computed by the algorithms discussed above (fig. C3). The largest differences in the two computations occurred during 1987–90, when the lake was declining and the WDPP was in operation. The maximum difference was about 580 acre-ft/d, or 19 percent in 1987. During 1987–98, the model-computed fill flow averaged 611 acre-ft/d and the flow computed by equation C8 averaged 503 acre-ft/d, or about 21 percent lower than that computed by the model.

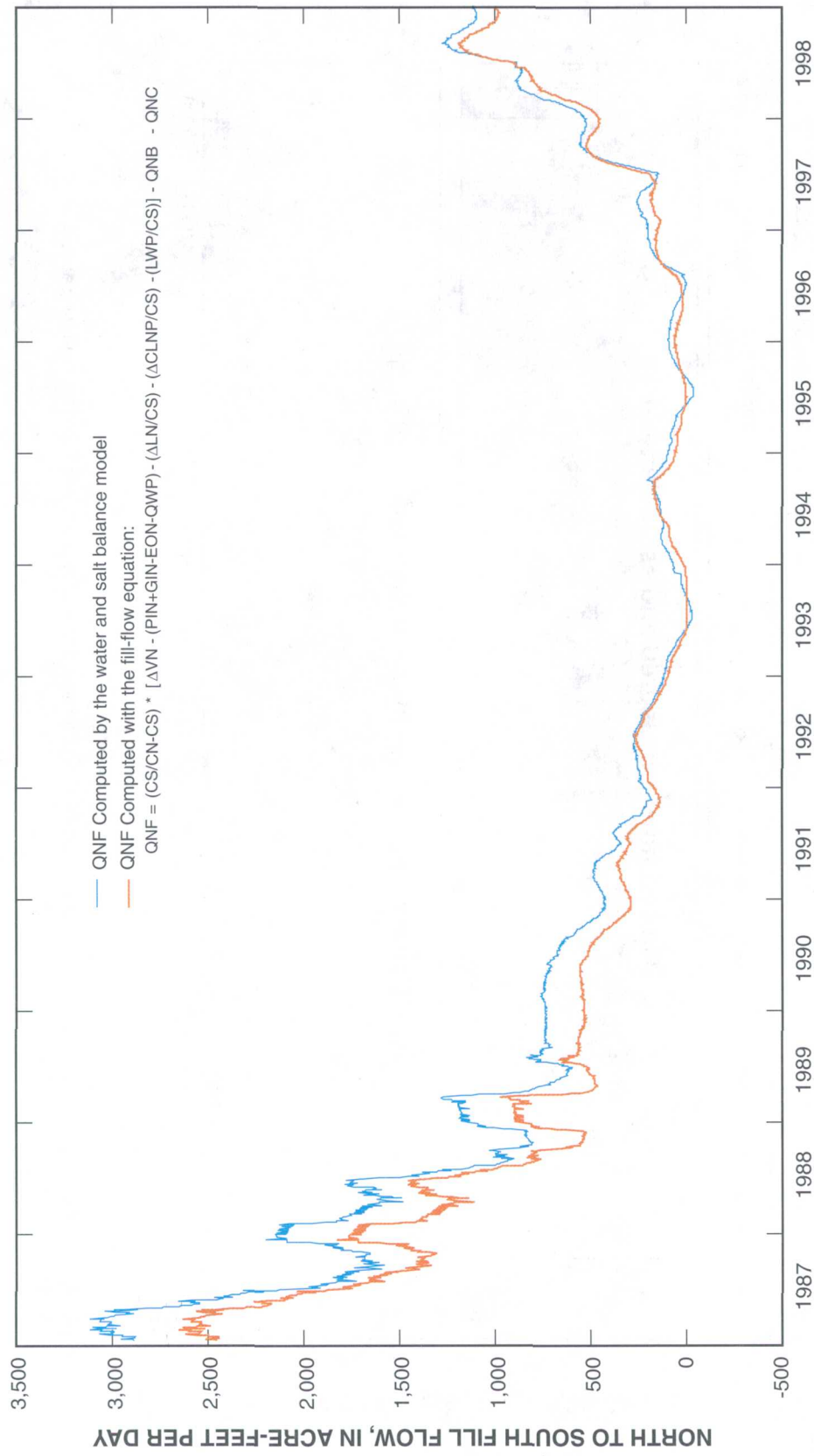
Each of the terms on the right side of equation C8 has a potential error that affects the calculation of  $QNF$ . The amount of error that can be attributed to each parameter depends largely on how well it was measured or estimated, and how large the value is relative to the other parameters. During model calibration, 1987–98, the significance of the parameters changed. For example, north-to-south flows through the breach ( $QNB$ ) only occurred during 1987–89 (fig. C4). Similarly, evaporation occurs primarily in the summer and precipitation occurs primarily in the winter and spring. A precipitated salt load ( $CLNP$ ) was not present during 1987–92 but was present during 1992–98. Also, pumpage to West Pond ( $QWP$  and  $LWP$ ) occurred only during 1987–89. Because culvert flows ( $QNC$ ) were not measured during 1987–95, they were estimated from measurements made during 1986 and 1996–98 (fig. C4). These estimates are subject to large errors because the culverts are often plugged with debris, and the size or shape of the opening cannot be determined without measurement. Because ground-water inflow ( $GIN$ ) is very small relative to the other parameters (fig. A2), even large errors would not have substantially affected the calculation of  $QNF$ .

$CS$  and  $CN$ :

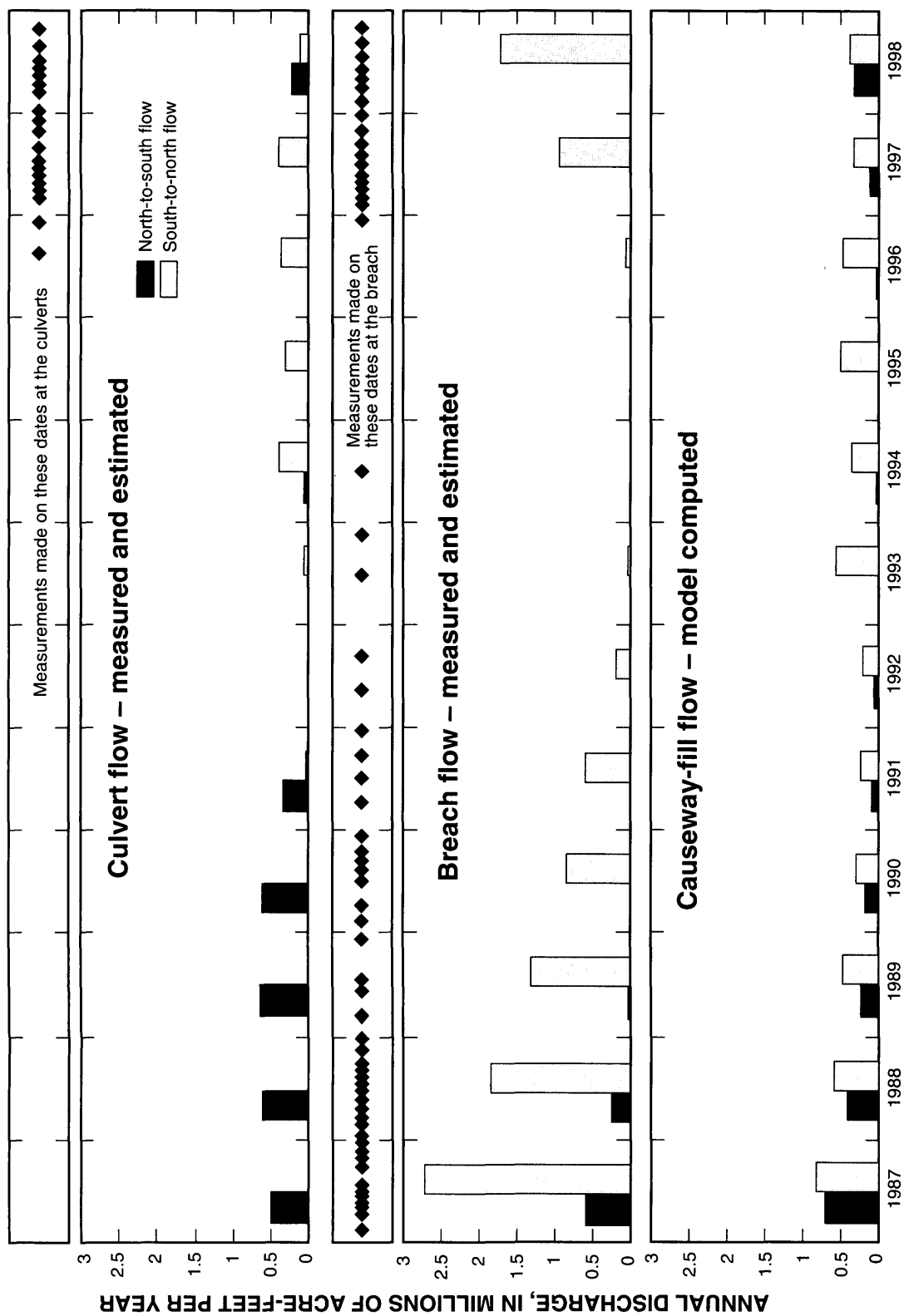
The values represent the average dissolved-solids concentration of the south and north parts, respectively. The averages are determined from measurements made at two to four monitoring sites on the lake. How well the sites represent the average for the north or south parts has not been statistically documented. Chemical analysis of the samples, which involves measuring specific gravity with a hydrometer or a densimeter, has some analytical error.

$\Delta VN$ :

Because continuous records of water-surface altitude are available for the north part of the lake during 1987–98, continuous records of the volume of the north part ( $VN$ ) can be computed with the water-surface altitude/volume relations. The amount of error associated with the change in volume of the north part ( $\Delta VN$ ) would be the result of errors in the water-surface altitude/volume relations that are derived from surface area of the north part at specified altitudes. The error associated



**Figure C3.** North-to-south flow through the causeway fill as computed from the fill flow model and from the water and salt balance equations for Great Salt Lake, Utah.



**Figure C4.** Measured and estimated flows through the culvert and breach and model-computed flows through the causeway fill for Great Salt Lake, Utah.

with this variable is believed to be smaller than that of any of the other parameters on the right side of equation C8.

$$PIN + GIN - EON - QWP:$$

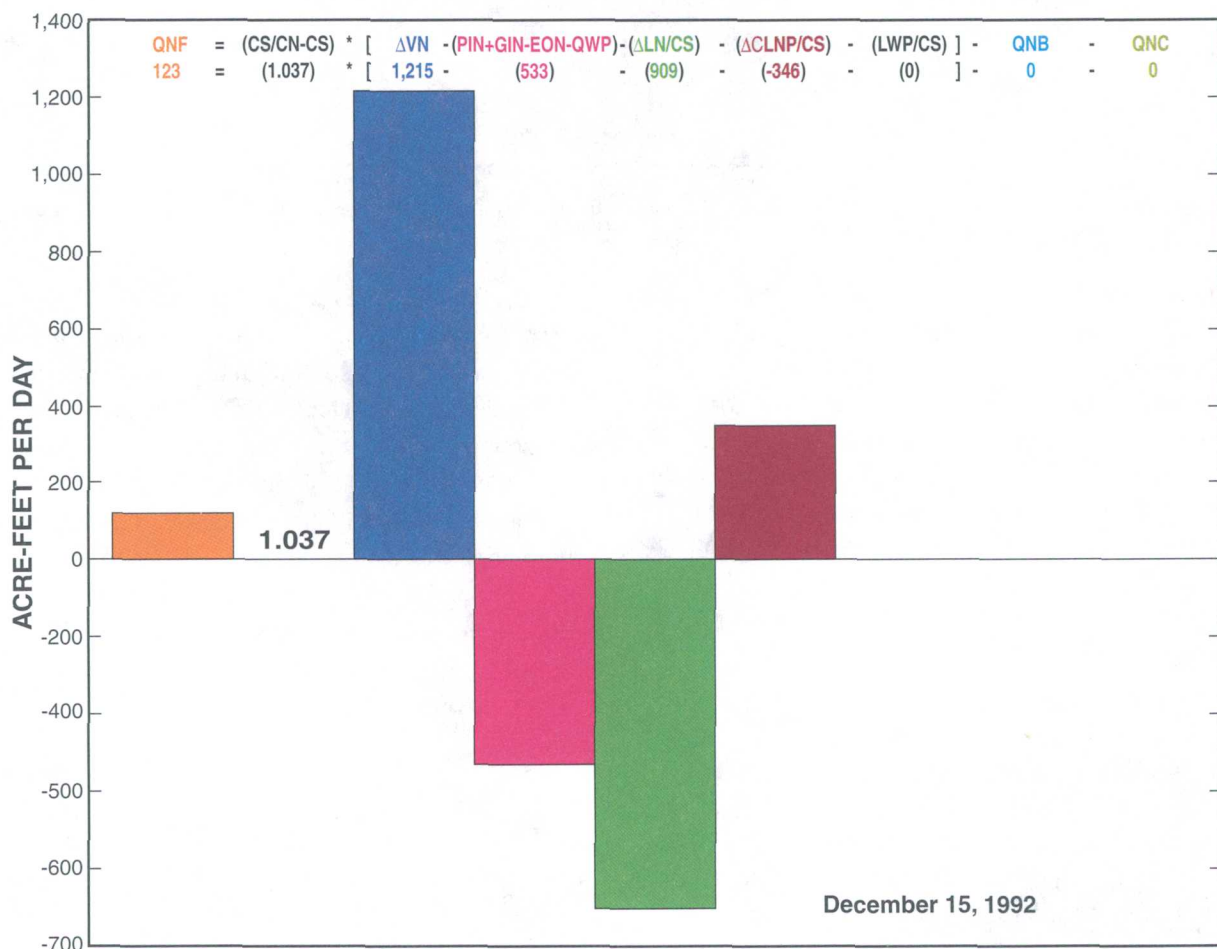
Precipitation (*PIN*) and evaporation (*EON*) are the largest numbers in this equation, and ground-water inflow (*GIN*) is almost negligible. Water pumped to West Pond (*QWP*) was a significant value during 1987–89 when the WDPP was in operation but was measured within an error of about 5 percent.

$$\Delta LN \text{ and } \Delta LNP:$$

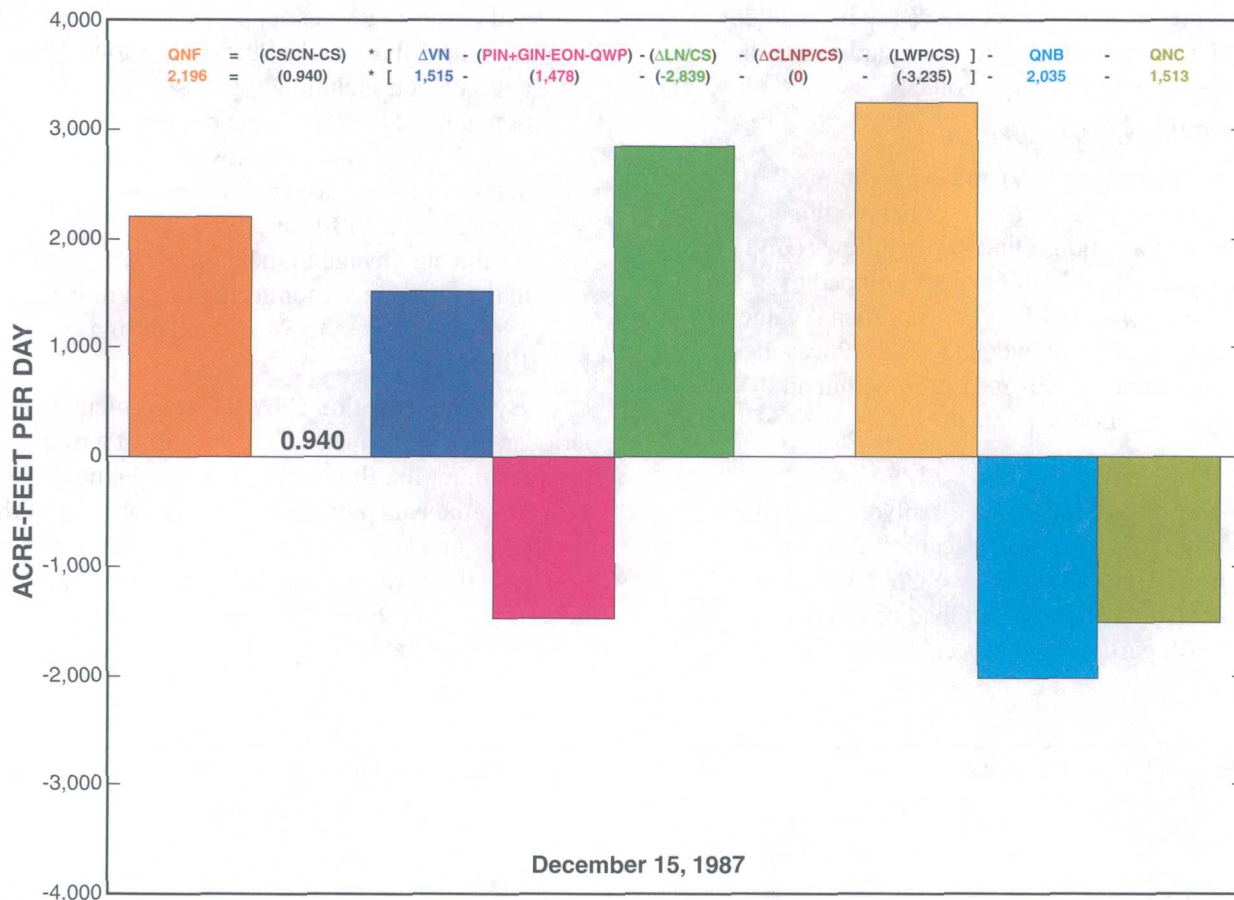
The change in load of dissolved salt in the north part ( $\Delta LN$ ) is as accurate as the parts used to compute it ( $LN = CN * VN$ ). The change of precipitated load of salt in the north part ( $\Delta LNP$ ) is a calculated value,

and the accuracy is not known but believed to be near that of *LN*. Because the total mass of salt, including the dissolved and precipitated loads, is large relative to annual inflow and withdrawals, the total mass is assumed to remain constant throughout a 100-year period. The only significant change in the total mass of salt in the lake, since monitoring began in the 1960s, is the loss to West Pond during 1987–89.

By using equation C8, *QNF* was calculated for periods when the terms on the right side of the equation were optimum for eliminating most of the potential error from the calculation. The values for each of the parameters on December 15, 1992, are shown in figure C5. About this time, the lake level was low enough that there was no flow through the breach (*QNB*), no precipitated salt load in the north part (*CLNP*), very little



**Figure C5.** Values for each parameter of the north-to-south fill-flow equation on December 15, 1992, Great Salt Lake, Utah. (See Glossary for definitions of parameters.)



**Figure C6.** Values for each parameter of the north-to-south fill-flow equation on December 15, 1987, Great Salt Lake, Utah. (See Glossary for definitions of parameters.)

evaporation (*EON*), and no outflow of water (*QWP*) or salt (*LWP*) to West Pond. Only values for *QNF*,  $\Delta VN$ , *PIN*, *GIN*, and  $\Delta LN$  were computed. The computed north-to-south flow (*QNF*) was 123 acre-ft/d. On December 15, 1992, the south part water-surface altitude was about 4,199 ft and all flow from north to south was through the older fill material (under 4,200 ft). Though the parameters on the right side of equation C8 were considered to have small errors, it would take only a 13-percent positive error in  $\Delta LN$  to reduce the calculated value of *QNF* to zero.

A similar calculation was made for the fill flow when the water-surface altitude was higher. On December 15, 1987, the south part water-surface altitude was about 4,209 ft. The computed north-to-south fill flow calculated with equation C8 was 2,196 acre-ft/d (fig. C6). On this day, the potential error was greater than that on December 15, 1992, because a greater number of parameter values were not equal to zero. Only the value for precipitated salt load was zero at this time. There also was a large amount of brine being pumped to West Pond and a considerable amount of flow

through the culverts, which has a potentially large error. The weighted hydraulic-conductivity value for the *QNF* flow layer was somewhat higher on December 15, 1987, than it was on December 15, 1992, because about 20 percent of the flow was through the more permeable new fill above 4,200 ft. Culvert flow, which is the largest potential source of error because of a lack of measurements, was estimated to be 1,513 acre-ft/d. A 100-percent positive error in the estimate of culvert flows would increase *QNF* from about 2,200 to 3,700 acre-ft/d, and a 100-percent negative error would decrease *QNF* to about 700 acre-ft/d.

During this study, the entire 1987–98 period was used for calibration because some of the parameters used in the calculations are zero or extremely small for part of the period and very large in other parts. For example, if fill flows were calibrated during 1987–92 when water-surface altitudes were high and most of the fill flow was through the new fill, the calibration would not have worked well for 1993–98 when most of the flow was through the old fill.

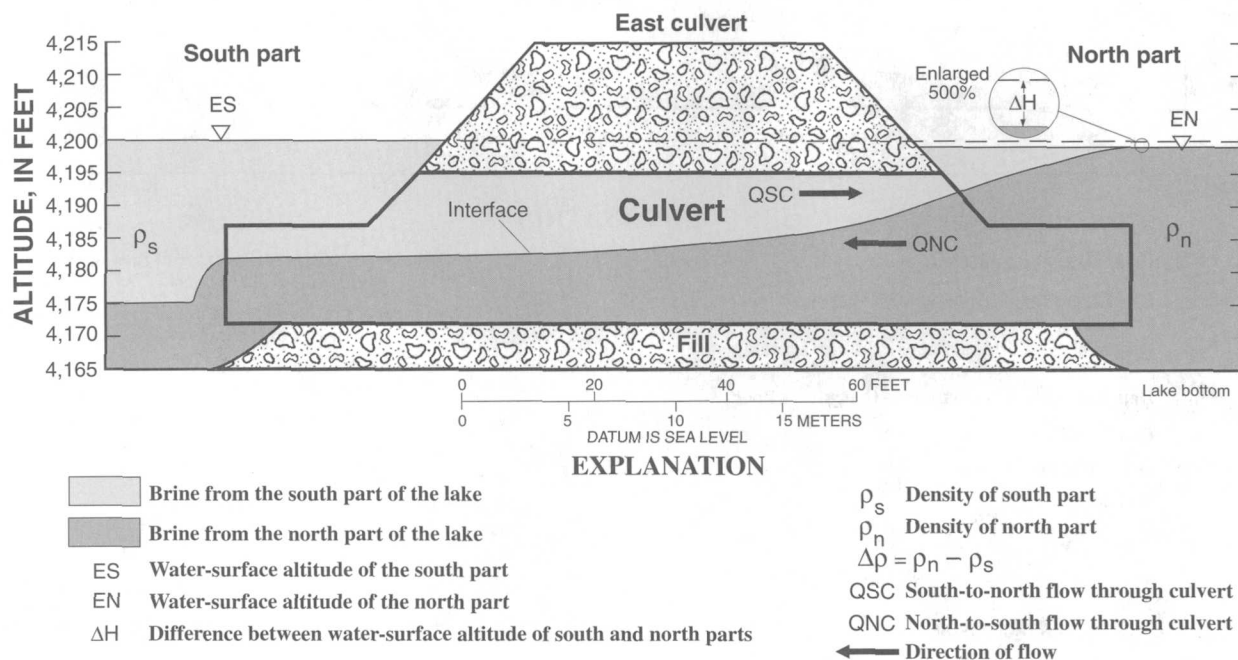
## APPENDIX D. FLOW THROUGH THE CAUSEWAY CULVERTS

During 1957–59 when the causeway was constructed, the two 15-ft-wide culverts were placed where the lake was deepest. In 1973, the altitude of the ceiling of the east culvert was about 4,203 ft and the ceiling of the west culvert was about 4,206 ft (Waddell and Bolke, 1973). Waddell and Bolke (1973, p. 47) stated that the distance from the bottom to the ceiling of the east culvert was 25.7 ft, but discharge measurements made at the culvert indicate that the opening, which may have partially filled with debris, was 23 ft deep. Since 1973 the culverts have settled, and by 1998, the altitude of the east culvert ceiling was about 4,195 ft (fig. D1), and the west culvert ceiling was about 4,198 ft, on the north ends.

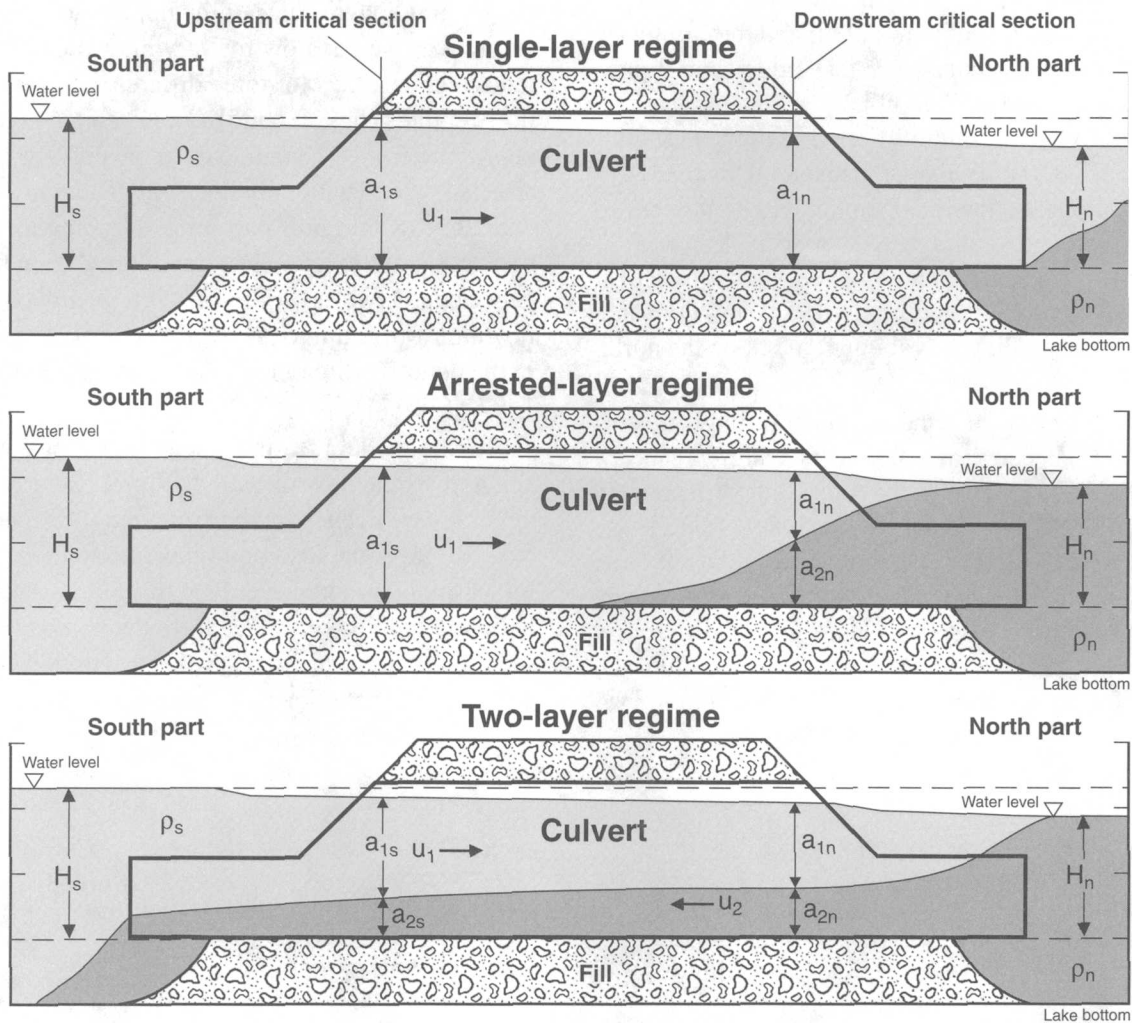
Two-way flow of brine can occur through the culverts (fig. D1) because of water-surface altitude and density differences between the south and north parts of the lake ( $\Delta H$  and  $\Delta \rho$ ). South-to-north flow ( $Q_{SC}$ ) through the upper part of the culverts is the result of a positive head difference ( $\Delta H$ ) at the causeway between the south and north parts. A positive density difference ( $\Delta \rho$ ) between the north and south parts creates the potential for north-to-south flow ( $Q_{NC}$ ) through the lower part of the culverts.

Holley and Waddell (1976) developed an algorithm for a rigorous treatment of the culvert flow through an unsubmerged culvert. The equations, which also work for the breach, had the capability of producing longitudinal profiles of the upper and interfacial surfaces as well as flow for varying water-surface altitudes and densities for three different unsubmerged flow regimes (figs. D2 and D3): (1) single layer with only brine from the south part in the culvert; (2) arrested wedge with only flow from south to north, but with a wedge of north-part brine intruding into the culvert and underlying the less dense brine from the south part; and (3) two-layer regime with the upper layer flowing from south to north and a lower layer flowing in the opposite direction (Wold, Thomas, and Waddell, 1997, p. 53).

The model identifies the proper flow condition and adjusts the flow through the upper layer and the upper layer thickness at the north end ( $a_{ln}$ , fig. D2) iteratively until boundary conditions are satisfied. Entrance losses are distributed evenly along side walls and the bidirectional flow interface from the upstream critical section to the downstream critical section. Holley and Waddell (1976) assumed a free upper water surface and did not consider flow through submerged culverts.



**Figure D1.** Schematic cross section of the east culvert in the causeway across Great Salt Lake, Utah, showing bidirectional, stratified flow, and related hydraulic properties.



#### EXPLANATION

- Brine from the south part of the lake
- Brine from the north part of the lake

$H_s$  Depth of the south part above the culvert floor

$H_n$  Depth of the north part above the culvert floor

$\rho_s$  Density of south part

$\rho_n$  Density of north part

$a_{1s}$  Depth of the upper layer of flow at the south end of the culvert

$a_{1n}$  Depth of the upper layer of flow at the north end of the culvert

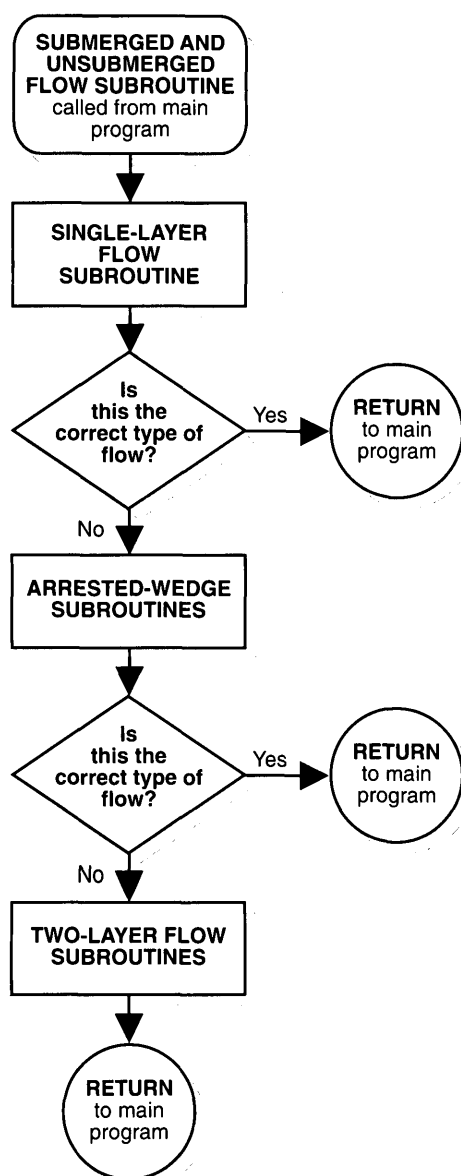
$a_{2s}$  Depth of the lower layer of flow at the south end of the culvert

$a_{2n}$  Depth of the lower layer of flow at the north end of the culvert

$u_1 \rightarrow$  Velocity of the upper flow layer

$\leftarrow u_2$  Velocity of the lower flow layer

**Figure D2.** Schematic cross sections showing flow regimes modeled for unsubmerged culverts in Great Salt Lake, Utah.



**Figure D3.** Flow chart of subroutine used to compute flow through submerged and unsubmerged culverts, and the breach in the causeway across Great Salt Lake, Utah.

To compute  $QSC$  and  $QNC$  with the equations of Holley and Waddell (1976), the density of brine near the culverts was used to estimate the density of brine moving from north to south through the culverts. A method for estimating the density of the lower layer brine as a function of  $\rho_n$  and  $QSC$  is described in appendix E.

The altitude of the culvert bottom is important in determining  $QNC$ . The culverts are often partially or completely plugged as a result of storms filling them with debris, effectively raising the bottom of the culverts. During periods of submergence, wave action can

quickly fill the culvert with cobbles and gravel. After attempts to clean the submerged culverts, it was difficult to determine how effectively the debris had been cleared. For these reasons, the model of Wold, Thomas, and Waddell (1997) included code that set the culvert flow to zero whenever submergence occurred. Some flow probably occurred through the debris but would have been insignificant when compared to flow through clean culverts.

The equations of Holley and Waddell (1976) did not account for submerged flow. To determine how the lake might respond to clean and free-flowing submerged culverts, Holley derived culvert equations that are valid for submerged flow (eqs. D1-D10) in 1998 (E.R. Holly, University of Texas at Austin, written commun., 1998). The modified equations of Holley have the capability of computing flow for varying head and density differences for four different submerged flow regimes (fig. D4). These equations were incorporated into the current model, giving it the capability to simulate flow through clean culverts in both submerged and unsubmerged conditions (figs. D3 and D4).

Critical flow at each end of the culvert is defined by the equation:

$$F_1^2 + F_2^2 - \epsilon F_1^2 F_2^2 - 1 = 0 \quad (D1)$$

where

$$\epsilon = \frac{\rho_n - \rho_s}{\rho_n}, \quad (D2)$$

and

$$F_i = \frac{u_i}{\sqrt{\epsilon g a_i}}, \quad (i = 1, 2) \quad (D3)$$

$F$  = densimetric Froude number (subscript denotes flow layer: upper = 1 and lower = 2);

$\epsilon$  = ratio of the density difference between the north and south parts of the lake to the north part density;

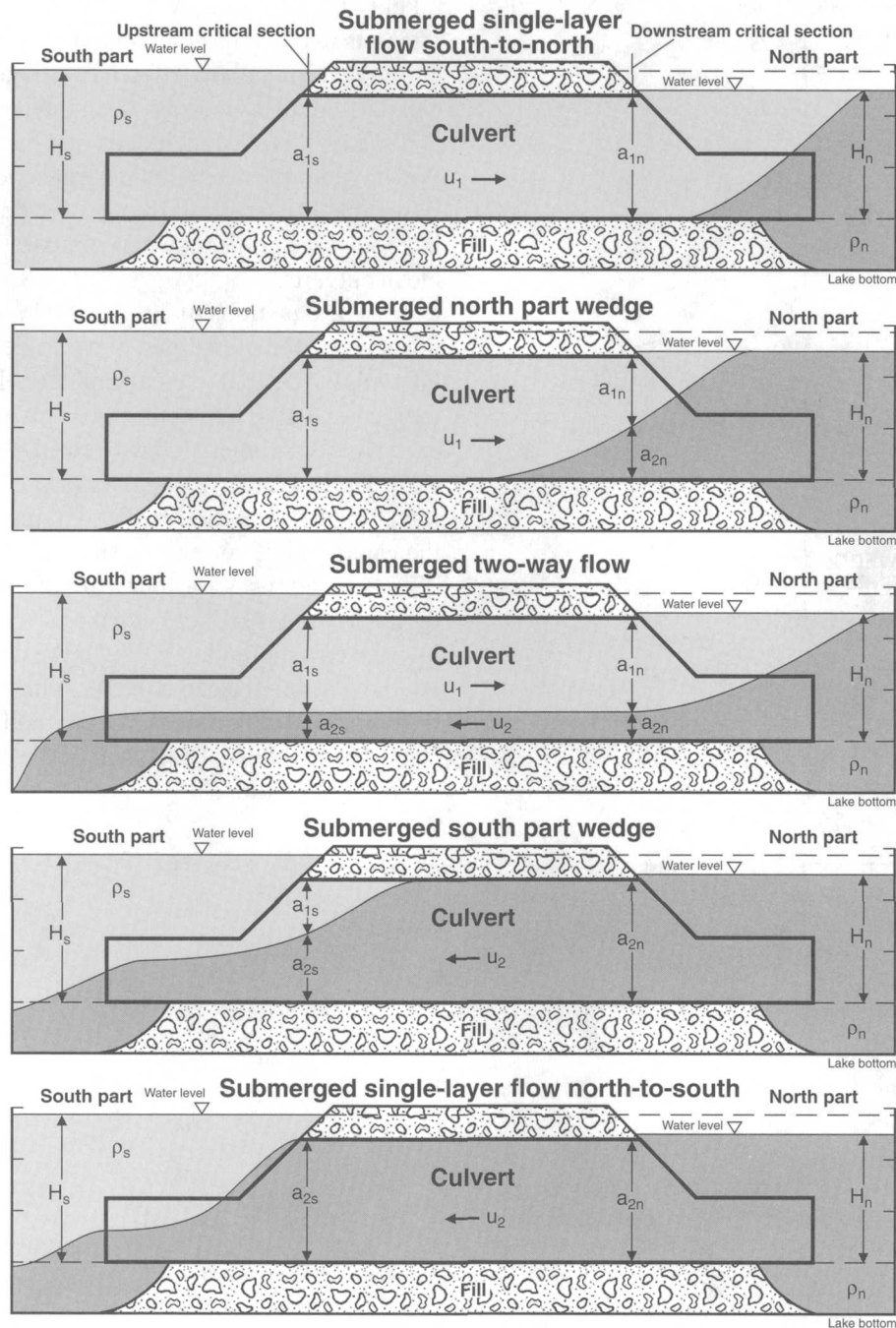
$i$  = layer number (subscript denotes flow layer: upper = 1 and lower = 2);

$u$  = velocity, in ft/s (flow divided by the cross-sectional area);


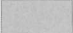
$g$  = gravitational constant (32.2 ft/s);

$a$  = layer thickness, in ft (subscript denotes flow layer: upper = 1 and lower = 2); and

$\rho$  = fluid density, in g/mL (subscript denotes part of lake: south =  $s$  and north =  $n$ ).



#### EXPLANATION

	Brine from the south part of the lake	$a_{1s}$	Depth of the upper layer of flow at the south end of the culvert
	Brine from the north part of the lake	$a_{1n}$	Depth of the upper layer of flow at the north end of the culvert
$H_s$	Depth of the south part above the culvert floor	$a_{2s}$	Depth of the lower layer of flow at the south end of the culvert
$H_n$	Depth of the north part above the culvert floor	$a_{2n}$	Depth of the lower layer of flow at the north end of the culvert
$\rho_s$	Density of south part	$u_1 \rightarrow$	Velocity of the upper flow layer
$\rho_n$	Density of north part	$\leftarrow u_2$	Velocity of the lower flow layer

**Figure D4.** Schematic cross sections showing flow regimes modeled for submerged culverts in the causeway across Great Salt Lake, Utah.

Holley determined that the equation for critical flow under submerged conditions remained the same as equation D1 above. From the general equation for momentum and the boundary conditions of a submerged culvert, Holley derived the equations for the depth of the culvert versus distance along the barrel to be as follows:

$$\frac{dx}{da_1} = \frac{\phi}{\alpha + (1 - F_2^2) \left[ \frac{\alpha + \beta - \phi \left( \frac{dD}{dx} \right)}{\kappa} \right]} \quad (D4)$$

and

$$\frac{dx}{da_2} = \frac{\phi}{\beta - (1 - \epsilon) F_1^2 \left[ \frac{\alpha + \beta - \phi \left( \frac{dD}{dx} \right)}{\kappa} \right]} \quad (D5)$$

where

$$\phi = F_1^2 + F_2^2 - \epsilon F_1^2 F_2^2 - 1; \quad (D6)$$

$$\alpha = \left( \frac{1}{\epsilon} - F_2^2 \right) T_1 - \frac{T_2}{\epsilon} + F_2^2 S_0; \quad (D7)$$

$$\beta = \left( 1 - \frac{1}{\epsilon} \right) T_1 + \left( \frac{1}{\epsilon} - F_1^2 \right) T_2 + (F_1^2 - 1) S_0; \quad (D8)$$

$$\kappa = F_1^2 + F_2^2 - \epsilon F_1^2 - 1; \quad (D9)$$

$$T_1 = \frac{2a_1(E_1 + W_1) + B(2E_1 + \Lambda_1 + S_1)}{g\rho_s a_1 B}; \quad (D10)$$

$$T_2 = \frac{2a_2(E_2 + W_2) + B(\Lambda_2 + Z + 2E_2)}{g\rho_n a_2 B}; \quad (D11)$$

$B$  = culvert width, in ft;

$D$  = culvert depth, in ft;

$E$  = entrance losses expressed as a force per square foot;

$\Lambda$  = interfacial losses expressed as a force per square foot;

$S$  = slope (subscript denotes: 0 = bottom, 1 = interface);

$W$  = wall losses expressed as a force per square foot;

$X$  = distance in the horizontal direction, in ft;

$Z$  = bottom shear; and

$\alpha, \beta, \phi, \kappa, T_1, T_2$  = mathematical shortcuts that do not represent anything physical.

With the submerged-flow equations incorporated in the model, the additional flow regimes shown in figure D4 can now be analyzed. Because the condition of submerged flow through clean, open culverts has never occurred in the causeway, there have been no measurements with which to check the theoretical flows.

During 1987–98, the culverts were partially, and at times completely, filled with debris. The variability of the size and shape of the culvert openings prevented simulations of submerged culvert flow during the calibration of the model, so flow estimates based on measurements made during 1986 and 1996–98 (table D1) were used instead.

**Table D1.** Water-surface altitude and brine density in Great Salt Lake, Utah, and flow through the east and west culverts in the causeway across Great Salt Lake, Utah, 1986–98

[g/mL, grams per milliliter; ft<sup>3</sup>/s, cubic feet per second. A dash (—) indicates no measurement was made; water-surface altitudes are estimates at the culverts, based on reported altitudes at the Saline (10010100) and Promontory Point (10010050) gages; reported densities are time-interpolated average values for the south or north part of the lake]

Date	Water-surface altitude during measurement of flow, in feet		Water-surface altitude difference across causeway, in feet	Average brine density, in g/mL		Brine density difference across causeway, in g/mL	Flow through the east culvert, in ft <sup>3</sup> /s		Flow through the west culvert, in ft <sup>3</sup> /s	
	South Part	North Part		South Part	North Part		South to North	North to South	South to North	North to South
05/20/1986	<sup>1</sup> 4,211.2	4,210.5	0.7	1.043	1.120	0.077	0	282	0	67.5
09/24/1996	<sup>1</sup> 4,198.3	4,197.0	1.3	1.086	1.219	.133	<sup>2</sup> 300	<sup>2</sup> 0	<sup>2</sup> 5	<sup>2</sup> 0
12/09/1996	<sup>1</sup> 4,198.4	4,196.9	1.5	1.086	1.218	.132	<sup>2</sup> 300	<sup>2</sup> 0	<sup>2</sup> 300	<sup>2</sup> 0
03/20/1997	4,200.1	4,197.9	2.2	1.076	1.209	.133	468	0	108	0
04/14/1997	4,200.4	4,198.0	2.4	1.074	1.209	.135	442	0	132	0
05/07/1997	4,200.7	4,198.4	2.3	1.071	1.209	.138	733	0	227	0
05/29/1997	4,200.9	4,198.5	2.4	1.068	1.209	.141	809	0	167	0
06/19/1997	4,201.3	4,198.7	2.6	1.066	1.210	.144	574	0	94	0
07/09/1997	4,201.0	4,198.6	2.4	1.066	1.211	.145	741	0	—	—
07/18/1997	4,200.8	4,198.9	1.9	1.066	1.212	.146	—	—	137	0
09/04/1997	4,200.2	4,198.7	1.5	1.069	1.218	.149	496	0	51	0
11/04/1997	4,199.8	4,198.6	1.2	1.070	1.220	.150	354	0	59	0
12/04/1997	4,200.1	4,198.9	1.2	1.069	1.218	.149	353	0	65	0
01/22/1998	4,200.6	4,199.3	1.3	1.065	1.211	.146	312	0	—	—
03/11/1998	4,201.5	4,200.1	1.4	1.060	1.202	.142	312	0	—	—
04/22/1998	4,202.1	4,200.9	1.2	1.058	1.200	.142	—	—	25	0
04/28/1998	4,202.2	4,201.0	1.2	1.057	1.200	.143	87	0	—	—
05/14/1998	4,202.4	4,201.2	1.2	1.055	1.200	.145	—	—	55	0
06/18/1998	4,202.9	4,201.6	1.3	1.051	1.201	.150	69	3	2	2
07/20/1998	4,202.7	4,201.8	0.9	1.053	1.204	.151	26	12	0	0
09/01/1998	4,201.9	4,201.5	0.4	1.056	1.212	.156	0	401	0	0
10/14/1998	4,201.8	4,201.4	0.4	1.059	1.215	.156	0	297	0	0

<sup>1</sup> Data from the Boat Harbor gage (10010000), corrected to the datum at the Saline gage (10010100).

<sup>2</sup> Estimated based on observations.

## APPENDIX E. FLOW THROUGH THE CAUSEWAY BREACH

A 290-ft-wide breach near the west side of Great Salt Lake (fig. 2) was opened on August 1, 1984. The altitude of the bottom of the breach was about 4,200 ft, until August of 1996 when it was deepened to an effective depth of 4,198 ft by the Union Pacific Railroad Company.

Similar to that of the culvert openings, two-way unsubmerged flow of brine can occur through the breach because of altitude and density differences between the south and north parts of the lake ( $\Delta H$  and  $\Delta \rho$ ). Only unsubmerged flows have occurred at the breach; the altitude of the top of the breach is about 4,214 ft. The flow through the breach ( $Q_{SB}$  and  $Q_{NB}$ ) was measured by using modified streamflow measurement techniques (table E1). Levels for altitude control were run to benchmark FMK 120 1966 (fig. 2), and the head difference at the causeway was determined between the south and north parts of the lake. The altitude of the bottom of the breach was determined as part of the flow measurements. Brine samples were collected at selected depths from within the breach opening to determine the depth of the interface between the two layers of flow.

During most of 1987–90, two-layer flow was observed; thereafter, flows that occurred were from south to north until late 1998, when two-layer flow returned (table E1). For unsubmerged flows, the hydraulics governing flow through the breach and culverts are similar, so the equations of Holley and Waddell (1976) were used in the model to compute breach flow (appendix D).

To compute  $Q_{SB}$  and  $Q_{NB}$  with the equations of Holley and Waddell (1976), the density of the brine near the breach is used to estimate the density of brine moving from north to south through the breach. As brine from the south part enters the breach, it forms the upper layer of brine moving through the breach, and after exiting the breach, spreads out over the surface of the north part and mixes with brine from the north part. This mixing causes brine moving from north to south

through the breach to be slightly lower in density than the average of brine from the north part. A previous study by Wold, Thomas, and Waddell (1997, p. 58) determined that the effect of mixing is related to the amount of south-to-north flow. The brine density used as a boundary condition for computing flow through the breach is computed from equation E1:

$$\text{Density of brine near breach} = \rho_n [1 - (3 \times 10^{-6}) Q_{SB}] \quad (\text{E1})$$

where

$\rho_n$  = average density of brine in north part, in g/mL; and

$Q_{SB}$  = south-to-north flow through breach from previous time step, in  $\text{ft}^3/\text{s}$ .

The cross-sectional opening of the breach is a trapezoidal shape with the east and west sides of the breach sloping into the lake. The equations of Holley and Waddell (1976) assume that openings in the causeway have vertical walls. The cross-sectional area of the trapezoid, which is formed by the sides of the breach, the water-surface altitude, and the bottom of the breach, was estimated and (table E1) then used in conjunction with the equations of Holley and Waddell (1976) to compute breach flow.

Correspondence between the computed and measured values of  $Q_{SB}$  and  $Q_{NB}$ , respectively, is shown in figures E1 and E2. The standard error of estimate for computed and measured breach flow was  $722 \text{ ft}^3/\text{s}$ , or 30 percent of the mean for south-to-north flow, and  $294 \text{ ft}^3/\text{s}$ , or 116 percent of the mean for north-to-south flow. The differences between computed and measured flows are due to a combination of measurement errors and the sum of errors in simulating flows. Measurement errors are the result of difficulty in determining a precise depth of interface between the layers of bidirectional flow and difficulty in determining accurate mean water-surface altitudes for a field measurement on days when the lake is turbulent and flows unsteady. Model errors are the result of the sensitivity of computed flows to errors in head difference and differences between model-simulated and actual physical characteristics of the breach.

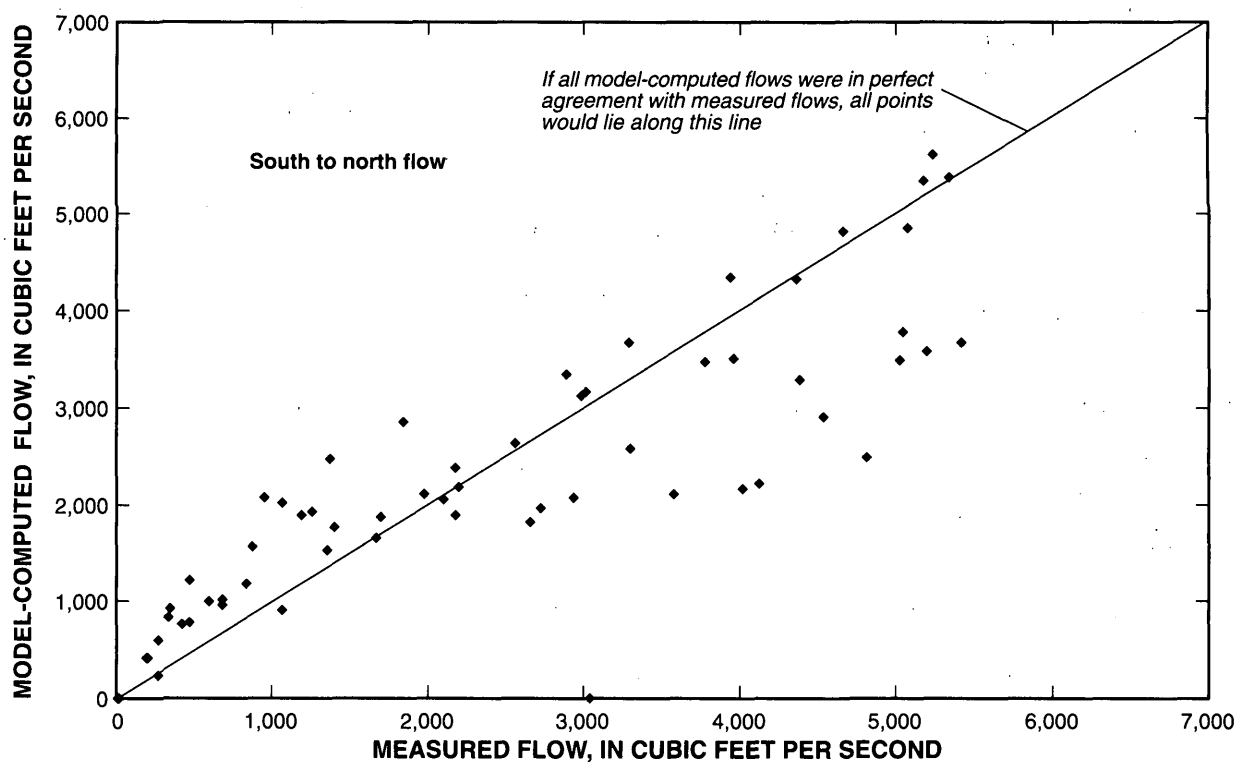
**Table E1.** Water-surface altitude, head difference, and brine density in Great Salt Lake and flow through the breach in the causeway across Great Salt Lake, Utah, 1987–98

[Data from Remillard and others (1987, 1988, 1989, 1990, 1991, 1992, 1993, 1994, 1995), and Herbert and others (1996, 1997, 1998, 1999). ES, water-surface altitude of south part; EN, water-surface altitude of north part;  $\Delta H$ , head difference;  $\rho_s$ , average density of south part;  $\rho_n$ , average density of north part;  $\Delta\rho$ , density difference; QSB, south-to-north flow through breach; and QNB, north-to-south flow through breach. (These terms are the same as those used in equations and text throughout this report); ft, feet; g/mL, grams per milliliter; ft<sup>3</sup>/s, cubic feet per second;  $\pm$ , plus or minus;  $\pm >$ , plus or minus greater than; water-surface altitudes are reported to the nearest tenth of a foot;  $\pm$  tolerances reflect the variability of the unrounded values during the measurement; water-surface altitude difference tolerances of greater than  $\pm 0.15$  ft indicate unsteady conditions at the breach due to wind and waves; some reported densities are interpolations between measured values]

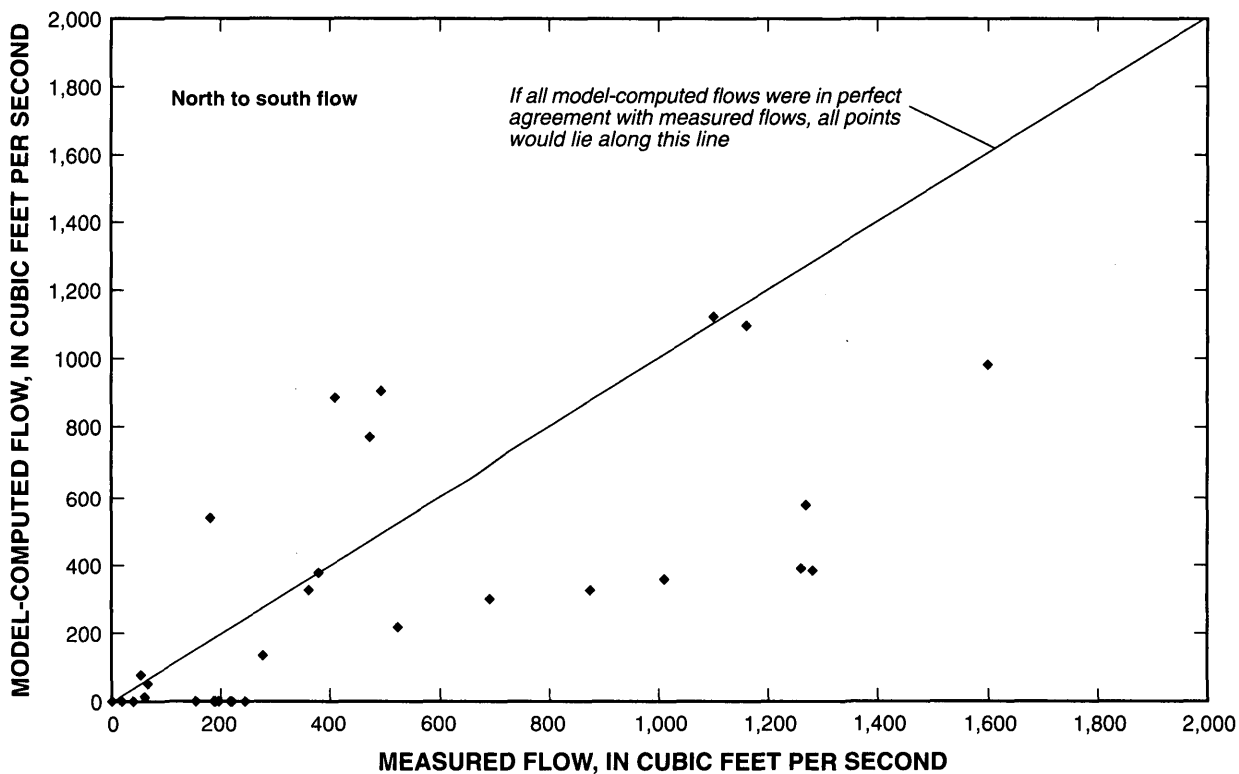
Date	Water-surface altitude during measurement of flow, in ft		Water-surface altitude difference across causeway, in feet ( $\Delta H$ )	Average brine density, in g/mL		Brine density difference, in g/mL ( $\Delta\rho$ )	Measured flow through the breach, in ft <sup>3</sup> /s		Model-computed flow through the breach, in ft <sup>3</sup> /s	
	South Part (ES)	North Part (EN)		South part ( $\rho_s$ )	North part ( $\rho_n$ )		South to north (QSB)	North to south (QNB)	South to north (QSB)	North to south (QNB)
01/13/1987	4,211.1 $\pm$ .08	4,210.5 $\pm$ .09	0.6 $\pm$ .17	1.053	1.130	0.077	5,180	1,010	5,350	359
03/03/1987	4,211.4 $\pm$ .04	4,210.8 $\pm$ .04	.6 $\pm$ .08	1.052	1.126	.074	5,240	1,280	5,620	382
04/07/1987	4,211.5 $\pm$ .03	4,210.9 $\pm$ >.10	.6 $\pm$ >.13	1.052	1.124	.072	5,340	1,270	5,390	576
05/05/1987	4,211.4 $\pm$ .07	4,210.9 $\pm$ .08	.5 $\pm$ .15	1.053	1.123	.070	3,940	1,600	4,340	980
05/19/1987	4,211.3 $\pm$ >.10	4,210.9 $\pm$ >.10	.4 $\pm$ >.20	1.052	1.122	.070	5,200	1,100	3,580	1,120
06/02/1987	4,211.2 $\pm$ >.10	4,210.8 $\pm$ .10	.4 $\pm$ >.20	1.052	1.121	.069	5,020	1,160	3,490	1,100
06/30/1987	4,210.9 $\pm$ >.10	4,210.4 $\pm$ >.10	.5 $\pm$ >.20	1.053	1.122	.069	5,070	876	4,850	329
08/11/1987	4,210.1 $\pm$ >.10	4,209.7 $\pm$ >.10	.4 $\pm$ >.20	1.055	1.125	.070	3,290	1,260	3,680	391
09/22/1987	4,209.4 $\pm$ .05	4,209.0 $\pm$ .03	.4 $\pm$ .08	1.059	1.127	.068	5,040	276	3,790	136
10/27/1987	4,209.1 $\pm$ .03	4,208.7 $\pm$ .06	.4 $\pm$ .09	1.061	1.128	.067	3,960	522	3,500	218
11/23/1987	4,209.1 $\pm$ .10	4,208.7 $\pm$ >.10	.4 $\pm$ >.20	1.061	1.127	.066	4,380	362	3,300	329
12/28/1987	4,209.0 $\pm$ >.10	4,208.7 $\pm$ .07	.3 $\pm$ >.17	1.061	1.126	.065	4,020	408	2,160	884
01/27/1988	4,209.0 $\pm$ .09	4,208.8 $\pm$ >.10	.2 $\pm$ >.19	1.061	1.124	.063	3,040	922	0	2,380
02/26/1988	4,209.1 $\pm$ .04	4,208.8 $\pm$ .02	.3 $\pm$ .06	1.062	1.123	.061	4,120	494	2,210	905
03/29/1988	4,209.0 $\pm$ >.10	4,208.7 $\pm$ >.10	.3 $\pm$ >.20	1.062	1.123	.061	4,810	181	2,490	538
04/26/1988	4,209.0 $\pm$ >.10	4,208.5 $\pm$ >.10	.5 $\pm$ >.20	1.062	1.122	.060	4,660	188	4,820	0
05/20/1988	4,208.8 $\pm$ .08	4,208.5 $\pm$ >.10	.3 $\pm$ >.18	1.061	1.121	.060	3,300	378	2,570	379
06/27/1988	4,208.3 $\pm$ >.10	4,208.0 $\pm$ >.10	.3 $\pm$ >.20	1.062	1.123	.061	2,720	472	1,960	769
07/26/1988	4,207.6 $\pm$ .03	4,207.3 $\pm$ .06	.3 $\pm$ .09	1.065	1.126	.061	2,200	691	2,180	300
08/29/1988	4,207.0 $\pm$ .04	4,206.6 $\pm$ .07	.4 $\pm$ .11	1.068	1.130	.062	2,980	187	3,120	0
09/27/1988	4,206.3 $\pm$ >.10	4,206.0 $\pm$ >.10	.3 $\pm$ >.20	1.070	1.133	.063	3,580	244	2,110	0
10/31/1988	4,206.0 $\pm$ >.10	4,205.7 $\pm$ .06	.3 $\pm$ >.16	1.072	1.134	.062	2,930	0	2,060	0
12/05/1988	4,205.9 $\pm$ >.10	4,205.6 $\pm$ .10	.3 $\pm$ >.20	1.072	1.132	.060	2,660	53	1,810	79
02/24/1989	4,206.0 $\pm$ >.10	4,205.7 $\pm$ >.10	.3 $\pm$ >.20	1.071	1.129	.058	2,100	66	2,050	49
05/18/1989	4,206.1 $\pm$ >.10	4,205.7 $\pm$ >.10	.4 $\pm$ >.20	1.070	1.130	.060	4,540	0	2,910	0
06/28/1989	4,205.4 $\pm$ >.10	4,205.1 $\pm$ .07	.3 $\pm$ >.17	1.072	1.132	.060	2,180	18	1,890	0
11/16/1989	4,203.8 $\pm$ >.10	4,203.4 $\pm$ >.10	.4 $\pm$ >.20	1.082	1.147	.065	1,260	0	1,920	0
01/26/1990	4,203.8 $\pm$ >.10	4,203.7 $\pm$ .10	.1 $\pm$ >.20	1.081	1.145	.064	683	217	972	0
03/26/1990	4,204.1 $\pm$ >.10	4,203.7 $\pm$ .04	.4 $\pm$ >.14	1.081	1.144	.063	954	39	2,060	0
06/05/1990	4,203.7 $\pm$ >.10	4,203.3 $\pm$ .05	.4 $\pm$ >.15	1.081	1.146	.065	468	220	1,210	0
07/06/1990	4,203.2 $\pm$ >.10	4,203.0 $\pm$ .05	.2 $\pm$ >.15	1.083	1.151	.068	336	196	831	0
08/10/1990	4,202.5 $\pm$ >.10	4,202.3 $\pm$ .05	.2 $\pm$ >.15	1.088	1.158	.070	592	0	1,010	0
09/19/1990	4,202.0 $\pm$ >.10	4,201.6 $\pm$ .05	.4 $\pm$ >.15	1.093	1.167	.074	468	0	790	0
11/29/1990	4,201.6 $\pm$ .05	4,201.0 $\pm$ .05	.6 $\pm$ .10	1.096	1.169	.073	425	0	765	0
03/19/1991	4,202.0 $\pm$ .05	4,201.3 $\pm$ .05	.7 $\pm$ .10	1.094	1.166	.072	835	0	1,170	0
06/25/1991	4,202.0 $\pm$ .04	4,201.2 $\pm$ .04	0.8 $\pm$ .08	1.092	1.170	0.078	684	0	1,020	0
09/12/1991	4,200.7 $\pm$ >.10	4,200.1 $\pm$ >.10	.6 $\pm$ >.20	1.101	1.187	.086	199	0	415	0
12/06/1991	4,200.5 $\pm$ .05	4,199.5 $\pm$ .10	1.0 $\pm$ .15	1.102	1.190	.088	187	0	415	0
04/17/1992	4,201.2 $\pm$ .05	4,199.9 $\pm$ .05	1.3 $\pm$ .10	1.098	1.190	.092	342	0	936	0
08/20/1992	4,199.4 $\pm$ >.10	4,198.0 $\pm$ >.10	1.4 $\pm$ >.20	1.108	1.215	.107	18	0	0	0
09/29/1992	4,198.8 $\pm$ .04	4,197.5 $\pm$ .04	1.3 $\pm$ .08	1.113	1.219	.106	22	0	0	0
06/10/1993	4,200.7 $\pm$ .05	4,197.4 $\pm$ .04	3.3 $\pm$ .09	1.097	1.218	.121	271	0	607	0

**Table E1.** Water-surface altitude, head difference, and brine density in Great Salt Lake and flow through the breach in the causeway across Great Salt Lake, Utah, 1987–98—Continued

Date	Water-surface altitude during measurement of flow, in ft		Water-surface altitude difference across causeway, in feet ( $\Delta H$ )	Average brine density, in g/mL		Brine density difference, in g/mL ( $\Delta \rho$ )	Measured flow through the breach, in ft <sup>3</sup> /s		Model-computed flow through the breach, in ft <sup>3</sup> /s	
	South Part (ES)	North Part (EN)		South part ( $\rho_s$ )	North part ( $\rho_n$ )		South to north (QSB)	North to south (QNB)	South to north (QSB)	North to south (QNB)
10/28/1993	4,199.7 $\pm$ >.10	4,196.6 $\pm$ .04	3.1 $\pm$ >.14	1.104	1.220	.116	23	0	0	0
06/16/1994	4,199.8 $\pm$ >.10	4,197.8 $\pm$ >.10	2.0 $\pm$ >.20	1.095	1.217	.122	14	0	0	0
12/19/1996	4,198.5 $\pm$ .05	4,197.0 $\pm$ .04	1.5 $\pm$ .09	1.085	1.216	.131	271	0	229	0
02/11/1997	4,199.6 $\pm$ .04	4,197.6 $\pm$ .05	2.0 $\pm$ .09	1.079	1.211	.132	877	0	1,560	0
03/20/1997	4,200.1 $\pm$ .04	4,197.9 $\pm$ .04	2.2 $\pm$ .08	1.076	1.209	.133	1,060	0	2,010	0
04/14/1997	4,200.4 $\pm$ .05	4,198.0 $\pm$ .05	2.4 $\pm$ .10	1.074	1.209	.135	1,370	0	2,470	0
05/07/1997	4,200.7 $\pm$ .05	4,198.4 $\pm$ .05	2.3 $\pm$ .10	1.071	1.209	.138	1,700	0	1,870	0
05/29/1997	4,200.9 $\pm$ .04	4,198.5 $\pm$ .05	2.4 $\pm$ .09	1.068	1.209	.141	1,980	0	2,110	0
06/19/1997	4,201.3 $\pm$ .05	4,198.7 $\pm$ .04	2.6 $\pm$ .09	1.066	1.210	.144	2,560	0	2,640	0
07/09/1997	4,201.0 $\pm$ .05	4,198.6 $\pm$ .04	2.4 $\pm$ .09	1.066	1.211	.145	2,180	0	2,380	0
08/12/1997	4,200.5 $\pm$ >.10	4,198.6 $\pm$ >.10	1.9 $\pm$ >.20	1.068	1.215	.147	1,670	0	1,650	0
10/20/1997	4,199.8 $\pm$ .04	4,198.7 $\pm$ .05	1.1 $\pm$ .09	1.070	1.220	.150	1,060	0	911	0
12/03/1997	4,200.0 $\pm$ .04	4,198.9 $\pm$ .05	1.1 $\pm$ .09	1.069	1.218	.149	1,400	0	1,760	0
01/21/1998	4,200.6 $\pm$ .04	4,299.3 $\pm$ .02	1.3 $\pm$ .06	1.065	1.210	.145	1,840	0	2,850	0
03/11/1998	4,201.5 $\pm$ .05	4,200.1 $\pm$ .02	1.4 $\pm$ .07	1.060	1.202	.142	2,890	0	3,340	0
04/22/1998	4,202.1 $\pm$ .02	4,200.9 $\pm$ .02	1.2 $\pm$ .04	1.058	1.200	.142	3,780	0	3,470	0
05/13/1998	4,202.5 $\pm$ >.10	4,201.1 $\pm$ .05	1.4 $\pm$ >.15	1.056	1.200	.144	5,420	0	3,680	0
06/22/1998	4,202.9 $\pm$ .10	4,201.8 $\pm$ .02	1.1 $\pm$ .12	1.053	1.201	.148	4,360	0	4,330	0
07/20/1998	4,202.7 $\pm$ .05	4,201.8 $\pm$ .05	.9 $\pm$ .10	1.053	1.204	.151	3,010	0	3,160	0
09/01/1998	4,201.9 $\pm$ .02	4,201.5 $\pm$ .02	.4 $\pm$ .04	1.056	1.212	.156	1,190	61	1,890	13
10/27/1998	4,201.8 $\pm$ .05	4,201.3 $\pm$ .03	.5 $\pm$ .08	1.060	1.215	.155	1,350	152	1,520	0



**Figure E1.** Comparison of model-computed and measured south-to-north flow through the breach in the causeway across Great Salt Lake, Utah, 1987–98.



**Figure E2.** Comparison of model-computed and measured north-to-south flow through the breach in the causeway across Great Salt Lake, Utah, 1987–98.

## APPENDIX F. INITIAL CONDITIONS AND INPUT USED FOR CALIBRATION OF WATER AND SALT BALANCE MODEL

Inflow data from 1987–98 were used as input during calibration of the water and salt balance model. The compilation of these data are discussed in appendix A. The physical and chemical conditions of the lake on January 1, 1987, were used as initial conditions for the 1987–98 model calibration period and are listed below:

### Initial Lake Conditions

Dissolved salt load in south part	<i>LS</i>	2.08 billion tons
Dissolved salt load in deep brine layer of south part	<i>LSL</i>	0.0 billion tons
Dissolved salt load in north part	<i>LN</i>	3.0 billion tons
Cumulative precipitated salt load in north part	<i>CLNP</i>	0.0 billion tons
Dissolved chloride (Cl) load in south part	<i>CILS</i>	1.087 billion tons
Dissolved chloride (Cl) load in north part	<i>CILN</i>	1.348 billion tons
Dissolved magnesium (Mg) load in south part	<i>MgLS</i>	0.070 billion tons
Dissolved magnesium (Mg) load in north part	<i>MgLN</i>	0.070 billion tons
Dissolved potassium (K) load in south part	<i>KLS</i>	0.039 billion tons
Dissolved potassium (K) load in north part	<i>KLN</i>	0.051 billion tons
Dissolved sodium (Na) load in south part	<i>NaLS</i>	0.610 billion tons
Dissolved sodium (Na) load in north part	<i>NaLN</i>	0.771 billion tons
Water-surface altitude of south part	<i>ES</i>	4,210.97 ft
Difference between water-surface altitude of south and north parts at the causeway (head difference)	$\Delta H$	0.60 ft

### Causeway Conditions

Hydraulic conductivity reduction factor of new fill layer (same as in 1973 (Waddell and Bolke, 1973))	1.0
Hydraulic conductivity reduction factor of old fill layer (10 percent of the value used in 1973 (Waddell and Bolke, 1973))	0.1
Average altitude of interface between old and new fill layers	4,200 ft
Average altitude at top of non-permeable fill layer	4,175 ft
Breach width at altitude 4,200.0 ft	200 ft
Breach width at altitude 4,210.0 ft	290 ft
Breach width at altitude 4,214.0 ft	290 ft
Breach bottom altitude (deepened to 4,198 ft on August 1, 1996)	4,200 ft

Culvert flows were not computed for the model calibration. The culverts were frequently plugged during the calibration period, which prevented the use of theoretical equations to compute flow. Estimates of flow based on measurements were used instead.

Model calibration is discussed in the main body of this report. A constant time interval ( $T$ ) of 1.901 days was used in the model.



## GLOSSARY

Abbreviations	Where used
A	Only in the report
M	Water And Salt Balance Model (Main Routine)
1	CULV1 Subroutine
2	CULV2A Or CULV2B Subroutine
3	CULV3 Subroutine
I	INTER Subroutine
P	INTERP Subroutine
R	RINTER Subroutine
S	SLOPE Subroutine
T	INTER3 Subroutine
W	Water Balance Program

Report symbol	Water-Balance Program symbol	Water and Salt Balance Model symbol	Description	Unit	Where used
a1		A1	Thickness of the upper layer of channel flow	ft	123S
		A1BAR	Thickness of the upper layer at the layer midpoint	ft	123S
a1N		A1N	Upper layer thickness at north end critical section	ft	123
		A1NMAX	Maximum trial value for A1N	ft	1
		A1NMIN	Minimum trial value for A1N	ft	1
		A1NTRY	Trial value for A1N	ft	1
a1S		A1S	Upper layer thickness at south end critical section	ft	123
a2		A2	Thickness of the lower layer of channel flow	ft	123S
		A2BAR	Thickness of the lower layer at the layer midpoint	ft	123S
a2N		A2N	Lower layer thickness at north end critical section	ft	123
a2S		A2S	Lower layer thickness at south end critical section	ft	123
	AAPEN		An array that is a table of average annual precipitation and evaporation for the north part	in.	W
	AAPES		An array that is a table of average annual precipitation and evaporation for the south part	in.	W
		ADN	Downstream value of A1	ft	1
		AH1	Pressure head at upstream end of channel	ft	1
		ALBL	Cross-sectional area of the lower breach flow layer	ft <sup>2</sup>	M
α		ALPHA	(1./EPS-F2)*T1-T2/EPS+F2*SZ; a variable used to calculate DA1/DX and DA2/DX	no units	S
		ALWP(IN)	Loss of dissolved solids to west pond from the north part as part of the WDPP (negative values indicate return flow)	billions of tons/month	M
		AMBN(IN)	Mean (north-to-south) breach flow for each month (measured)	ft <sup>3</sup> /s	M
		AMBS(IN)	Mean (south-to-north) breach flow for each month (measured)	ft <sup>3</sup> /s	M

Report symbol	Water-Balance Program symbol	Water and Salt Balance Model symbol	Description	Unit	Where used
		AMECN(IN)	Mean (north-to-south) east culvert flow for each month (measured)	ft <sup>3</sup> /s	M
		AMECS(IN)	Mean (south-to-north) east culvert flow for each month (measured)	ft <sup>3</sup> /s	M
		AMWCN(IN)	Mean (north-to-south) west culvert flow for each month (measured)	ft <sup>3</sup> /s	M
		AMWCS(IN)	Mean (south-to-north) west culvert flow for each month (measured)	ft <sup>3</sup> /s	M
AN	AN	AN	Surface area of the north part of the lake	acres	MPW
EON	AQENXC	AQEN(IN)	Evaporation from the north part as computed in the water-balance program	acre-ft/d	MW
EOS	AQESXC	AQES(IN)	Evaporation from the south part as computed in the water-balance program	acre-ft/d	MW
	AQINX	AQIN(IN)	Ground water and precipitation inflow to the north part	acre-ft/d	MW
	AQISX	AQIS(IN)	Surface water, ground water, and precipitation inflow to the south part	acre-ft/d	MW
	QWP	WESTP	AQWP(IN)	Loss of water to the West Pond from the north part as part of the WDPP (negative values indicate return flow)	acre-ft/month
AS	AS	AS	Surface area of the south part of the lake	acres	MPW
		AUBL	Cross-sectional area of the upper breach flow layer	ft <sup>2</sup>	M
		AX1	Change in A1 with respect to X	no units	S
		AX2	Change in A2 with respect to X	no units	S
	AQENX	AXEN(IN)	Monthly freshwater evaporation rate from the north part (computed in the water-balance program)	ft/day	MW
	AQESX	AXES(IN)	Monthly freshwater evaporation rate from the south part (computed in the water-balance program)	ft/day	MW
	β		BETA	(1.-1./EPS)*T1+(1./EPS-F1SQ)*T2+(F1SQ-1.)*SZ; a variable used to calculate DA1/DX and DA2/DX	no units
		BSLOPE	Increase of trapezoidal breach width with every increased foot of altitude	ft	M
		CAC	Constant used to convert ft <sup>3</sup> /s to acre-ft/d	ft <sup>3</sup> /s*(day/acre-ft)	M
	CAUS	CAUS	Net flow through causeway from south-to-north	acre-ft/month	W
	CHANB(ICHN)	Elevation of the bottom of channel (ICHN) (elevation = altitude - 4,000 ft)	ft	M	
	CHANB2(1)	Elevation of the bottom of the breach after it was deepened (at TSBD) (elevation = altitude - 4,000 ft)	ft	M	
	CHANT(ICHN)	Elevation of the top of channel (ICHN) (elevation = altitude - 4,000 ft)	ft	M	
B		CHANW(ICHN)	Width of the channel (ICHN)	ft	M
		CHNW	Width of the channel ('B' in the subroutines)	ft	M123
		CICN	Chloride (Cl) concentration in the north part	tons/acre-ft	M

Report symbol	Water-Balance Program symbol	Water and Salt Balance Model symbol	Description	Unit	Where used
		CICS	Chloride (Cl) concentration in the south part	tons/acre-ft	M
CILN		CILN	Dissolved chloride (Cl) load in the north part	tons	M
CILS		CILS	Dissolved chloride (Cl) load in the south part	tons	M
		CILWP	Loss of chloride from the north part to west pond due to the WDPP (negative values indicate chloride returning)	tons/time step	M
CLNP		CLNPPT	Cumulative (total) precipitated salt load in the north part	tons	M
CLSP			Cumulative (total) precipitated salt load in the south part	tons	A
CN	CN	CN	Concentration of dissolved solids in the north part	g/L	M
		COEF	Used to determine X when integration goes past downstream Pressure head	no units	2
CS	CS	CS	Concentration of dissolved solids in the south part	g/L	M
CULV1			Subroutine used to calculate two-way flow	no units	A
D			Depth of culvert	ft	A
		DA	Change in Pressure head	ft	12
		DA1	Change in upper layer thickness	ft	12
		DA1DX	Change in A1 with respect to X	no units	12
		DA2	Change in A2	ft	12
		DA2DX	Change in A2 with respect to X	no units	12
		DADX	Change in surface with respect to X	no units	12
		DAY	Approximate day of the month at the end of a time step	no units	M
		DD	Density difference; used in fill flow matrix interpolations	g/mL	T
		DDEP	Change in Pressure head	no units	3
		DDF	Density difference; used in fill flow matrix interpolations	g/mL	T
		DDM	Density difference; used in fill flow matrix interpolations	g/mL	T
		DELA1	Change in A1 for two layer integration with respect to X	no units	123
		DENOM	Denominator term to determine DA/DX	no units	S
		DENSITY	Density of brines (north or south) used in single layer flow subroutine	lbs/ft <sup>3</sup>	3
	DIFFN		Difference between measured and computed North part water-surface altitude for a given time step	ft	W
	DIFFS		Difference between measured and computed South part water-surface altitude for a given time step	ft	W
	DIFVS		Difference between computed and measured south part volume for a given time step	acre-ft	W
		DNSTRM	Downstream water depth (can be critical section)	ft	3
$\Delta\rho$		DP	Difference in density between the north and south parts ( $\rho_n - \rho_s$ )	g/mL	MT

Report symbol	Water-Balance Program symbol	Water and Salt Balance Model symbol	Description	Unit	Where used
		DS	Density of the south part; used in fill flow matrix interpolations	g/mL	T
		DSM	Density of the south part; used in fill flow matrix interpolations	g/mL	T
		DX	Change in X, calculated from DA and slope	ft	23
		DX1	Change in X, calculated from change of A1	ft	12
		DX2	Change in X, calculated from change of A2	ft	12
		DXBAR	Average of DX1 and DX2	ft	12
EAAN	EAAN		1931–73 average annual fresh water evaporation for the north part	in.	W
EAAS	EAAS		1931–73 average annual fresh water evaporation for the south part	in.	W
EAI	EAI		Annual fraction of EAAN and EAAS used to calibrate the water-balance program	no units	W
	EAN		Annual evaporation from north part	in.	W
	EAS		Annual evaporation from south part	in.	W
	EAV		Integer counter	no units	W
	EAVMAX		Number of rows in the altitude-area-volume tables	no units	W
	EAVNUM		Integer counter	no units	W
	EAVVAL		Integer counter	no units	W
	EAVVALN		Integer counter	no units	W
	EAVVALS		Integer counter	no units	W
		EBBR	Elevation of the bottom of the rectangular part of breach (elevation = altitude - 4,000)	ft	M
		EGL	Array of energy gradeline from upstream to downstream	ft	2
		EGLN	Pressure head, north end	ft	2
	ELEV		Integer counter	no units	W
		ELN	Water-surface altitude of the north part; used in fill flow matrix interpolations	ft	T
EMI	EMI		Monthly fraction of annual evaporation	no units	W
	EMN		Monthly evaporation from the north part	acre-ft	W
	EMS		Monthly evaporation from the south part	acre-ft	W
EN	EN		Water-surface altitude of the north part, after time step	ft	W
		EN	Water-surface altitude of the north part; used in fill flow matrix interpolations	ft	T
	ENI		North part water-surface altitude at beginning of time step (computed)	ft	W
	ENIFIRST		Initial north part water-surface altitude	ft	W
		ENM	Water-surface altitude of the north part; used in fill flow matrix interpolations	ft	T
	ENMES		North part water-surface altitude at beginning of time step (measured)	ft	W
E		ENTRN1	An entrance loss coefficient for the lower layer at the north end of a channel based on the Velocity of the lower layer	slugs/ft <sup>2</sup>	M123

Report symbol	Water-Balance Program symbol	Water and Salt Balance Model symbol	Description	Unit	Where used
E		ENTRN2	An entrance loss coefficient for the lower layer at the north end of a channel based on the velocity of the lower layer; model adds effects of ENTRN1 and ENTRN2 for total entrance loss at the north end	slugs/ft <sup>2</sup>	M123
E		ENTRS	Entrance loss coefficient for the upper layer at the south end of a channel	slugs/ft <sup>2</sup>	M123
	EP		Integer counter	no units	W
ε		EPS	(RHO2 - RHO1)/RHO2	no units	M123
ES	ES		Water-surface altitude of the south part, after time step	ft	W
	ESI		South part water-surface altitude at beginning of time step (computed)	ft	W
	ESIFIRST		Initial south part water-surface altitude	ft	W
	ESMES		South part water-surface altitude at beginning of time step (measured)	ft	W
		ETLL	Elevation of the top of the lower flow layer at the middle of the breach (elevation = altitude - 4,000)	ft	M
		ETUL	Elevation of the top of the upper flow layer at the middle of the breach (elevation = altitude - 4,000)	ft	M
		F1SQ	Upper layer densimetric froude number squared	no units	S1
		F2SQ	Lower layer densimetric froude number squared	no units	S1
		FBBE	Average elevation below which the fill is not permeable (at the beginning of the modeling period) (elevation = altitude - 4,000)	ft	M
		FBE	Average elevation below which the fill is not permeable (at a given time step)	ft	M
		FBEI	Average elevation of the interface between the old and new fill layers (at the beginning of the modeling period) (elevation = altitude - 4,000)	ft	M
		FBNP	Correction factor to relate the permeability of the new (upper) fill layer to the permeability of the fill in 1973 (at the beginning of the modeling period)	no units	M
		FBOP	Correction factor to relate the permeability of the old (lower) fill layer to the permeability of the fill in 1973 (at the beginning of the modeling period)	no units	M
WKN		FCFN	Correction factor to adjust the (north-to-south) fill flows for changes in fill permeability from 1973 conditions to the conditions present at the current time step	no units	M
WKS		FCFS	Correction factor to adjust the (south-to-north) fill flows for changes in fill permeability from 1973 conditions to the conditions present at the current time step	no units	M
		FCN	Temporary north part dissolved-solids concentration used to determine if there is precipitation or resolution of salt in the north part during the time step	tons/acre-ft	M

Report symbol	Water-Balance Program symbol	Water and Salt Balance Model symbol	Description	Unit	Where used
F		FCOEF	Correction factor to reduce NI & FI (subroutine friction coefficients) relative to the value obtained assuming a smooth surface	no units	MS
		FDENSITY	Densimetric froude number	no units	3
		FEBE	Average elevation below which the fill is not permeable (at the end of the modeling period) (elevation = altitude - 4,000)	ft	M
		FEEI	Average elevation of the interface between the old and new fill layers (at the end of the modeling period) (elevation = altitude - 4,000)	ft	M
		FEI	Average elevation of the interface between the old and new fill layers (at a given time step) (elevation = altitude - 4,000)	ft	M
		FENP	Correction factor to relate the permeability of the new (upper) fill layer to the permeability of the fill in 1973 (at the end of the modeling period)	no units	M
		FEOP	Correction factor to relate the permeability of the old (lower) fill layer to the permeability of the fill in 1973 (at the end of the modeling period)	no units	M
Λ		FI	Interfacial friction factor	no units	S
		FL	North to south channel length (the same for all channels)	ft	M
φ		FLHS	$F1SQ + F2SQ - EPS * F1SQ * F2SQ - 1$ ; a measure of whether flow is supercritical ( $> 1.0$ ) or subcritical ( $< 1.0$ )	no units	1
QNF		FN	Fill flow (north-to-south) for a given time step	ft <sup>3</sup> /s	M
QIF		FNE	Average elevation of the top of the (north-to-south) fill flow layer (elevation = altitude - 4,000)	ft	M
K <sub>new</sub>		FNP	Correction factor to relate the permeability of the new (upper) fill layer to the permeability of the fill in 1973 (at a given time step)	no units	M
K <sub>old</sub>		FOP	Correction factor to relate the permeability of the old (lower) fill layer to the permeability of the fill in 1973 (at a given time step)	no units	M
		FR1SQ	Froude number (not densimetric)	no units	2
		FR2SQ	Froude number (not densimetric)	no units	2
		FRDN	Downstream froude number	no units	3
		FRN	Densimetric froude number calculated at point	no units	3
		FRNSQ	Densimetric froude number squared	no units	3
QSF		FS	Fill flow (south-to-north) for a given time step	ft <sup>3</sup> /s	M
AE		FSE	Average altitude of the top of the (south-to-north) fill flow layer	ft	M
CF W	FTFC	FT	Force from soffit flow resistance	slugs/ft <sup>2</sup>	23S
			Feet to inches conversion (1.0/12.0)	no units	W
		FW	Force from wall flow resistance	slugs/ft <sup>2</sup>	3
		FW1	Force from wall flow resistance - upper layer	slugs/ft <sup>2</sup>	3
		FW2	Force from wall flow resistance - lower layer	slugs/ft <sup>2</sup>	3
Z		FZ	Force from bottom flow resistance - lower layer	slugs/ft <sup>2</sup>	23S

Report symbol	Water-Balance Program symbol	Water and Salt Balance Model symbol	Description	Unit	Where used
g		G	Gravitational constant (32.2 ft/s)	ft/s	M123S
GIN			Ground-water inflow to the north part	acre-ft/d	A
GIS			Ground-water inflow to the south part	acre-ft/d	A
		H1N	Pressure head at north end of channel	ft	2
		HAVG	Average of north and south part elevation head	ft	M
ΔH		HD	Water-surface altitude difference between the north and south parts of the lake	ft	MT
		HDEP	Head at inlet of channel	ft	3
		HDF	Water-surface altitude difference between the north and south parts of the lake; used for fill flow matrix interpolation	ft	T
		HDM	Water-surface altitude difference between the north and south parts of the lake; used for fill flow matrix interpolation	ft	T
		HDN	Head at outlet of channel	ft	3
D		HEIGHT	Distance from top of culvert to bottom	ft	M123S
HN		HN	Height of the north part water-surface above the channel bottom (LEN-CHANB(ICHN))	ft	M123
HS		HS	Height of the south part water surface above the channel bottom (LES-CHANB(ICHN))	ft	M123
		HSTRY	Computed south part head to be compared with actual	ft	1
		HVNC	Change in volume of north part (computed)	acre-ft	W
		HVNM	Change in volume of north part (measured)	acre-ft	W
		HVOLN	Difference between measured and computed north part volumes for a given time step (HVNM-HVNC)	acre-ft	W
		HVOLS	Difference between measured and computed south part volumes for a given time step	acre-ft	W
		HVSC	Change in volume of south part (computed)	acre-ft	W
		HVSM	Change in volume of south part (measured)	acre-ft	W
I		I	Loop counter used throughout the model, generally indicates the current time step	no units	MPRT
		IA1N	Loop counter used for A1N trial loop	no units	1
		IA1S	Loop counter used to calculate A1S	no units	1
		IAS	Loop counter	no units	23
		ICHN	Counter that designates which channel flow is being computed for in a run through the channel flow loop (breach: ICHN=1, culverts: ICHN=2)	no units	M
		IDX	Loop counter for matching DX1 and DX2	no units	12
		IF	Loop counter for calculating FI	no units	S
		IN	Counter from 1 to N that designates the month that corresponds to a variable read in from the input file	no units	M
		INFLOCAL	Inflow calibration constant	no units	W
		IM	Integer counter	no units	T
		IQ1	Loop counter for calculating Q	no units	12

Report symbol	Water-Balance Program symbol	Water and Salt Balance Model symbol	Description	Unit	Where used
		IX	Integration counter	no units	12
		J	Loop counter used to read in variables	no units	MT
		JJ	Loop counter used to read in variables	no units	M
		JJJ	Loop counter used to read in variables	no units	M
		JM	Integer counter	no units	T
		JQMAX	Equals 1 if iterations to find Q for an A1 failed	no units	1
		K	Loop counter	no units	MT
K		KAPPA	F1SQ+F2SQ-EPS*F1SQ-1.0; a variable used to calculate DA/DX	no units	S
		KCN	Potassium (K) concentration in the north part	tons/acre-ft	M
		KCS	Potassium (K) concentration in the south part	tons/acre-ft	M
KLN		KLN	Dissolved potassium (K) load in the north part	tons	M
KLS		KLS	Dissolved potassium (K) load in the south part	tons	M
		KLWP	Loss of potassium (K) from the north part to west pond due to the WDPP (negative values indicate potassium returning)	tons	M
		KM	Integer counter	no units	T
		L	Integer counter	no units	T
		LEN	Water-surface elevation of the north part (elevation = altitude - 4,000)	ft	MPRT
		LES	Water-surface elevation of the south part (elevation = altitude - 4,000)	ft	MPR
		LLACF	Breach lower flow layer area correction factor	no units	M
LN		LN	Dissolved-solids load in the north part of the lake	tons	M
LNP		LNPPT	Amount of new precipitated salt in the north part during a given time step	tons	M
LS		LS	Dissolved-solids load in the north part of the lake	tons	M
LSD			Amount of salt re-entering solution in the south part during a given time step	tons	A
LSL			Dissolved-solids load in the deep brine layer of the south part	tons	A
LSP			Amount of new precipitated salt in the south part during a given time step	tons	A
LT			Total salt load in the lake, both dissolved and precipitated	tons	A
LWP		LWP(I)	Loss of dissolved solids from the north part to west pond due to the WDPP (negative values indicate salt returning)	tons/time step	M
		MATRIX	An array that is an interpolation matrix of (south-to-north) fill flows for various $\Delta H$ and $\Delta p$ combinations	no units	MT
		MAXINT	Integer counter	no units	T
QNB		MBN(I)	Measured (north-to-south) breach flow for a time step	ft <sup>3</sup> /s	M
QSB		MBS(I)	Measured (south-to-north) breach flow for a time step	ft <sup>3</sup> /s	M
		MCHAN	Maximum dimension for number of channels	no units	M

Report symbol	Water-Balance Program symbol	Water and Salt Balance Model symbol	Description	Unit	Where used
MgLN MgLS		MECN(I)	Measured (north-to-south) east culvert flow for a time step	ft <sup>3</sup> /s	M
		MECS(I)	Measured (south-to-north) east culvert flow for a time step	ft <sup>3</sup> /s	M
		MgCN	Magnesium (Mg) concentration in the north part	tons/acre-ft	M
		MgCS	Magnesium (Mg) concentration in the south part	tons/acre-ft	M
		MgLN	Dissolved magnesium (Mg) load in the north part	tons	M
		MgLS	Dissolved magnesium (Mg) load in the south part	tons	M
		MgLWP	Loss of magnesium from the north part to West Pond due to the WDPP (negative values indicate magnesium returning)	tons	M
CM	MON	MONTH	Month that the current time step falls in (model uses 12, 30.5 day months/year)	no units	MW
NaLN NaLS		MWCN(I)	Measured (north-to-south) west culvert flow for a time step	ft <sup>3</sup> /s	M
		MWCS(I)	Measured (south-to-north) west culvert flow for a time step	ft <sup>3</sup> /s	M
		N	The number of months in the model run	no units	M
		NaCN	Sodium (Na) concentration in the north part	tons/acre-ft	M
		NaCS	Sodium (Na) concentration in the south part	tons/acre-ft	M
		NaLN	Dissolved sodium (Na) load in the north part	tons	M
		NaLS	Dissolved sodium (Na) load in the south part	tons	M
		NaLWP	Loss of sodium from the north part to West Pond due to the WDPP (negative values indicate sodium returning)	tons	M
		NCHAN	The number of channels for which the model will compute flow	no units	M
		NDA1	An integration flag, for the first iteration (1, otherwise 2)	no units	1
EAVN		NDA2	Number of integration steps	no units	2
		NI	Manning's N value for the interface	no units	M123S
		NORTH	An array that is a table of lake surface areas and volumes for given lake water-surface altitudes for the north part	ft, acres, acre-ft	MPRW
		NPROG	A flag indicating whether the flow regime analyzed was correct, or whether the next flow regime should be analyzed, 1=two-layer flow, 2=arrested wedge, 3=single layer	no units	M123
		NQ	Number of valid flows analyzed for an assumed A1	no units	1
		NSTEP	Number of integration steps	no units	23
		NSTOP	A flag to determine whether critical flow has been reached	no units	1S
		NT	Manning's N value for top of culvert	no units	MS
		NTS	Number of time steps in the model	no units	M
		NW1	Manning's N value used in the culvert subroutines	no units	M123S
		NW2	Manning's N value used in the culvert subroutines	no units	M123S
		NZ	Manning's N value used in the culvert subroutines	no units	M123S

Report symbol	Water-Balance Program symbol	Water and Salt Balance Model symbol	Description	Unit	Where used
PAAN	PAAN		Average annual (1931–73) precipitation for north part	in.	W
PAAOGSF	PAAOG		Average annual (1931–73) precipitation at Ogden (16.43)	in.	W
PAAS	PAAS		Average annual (1931–73) precipitation for south part	in.	W
PAASLC	PAASLC		Average annual (1931–73) precipitation for SLC airport (14.69)	in.	W
PAATool	PAATO		Average annual (1931–73) precipitation at Tooele (16.05)	in.	W
		PF20	Density of freshwater at 20° C	g/mL	M
PRT	PFAC		Combined annual percent of average annual precipitation at Ogden, Salt Lake City and Tooele	no units	W
		PFT	Density of freshwater at TEMX	g/mL	M
		PHEAD2	Pressure head of layer 2	ft	23
		PHEADBAR	Pressure head at midpoint of integration step	ft	23
		PHEADDN	Pressure head downstream	ft	3
		PHEADN	Downstream pressure head	ft	2
		PHEADUP	Upstream pressure head	ft	3
PIN			Direct precipitation on the north part	acre-ft/d	A
PIS			Direct precipitation on the south part	acre-ft/d	A
	PMN		Monthly precipitation over the north part	acre-ft	W
PMOGSF	PMOG		Monthly precipitation at Ogden	in.	W
	PMS		Monthly precipitation over the south part	acre-ft	W
PMSLC	PMSLC		Monthly precipitation at SLC airport	in.	W
PMTool	PMTO		Monthly precipitation at Tooele	in.	W
$\rho_n$		PN	Density of the north part (at TEMX)	g/mL	M
	PRECIPCAL		Precipitation calibration constant	no units	W
$\rho_s$		PS	Density of the south part (at TEMX)	g/mL	MT
		Q1	(south-to-north) flow through channel (ICHN) computed in the culvert subroutines	ft <sup>3</sup> /s	M123S
		Q1F	(south-to-north) fill flow computed in the INTER3 subroutine	ft <sup>3</sup> /s	MT
		Q1PREV	Q1 from the previous time step, used in the culvert subroutines	ft <sup>3</sup> /s	M123
		Q1SQ	Square of upper layer flow	ft <sup>6</sup> /s <sup>2</sup>	1
		Q2	(north-to-south) flow through channel (ICHN) computed in the culvert subroutines	ft <sup>3</sup> /s	M123S
		Q2F	(north-to-south) fill flow computed in the INTER3 subroutine	ft <sup>3</sup> /s	MT
		Q2PREV	Q2 from the previous time step, used in the culvert subroutines	ft <sup>3</sup> /s	M123
		Q2SQ	Square of lower layer flow	ft <sup>6</sup> /s <sup>2</sup>	1
	QB		Monthly inflow of surface and ground water from the Bear River Basin	acre-ft	W
		QEN(I)	Evaporation from the north part for a given time step	acre-ft/time step	M

Report symbol	Water-Balance Program symbol	Water and Salt Balance Model symbol	Description	Unit	Where used
		QES(I)	Evaporation from the south part for a given time step	acre-ft/time step	M
		QFLOW	Trial flow rate	ft <sup>3</sup> /s	3
		QI	South-to-north fill flow	ft <sup>3</sup> /s	T
		QIN(I)	Ground water and precipitation inflow to the north part	acre-ft/time step	M
		QIS(I)	Surface water, ground water and precipitation inflow to the south part	acre-ft/time step	M
	QJ		Monthly inflow to Farmington Bay area from Jordan River Basin streams, streams in Davis County, and ground water	acre-ft	W
		QMAX	Maximum upper layer flow, for given lake water surface altitudes and densities	ft <sup>3</sup> /s	123
		QMIN	Minimum upper layer flow, starts at zero	ft <sup>3</sup> /s	123
QN		QN	Total flow through the causeway (north-to-south)	acre-ft/time step	M
		QNC(ICHN)	(north-to-south) flow through channel (ICHN) used in QN computations	ft <sup>3</sup> /s	M123S
QNC			North-to-south culvert flow	no units	A
		QQMAX	Initial QMAX for each A1 calculated in CULV1	ft <sup>3</sup> /s	1
QS		QS	Total flow through the causeway (south-to-north)	acre-ft/time step	M
	QS		Monthly inflow to the south part of lake from Goggin Drain, miscellaneous streams, and ground water	acre-ft	W
		QSC(ICHN)	(south-to-north) flow through channel (ICHN) used in QS computations	ft <sup>3</sup> /s	M123S
QSC			South-to-north culvert flow	no units	A
		QSN	South-to-north fill flow	ft <sup>3</sup> /s	T
		QSDN	South-to-north fill flow	ft <sup>3</sup> /s	T
	QSNET		Net inflow to the south part from all sources for a given time step	acre-ft	W
	QTN		Monthly ground water inflow to north part of lake	acre-ft	W
		QTRY	An array of valid flow estimates calculated in CULV1	ft <sup>3</sup> /s	1
	QTS		Monthly inflow to the south part of lake, equals QB + QW + QJ + QS	acre-ft	W
	QW		Monthly inflow to the south part from Weber River basin, miscellaneous streams, and ground water	acre-ft	W
		QWP(I)	Loss of water from the north part to West Pond due to the WDPP (negative values indicate return flow)	acre-ft/time step	M
		RATIO	Ratio of volumes used to calculate lake water surface altitude from the altitude-area-volume tables	no units	R
		REI	Reynolds number	no units	S
LND		RESOLN	Amount of salt re-entering solution in the north part during a given time step	tons	M
		RHO1	Density (specific gravity) of the south part at TEMX	slugs/ft <sup>3</sup>	M

Report symbol	Water-Balance Program symbol	Water and Salt Balance Model symbol	Description	Unit	Where used
		RHO2	Density (specific gravity) of the north part just north of a channel (ICHN) at TEMX	slugs/ft <sup>3</sup>	M
		RI1	Hydraulic radius related to upper layer interface	ft	S
		RI2	Hydraulic radius related to lower layer interface	ft	S
		RT	Hydraulic radius related to the top of the culvert	ft	23
		RT1	Hydraulic radius related to the top of the culvert	ft	S
	RTNC		Interpolation ratio for EAVN table (computed)	no units	W
	RTNM		Interpolation ratio for EAVN table (measured)	no units	W
	RTSC		Interpolation ratio for EAVS table (computed)	no units	W
	RTSM		Interpolation ratio for EAVS table (measured)	no units	W
		RW	Hydraulic radius related to culvert walls	ft	3
		RW1	Hydraulic radius related to upper layer walls	ft	2S
		RW2	Hydraulic radius related to lower layer walls	ft	2S
		RZ	Hydraulic radius related to culvert bottom	ft	23S
		SALL	Cross-sectional area of the lower layer of breach flow used in the culvert subroutines	ft <sup>2</sup>	M
		SAUL	Cross-sectional area of the upper layer of breach flow used in the culvert subroutines	ft <sup>2</sup>	M
SCFN	SCFN	SCFN	Correction factor to reduce the freshwater evaporation rate to the evaporation rate of the north part brine for the given time step's $\rho_n$	no units	MW
SCFS	SCFS	SCFS	Correction factor to reduce the freshwater evaporation rate to the evaporation rate of the south part brine for the given time step's $\rho_s$	no units	MW
		SENTR1	Coefficient for upper layer velocity head used to calculate entrance loss	no units	12S
		SENTR2	Coefficient for the difference between upper and lower layer velocity head used to calculate entrance loss	no units	12S
		SENTRAN	Coefficient for lower layer velocity head used to calculate entrance loss	no units	3
SIS			Surface-water inflow to the south part	no units	A
S		SLOPE	Subroutine used to compute hydraulic gradient	no units	A
	EAVS	SOUTH	An array that is a table of lake surface areas and volumes for given lake water-surface altitudes for the south part	ft, acres, acre-ft	MPRW
	EAVS1	SOUTH A	The array variable 'EAVS1' or 'SOUTH' before 1/1/94 when a dike owned by Magcorp was breached	ft, acres, acre-ft	MPRW
	EAVS2	SOUTH B	The array variable 'EAVS1' or 'SOUTH' after 1/1/94 when a dike owned by Magcorp was breached	ft, acres, acre-ft	MPRW
		SOUTONOR	Logical flag, true if either arrested wedge or single layer flow is from south-to-north	no units	3
		SZ	Slope of the culvert bottom	no units	M23S

Report symbol	Water-Balance Program symbol	Water and Salt Balance Model symbol	Description	Unit	Where used
T1		T1	For unsubmerged flow $T1 = (TAUI + TAUE1 + 2 \cdot A1BAR \cdot (TAUE1 + TAUW1) / CHNW) / (G \cdot RHO1 \cdot A1BAR)$ , and for submerged flow $(TAUT1 + TAUI + 2 \cdot TAUE1 + 2 \cdot A1BAR \cdot (TAUE1 + TAUW1) / CHNW) / (G \cdot RHO1 \cdot A1BAR)$ , used to calculate DA/DX	no units	S
T2		T2	$(TAUZ + 2 \cdot TAUE2 - TAUI + 2 \cdot A2BAR \cdot (TAUE2 + TAUW2) / CHNW) / (G \cdot RHO2 \cdot A2BAR)$ , used to calculate DA/DX	no units	S
		TAUE	Entrance losses expressed as a force	slugs	3
		TAUE1	Upper layer entrance losses expressed as a force	slugs	2S
		TAUE2	Lower layer entrance losses expressed as a force	slugs	2S
		TAUI	Interfacial head losses expressed as a force	slugs	23S
		TAUT	Soffit head losses expressed as a force	slugs	23
		TAUT1	Soffit head losses expressed as a force	slugs	S
		TAUW	Wall head losses expressed as a force	slugs	3
		TAUW1	Upper layer wall head losses expressed as a force	slugs	2S
		TAUW2	Lower layer wall head losses expressed as a force	slugs	2S
		TAUZ	Culvert bottom head losses expressed as a force	slugs	23S
		TEMX	Rough average monthly water temperature of the lake	°C	M
		TOLDX	Tolerance between X and FL	ft	M123
		TOLHS	Tolerance between hs and end of integration value	ft	M123
		TOLQ1	Tolerance for flow bracketing	ft <sup>3</sup> /s	M123
		TOLX	Tolerance between X and FL	ft	M123
		TOTHEAD1	Pressure head of upper layer, beginning of integration step	ft	12S
		TOTHEADBAR	Pressure head of upper layer, middle of integration step	ft	1
		TOTHEADS	Total pressure head, south end of culvert	ft	2
		TRY	Trial value iteratively refined numerically	no units	123S
T		TS	Length of one time step	days	M
		TSBD	time step it is assumed that the breach was deepened	no units	M
		TSPM	time steps per month	no units	M
		TT	Array holding values for TT1..TT9 for breach and culverts	no units	M
		TT1	Ratio of interfacial to upper wall Manning's N, used to calculate hydraulic radius	no units	M23S
		TT2	Ratio of interfacial to lower wall Manning's N	no units	M2S
		TT3	Ratio of culvert bottom to lower wall Manning's N	no units	M23S
		TT4	Ratio of culvert bottom to interfacial Manning's N	no units	M23S
		TT5	Ratio of difference between upper and lower layer velocity to the upper layer velocity	no units	S
		TT6	Ratio of difference between upper and lower layer velocity to the lower layer velocity	no units	S
		TT7	Ratio of culvert top to interfacial Manning's N	no units	MS

Report symbol	Water-Balance Program symbol	Water and Salt Balance Model symbol	Description	Unit	Where used
u1	TWELVE	TT8	Ratio of culvert top to upper wall Manning's N	no units	M23S
		TT9	Ratio of culvert top to culvert bottom Manning's N	no units	M
			Number of months in a year	no units	W
		U1	Velocity of upper layer	ft/s	2S
		U1BAR	Velocity of upper layer at midpoint of integration step	ft/s	S
		U1N	Velocity of upper layer at north control section	ft/s	1
		U1S	Velocity of upper layer at south control section	ft/s	12
		U2	Velocity of lower layer	ft/s	2S
		U2BAR	Velocity of lower layer at midpoint of integration step	ft/s	S
		U2N	Velocity of lower layer at north control section	ft/s	12
u2		ULACF	Breach upper flow layer area correction factor	no units	M
		UPSTRM	Upstream pressure head at control section	ft	3
		UVEL	Velocity of flow at integration step	ft/s	3
		UVELUP	Velocity at upstream control section	ft/s	3
			Change in the volume of the north part over a time step	acre-ft/time step	A
ΔVN	VNC	VN	Volume of north part, after time step	acre-ft	MRW
		VNFIRST	Initial volume of the north part (measured)	acre-ft	W
		VNIC	Volume of the north part at the beginning of a time step based on computed water-surface altitude from previous time step	acre-ft	W
VS	VNM		Volume of north part (measured)	acre-ft	W
	VOLNUM		Integer counter	no units	W
	VSC	VS	Volume of north part, after time step	acre-ft	MRW
	VSFIRST		Initial volume of the south part (measured)	acre-ft	W
	VSIC		Volume of the south part at the beginning of a time step based on computed water-surface altitude from previous time step	acre-ft	W
X	VSM		Volume of south part (measured)	acre-ft	W
		WBB	Width of the breach bottom	ft	M
		X	Longitudinal channel coordinate; X=0 is at north end and +X direction is north thus, all X's in the channel are (-)	ft	M123S
		XEN(I)	Evaporation from the north part as computed in the wb program with AN and SCFN divided out	ft/time step	M
		XES(I)	Evaporation from the south part as computed in the wb program with AS and SCFS divided out	ft/time step	M
Y <sub>new</sub>		XTRY	Array of solutions (for X) for a given Q1 and A1	ft	12
			Average thickness of a fill flow layer within the new fill	ft	A
Y <sub>old</sub>			Average thickness of a fill flow layer within the old fill	ft	A
YNF		Y2F	Average thickness of the (north-to-south) fill flow layer at a given time step	ft	MT

Report symbol	Water- Balance Program symbol	Water and Salt Balance Model symbol	Description	Unit	Where used
YSF			Average thickness of the (south-to-north) fill flow layer at a given time step	ft	
	YR	YEAR	Year that the current time step falls in	no units	MW
	YEARFIRST		The first year of the modeling period	no units	W
	YEARMAX		Number of years in the modeling period	no units	W